

# The Durability of Metal-Honeycomb Sandwich Structure Exposed to High Humidity Conditions

*Andrew Rider*

Airframes and Engines Division  
Aeronautical and Maritime Research Laboratory

DSTO-TR-1276

## ABSTRACT

Metal-honeycomb structure plays an important role in the structural integrity of RAAF F-111 aircraft. When F-111 is retired from service honeycomb panels will have experienced extended exposure to hostile environments. The processes leading to degradation of metal-honeycomb sandwich structure and its effect on the structural integrity of F-111 structure is critical information required for successful, long term aircraft management.

The work presented in this report summarises initial investigations into the mechanical strength response of metal-honeycomb sandwich structure exposed to high humidity environments. Honeycomb sandwich panels constructed from core and structural adhesives materials currently used for repairs at RAAF-Amberley have been conditioned in high humidity environments and examined using flatwise tension, peel and bending tests. The durability performance of honeycomb panels depended on the construction materials and the mode of loading employed. In some cases, characterisation of the honeycomb revealed differences that could be related to the durability performance.

## RELEASE LIMITATION

*Approved for public release*

20020531 098

DEPARTMENT OF DEFENCE  
DEFENCE SCIENCE & TECHNOLOGY ORGANISATION

**DSTO**

AQ F02-08-1602

*Published by*

*DSTO Aeronautical and Maritime Research Laboratory  
506 Lorimer St  
Fishermans Bend Vic 3207 Australia*

*Telephone: (03) 9626 7000*

*Fax: (03) 9626 7999*

*© Commonwealth of Australia 2002*

*AR-012-154*

*March 2002*

**APPROVED FOR PUBLIC RELEASE**

# The Durability of Metal-Honeycomb Sandwich Structure Exposed to High Humidity Conditions

## Executive Summary

This report summarises research undertaken in AIR Task 97/121. This task was established to undertake preliminary investigations into the influence of environmental exposure on the mechanical properties of bonded panels. Bonded panels make a significant contribution to the structural integrity of F-111 aircraft and extended service relies, in part, on the successful maintenance of bonded panels. To date limited information is available on the influence of environmental exposure on the condition of bonded panels and repairs. The research provides important information that will assist in the maintenance and repair of bonded panels.

Honeycomb panels were constructed from material currently used for repair and maintenance of bonded panels at RAAF Base Amberley and conditioned in high humidity environments. Testing in peel, flat-wise tension and bending revealed degradation of mechanical properties depended on the material used to construct the panels as well as the loading mode. Mechanical testing of environmentally conditioned panels indicated that the reduction in strength was greater for peel compared to tensile loading. The reduction in panel strength also required less exposure in the humid environment for peel loading compared to tensile loading. The honeycomb material also dictated the relative durability performance. Alcore PAA treated honeycomb offered the best performance with Hexcel CR3 being notably better than the equivalent Alcore product.

Characterisation of the honeycomb core material revealed differences in the node bond adhesive and the surface coatings applied to the metal surfaces. PAA honeycomb had a thick polyamide polymeric layer. The superior performance of the PAA honeycomb samples was clearly linked to the hydrolytic stability of adhesive bonds formed with the polyamide layer. The Hexcel CR3 layer had a chromium oxide layer with a thin silicon containing organic layer, whereas the equivalent Alcore product, Duracore, only had a chromium oxide layer. The poor performance of the Duracore honeycomb appeared to be related to the absence of the organic layer present on the Hexcel CR3 surface, that clearly improved the hydrolytic strength of the adhesive bonds formed.

Fracture analysis and moisture diffusion modelling provided useful insight into the mechanisms leading to bond degradation of the honeycomb fillet bond. Initially, moisture diffusion to the honeycomb and adhesive interface leads to bond hydrolysis and degradation. At extended exposure periods, interfacial moisture can begin to hydrolyse the honeycomb coating, leading to fracture in a weakened hydrated layer. Modelling the decay of the tensile and peel strength on the basis of moisture diffusion in the fillet bond of the sandwich panel indicated that the concept of a critical

concentration of interfacial moisture could be employed to explain bond degradation processes. In the case of tensile loading of conditioned honeycomb samples, interfacial diffusion of moisture, in addition to moisture absorbed in the adhesive, may also be required for a critical concentration of moisture that leads to degradation of the fillet bond. The peel loading, however, suggested that moisture uptake of the adhesive was generally sufficient for bond degradation to proceed. The degradation of peel strength, therefore, appears to proceed with a lower critical concentration of water at the interface than in the case of tension loading.

Moisture uptake by sandwich panels suggested a preference for diffusion in the node bond direction. Radiographs suggested that cerium nitrate solution used for radiographic contrast is transported along the honeycomb walls and through the node bond adhesive at a faster rate than diffusion through the fillet bond adhesive.

Experiments conducted with bulk adhesive and honeycomb samples saturated with moisture indicated that recovery of panel strength through drying procedures should be possible. Fillet bonds in single sided sandwich panels and honeycomb node bonds indicated substantial recovery in dry strength after elevated temperature drying. Indirect paths for moisture escape in double sided bonded panels, however, would be expected to retard the drying rates and longer times would be needed to achieve recovery of dry mechanical strength.

Results presented in this report should assist personnel responsible for overseeing the maintenance of bonded panels on F-111. The analysis performed on the relative durability performance of a range of honeycomb materials and adhesives should assist with decisions such as selection of suitable materials for panel repair. Diffusion and drying experiments should also provide an indication of the importance of drying moisture laden panels and the potential recovery of mechanical properties that can be achieved. The information contained in this report will also assist with research being undertaken in AIR Task 00/140, the F-111 Teardown. Investigation of bonded panels from the F-111 fuselage will involve the use of Elcometer sampling tests to assess the mechanical state of the panel. Fracture analysis will also provide critical information of the panel service history. Both the Elcometer test and fracture analysis techniques have been developed through work undertaken and detailed in this report.

## Authors

### **Andrew Rider**

**Airframes and Engines Division**

*Andrew Rider joined Airframes and Engines Division at DSTO in 1988 as a Professional Officer Class 1. He has a Bachelor of Applied Science in Chemistry from Swinburne University of Technology and a PhD in Physical Chemistry from the University of New South Wales. He is currently employed as a Research Scientist and works within Airframes and Engines Division. He is involved in research to understand degradation mechanisms involved in bonded structure and repairs used on F-111 and F/A-18 fighter aircraft.*

---

# Contents

<b>1. INTRODUCTION.....</b>	<b>1</b>
<b>2. EXPERIMENTAL METHOD AND MATERIALS.....</b>	<b>1</b>
<b>2.1 Materials.....</b>	<b>1</b>
<b>2.2 Experimental Methods .....</b>	<b>1</b>
2.2.1 Honeycomb Sandwich Fabrication .....	1
2.2.1.1 Honeycomb Core Construction .....	2
2.2.2 Environmental Conditioning.....	4
2.2.3 Flatwise Tension Testing .....	4
2.2.4 Elcometer Testing .....	5
2.2.5 Climbing Drum Peel Testing .....	5
2.2.6 Testing of Flexural Properties of Honeycomb Specimens.....	5
2.2.7 Node Bond Peel Testing .....	8
2.2.8 Fracture Analysis and Surface Characterisation Studies.....	8
2.2.9 Honeycomb Sandwich Water Diffusion Studies.....	8
2.2.10 Honeycomb Sandwich Panel Failure Modes .....	9
2.2.11 FM-300 and FM-300-2K Water Diffusion Studies.....	10
<b>3. HONEYCOMB CHARACTERISATION .....</b>	<b>10</b>
<b>3.1 Hexcel CR3 Honeycomb.....</b>	<b>10</b>
<b>3.2 Alcore Dura-Core Honeycomb .....</b>	<b>12</b>
<b>3.3 Hexcel PAA Honeycomb .....</b>	<b>14</b>
<b>3.4 Alcore 5056 PAA Honeycomb .....</b>	<b>14</b>
<b>4. RESULTS .....</b>	<b>15</b>
<b>4.1 Flatwise Tension results .....</b>	<b>15</b>
4.1.1 FM-300, Hexcel CR3 Honeycomb, Strength versus Adhesion Area.....	15
4.1.2 FM-300, Hexcel CR3 Honeycomb, 95°C humid exposure.....	15
4.1.3 Dry Recovery Experiments for FM-300 and Hexcel CR3 Honeycomb. ....	16
4.1.4 FM-300, Hexcel CR3 and Alcore Honeycomb, 95°C humid exposure .....	17
4.1.5 FM-300, Hexcel CR3 and Alcore Honeycomb, 50°C and 70°C humid exposure....	18
<b>4.2 Pull-Off Tension (Elcometer) results .....</b>	<b>20</b>
4.2.1 FM-300, Hexcel CR3 Honeycomb, 95°C humid exposure .....	20
4.2.2 FM-300, Hexcel CR3 and Alcore Honeycomb, 70°C humid exposure .....	21
4.2.3 FM-300, Hexcel CR3 Honeycomb, Double versus Single Skin Exposure .....	22
4.2.4 FM-300-2K, Hexcel CR3 and Alcore Honeycomb, 70°C humid exposure .....	22
4.2.5 Adhesional Failure as a Function of Pull-Off Tension .....	23
<b>4.3 Peel results.....</b>	<b>24</b>
4.3.1 FM-300, Hexcel CR3 and Alcore Honeycomb, 70°C and 95°C humid exposure.....	24
4.3.2 FM-300-2K, Hexcel CR3 and Alcore Honeycomb, 70°C humid exposure .....	25
4.3.3 Adhesional Failure as a Function of Peel Torque .....	26
<b>4.4 Fracture Analysis.....</b>	<b>27</b>
4.4.1 Flat-wise Tension Failure Analysis of FM-300, Hexcel CR3 Honeycomb .....	27
4.4.2 Peel Failure Analysis of FM-300, Hexcel CR3 Honeycomb .....	33
4.4.3 Peel Failure Analysis of FM-300, Alcore Untreated Honeycomb .....	36
4.4.4 Elcometer Failure Analysis of FM-300, Hexcel CR3 Honeycomb .....	39
<b>4.5 Three and four Point Bending results.....</b>	<b>42</b>
4.5.1 Hexcel CR3 Honeycomb, Strength versus Adhesion Area.....	42
4.5.2 Hexcel CR3 Honeycomb, 95°C humid exposure.....	43
4.5.3 Asymmetric Beam Mechanical Properties.....	45
<b>4.6 Node Bond results .....</b>	<b>48</b>
4.6.1 Hexcel and Alcore Node Bond Peel strength versus Humid Exposure .....	48
4.6.2 Hexcel and Alcore Node Bond Peel strength versus Temperature .....	50

4.6.3	Hexcel CR3 Honeycomb, prebond node conditioning, pull-off strength .....	50
4.6.4	Hexcel CR3 Honeycomb, prebond node conditioning, bend strength .....	51
4.7	<b>Water Diffusion Tests</b> .....	<b>51</b>
4.7.1	Hexcel CR3 Honeycomb, Water uptake at 70°C .....	51
4.7.2	Hexcel CR3 Honeycomb, Water uptake at 70°C, Radiography tests .....	55
4.8	<b>Adhesive Water Diffusion results</b> .....	<b>56</b>
4.8.1	Mass Uptake Studies .....	56
4.8.2	Moisture Saturated Adhesive Drying Rate at 80°C .....	60
5.	<b>DISCUSSION</b> .....	<b>63</b>
5.1	<b>Honeycomb Characterisation</b> .....	<b>63</b>
5.1.1	Honeycomb Node Bonds .....	63
5.1.2	Honeycomb Surface Coatings .....	63
5.2	<b>Flat-wise Tension Testing</b> .....	<b>64</b>
5.3	<b>Modelling Moisture Degradation in Honeycomb Structure</b> .....	<b>64</b>
5.3.1	The Influence of Moisture on the Locus of Fracture .....	64
5.3.2	Bond Degradation as a Function of Moisture Diffusion Rates .....	66
5.3.2.1	Modelling the Decay of Tension Strength in Humid Environments .....	66
5.3.2.2	Modelling the Decay of Peel Strength in Humid Environments .....	70
5.4	<b>Moisture Diffusion in Bonded Honeycomb Structure</b> .....	<b>71</b>
5.4.1	Tension Strength .....	71
5.4.2	Peel Strength .....	72
5.4.3	General Comments on the Decay in Mechanical Properties caused by Moisture .....	73
5.5	<b>Beam Mechanical Properties</b> .....	<b>74</b>
5.6	<b>Node Bond Strength Influence on Honeycomb Panel Properties</b> .....	<b>74</b>
5.7	<b>Moisture Diffusion in Honeycomb Sandwich Panels</b> .....	<b>75</b>
6.	<b>CONCLUSIONS</b> .....	<b>75</b>
7.	<b>FUTURE WORK</b> .....	<b>78</b>
8.	<b>ACKNOWLEDGEMENTS</b> .....	<b>79</b>
9.	<b>REFERENCES</b> .....	<b>79</b>
<b>APPENDIX A: RADIOGRAPHIC ANALYSIS OF MOISTURE DIFFUSION IN METAL HONEYCOMB SANDWICH PANELS</b> .....		<b>81</b>
A.1	Control Specimen .....	81
A.2	Two Days Immersion in 70°C Cerium Solution .....	85
A.3	Three Days Immersion in 70°C Cerium Solution .....	89
A.4	Five Days Immersion in 70°C Cerium Solution .....	93
A.5	Ten Days Immersion in 70°C Cerium Solution .....	97
A.6	Discussion .....	101
A.7	Conclusion .....	102

# 1. Introduction

Bonded sandwich panel structural integrity is an important component in the successful maintenance and continued operation of RAAF F-111 aircraft through to the projected withdrawal date of 2020. F-111 airframe stiffness and strength is dependent on the integrity of bonded sandwich panel structure. Currently, limited knowledge exists as to the effect of environmental exposure on the mechanical integrity of bonded sandwich panels. Several examples of inflight loss of sandwich panels and panel skins have been reported together with ongoing repairs of honeycomb structure being undertaken at RAAF Amberley [1]. This indicates that bonded panels have the potential to limit the available F-111 flying hours in the future and increase the financial burden of aircraft maintenance.

The work presented in this report summarises research into the effect of environmental exposure on fundamental mechanical properties of honeycomb materials currently used for repairs by RAAF Amberley and to assess their relative performance against new and existing materials available from honeycomb and adhesives manufacturers. Information derived from these studies will provide the necessary support for tasks such as AIR 00/140, the F-111 Fuselage Teardown program and AIR 98/186, which aims to model the influence of degradation on panel mechanical properties.

## 2. Experimental Methods and Materials

### 2.1 Materials

Materials used in the report are provided in Table 2.1 together with dimensions and manufacturing details.

### 2.2 Experimental Methods

#### 2.2.1 Honeycomb Sandwich Fabrication

5/8" thick honeycomb core, as described in Table 2.1, was vapour degreased in trichloroethylene (TCE) prior to all bonding operations, unless otherwise stated.

Aluminium Skin material received a standard *grit-blast and silane treatment* [2] [3]. Briefly, this involved degreasing the panel with MEK solvent using Kimwipes, scotchbrite abrasion with distilled water lubricant, debris removal with distilled water soaked Kimwipe tissues, drying and grit-blasting with alumina grit. The skin was then dipped in an aqueous solution of 1% v/v epoxy silane solution for 15 minutes and dried at 105°C for 30 minutes, prior to bonding.

FM-300 or FM-300-2K was bonded for 1 hour at 177°C and 120°C, respectively using a pressure of 40psi.

In some cases, only one skin was bonded to the honeycomb core with either FM-300 or FM-300-2K, prior to exposure to the conditioning environment. After removal from the conditioning environment the second skin was bonded using EA9309.3NA paste adhesive, unless otherwise stated, which had received a *grit-blast and silane treatment*.



**Table 2.1** Description and properties of materials used in report.

Material	Details
FM-300	177°C curing structural epoxy adhesive. Manufactured by Cytec
FM-300-2K	120°C curing structural epoxy adhesive. Manufactured by Cytec.
FM-73	120°C curing structural adhesive, manufactured by Cytec.
Alcore 5056 Untreated Honeycomb	Cell size 3/16", thickness 5/8", foil gauge 0.002", node adhesive: polyamide. 5056 Aluminium alloy. Manufactured by Alcore.
Alcore Dura-Core Honeycomb	Cell size 3/16", thickness 5/8", foil gauge 0.002", node adhesive: polyamide. 5056 Aluminium alloy. Foil has protective chromium based coating Manufactured by Alcore.
Alcore 5052 PAA Honeycomb	Cell size 3/16", thickness 5/8", foil gauge 0.002", node adhesive: polyamide. 5052 Aluminium alloy. Foil has protective phosphoric acid anodised (PAA) coating. Manufactured by Alcore.
Alcore 5056 PAA Honeycomb	Cell size 3/16", thickness 5/8", foil gauge 0.002", node adhesive: polyamide. 5056 Aluminium alloy. Foil has protective phosphoric acid anodised (PAA) coating. Manufactured by Alcore.
Hexcel CR3 Honeycomb	Cell size 3/16", thickness 5/8", foil gauge 0.002", node adhesive: nitrile rubber modified phenolic. 5056 Aluminium alloy. Foil has protective organo-metallic chromium based coating, different from Alcore. Manufactured by Hexcel.
Aluminium Skin material	Al-2024 T3 clad aluminium. 0.5mm thick. Supplied by H Aircraft Spares P/L, Mentone, Victoria.
Epoxy Silane	$\gamma$ -glycidoxypolytrimethoxysilane. A-187 from Union Carbide.
MEK	Methyl ethyl ketone, analytical grade reagent. Merck Chemicals.
Kimwipes	Fine Grade RN 4103, Kimberly-Clarke
Scotchbrite	8447 Scotchbrite from 3M.
Paste Adhesive	EA9309.3NA room temperature curing adhesive from Hysol-Dextor.
Humidity chamber	Air recirculating Condensing humidity chamber from Thermoline, model no SH60.
Alumina Grit	Refined aluminium oxide 50 $\mu$ m grit, S.S. White, No. 3, Coultronics Trading, NSN 5350-66-047-2439.
Distilled Water	0.4 $\mu$ S/cm, pH: 6.4.
TCE	Trichloroethylene solvent, high purity.

### 2.2.1.1 Honeycomb Core Construction

Figure 2.2.1.1 indicates the manner in which honeycomb core material is constructed together with the terms used to describe the core characteristics.

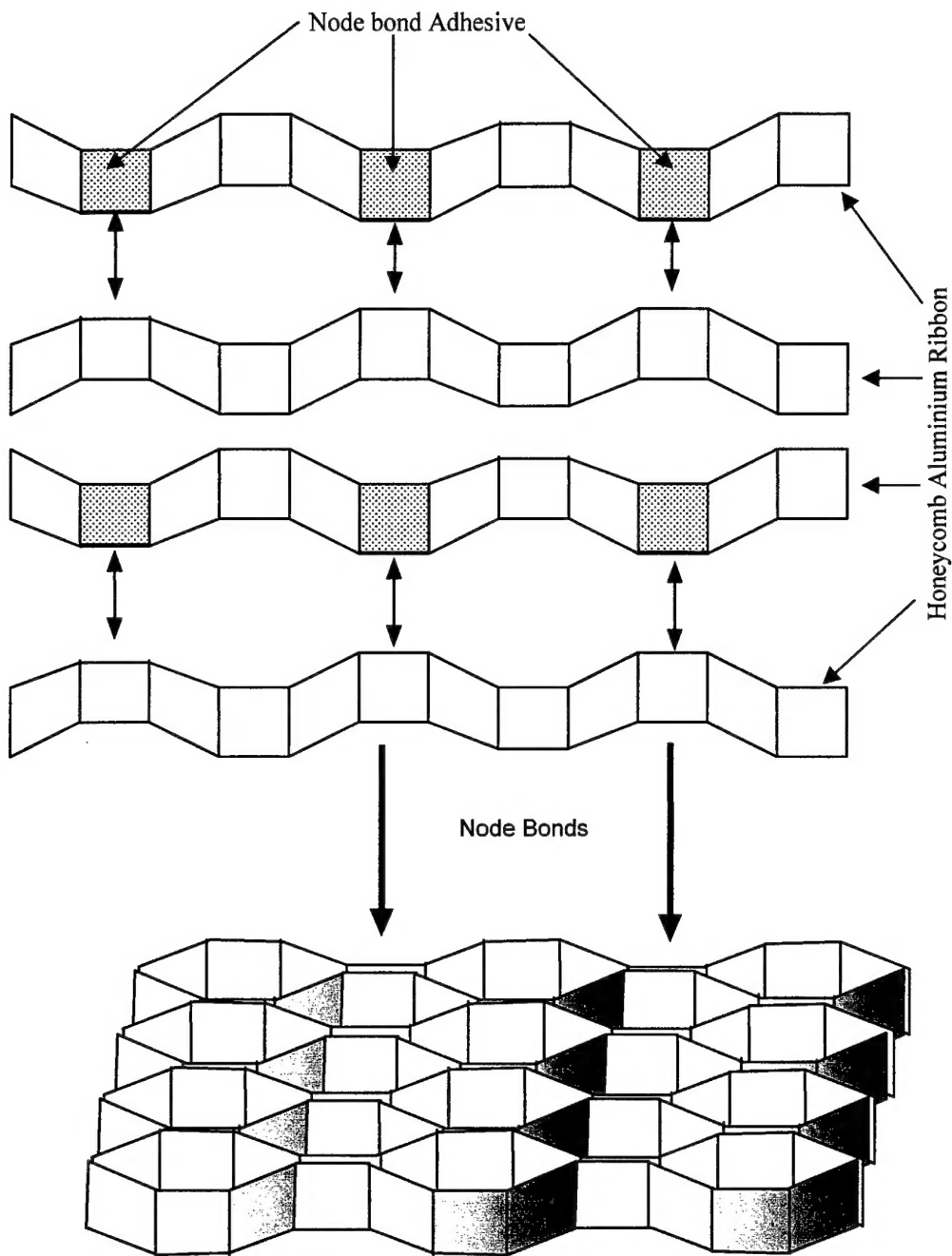


**Figure 2.2.1.1** Honeycomb core construction. Hexagonal cells are produced by bonding aluminium foil at points on the top and bottom wall of each cell, termed *node bonds*.

### 2.2.2 Environmental Conditioning

Honeycomb samples were exposed to the environments detailed in Table 2.2:

**Table 2.2** Honeycomb conditioning environments used

Environment	Test Environment Description
50°C/95%RH	50°C in a 95% relative humidity, created by suspension above saturated salt solution.
70°C/100%R.H.	70°C in a condensing humidity oven.
70°C/95%RH	70°C in a 95% relative humidity, created by suspension above saturated salt solution.
70°C, water immersion	70°C immersion in distilled water.
95°C, water immersion	95°C immersion in distilled water.

### 2.2.3 Flatwise Tension Testing

ASTM C 297-94 [4] was employed for flatwise tension testing of honeycomb sandwich panels. Samples of 51 mm x 51 mm cross-sectional area were loaded at 0.5mm/min and room temperature and ultimate load was recorded. A diagram of the test is shown in Figure 2.1. Double skin specimens were bonded to loading blocks for 16 hours at 80°C with FM-73 curing adhesive. Skins were prepared using the grit-blast silane treatment. Single skin specimens had the second skin bonded with FM-73, curing 16 hours at 80°C.

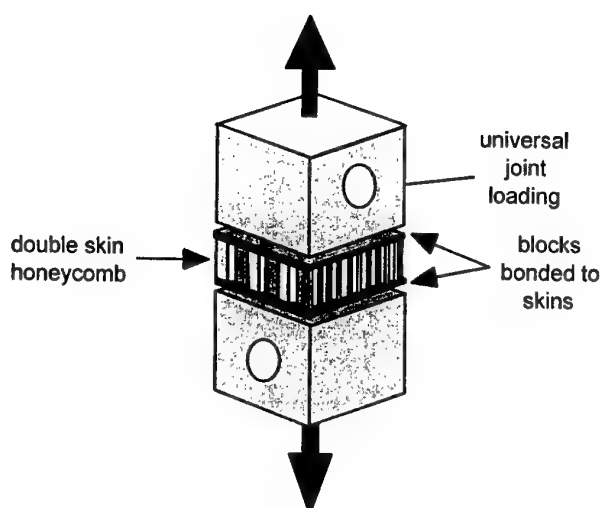


**Figure 2.1** Experimental arrangement for Flat-wise tension testing of Honeycomb sandwiches.

#### 2.2.4 Elcometer Testing

A modified version of the Flatwise tension test was employed for a second series of tests. The method described as the Elcometer test is based on ASTM D 4541-95 [5]. A diagram of the test and apparatus is shown in Figure 2.2.

The test method involves bonding a 1" diameter stub to the outer skin of the honeycomb sandwich panel with EA9309.3NA paste adhesive after pre-treating both skin and stub surfaces with the grit-blast and silane treatment. After allowing the adhesive to cure, a ring is cut out from the skin around the outer perimeter of the stub. Applying pressure to the piston, which reacts against the disk, detaches the skin from the honeycomb at a pressure equivalent to the load measured in the flatwise tension test used in section 2.2.3. Pressure applied to the piston insured 100psi was reached in 40 seconds, as specified in ASTM D 4541-95 [5]. Tests were conducted at room temperature.

#### 2.2.5 Climbing Drum Peel Testing

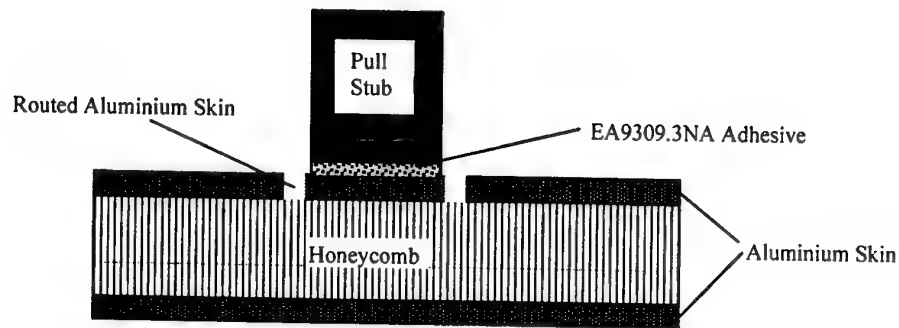
ASTM D 1781-98 [6] climbing drum peel test was employed to assess the peel resistance of adhesive bonds formed between the aluminium skin and honeycomb core material. Specimens had dimensions of 76mm x 305mm including the skin overlap for machine gripping. Average peel load values were used to determine the peel torque,  $T$  (mm.kg/mm), as specified in the standard. Specimens were tested at room temperature with a cross-head displacement of 25mm/min. The test geometry is indicated in Figure 2.3

#### 2.2.6 Testing of Flexural Properties of Honeycomb Specimens

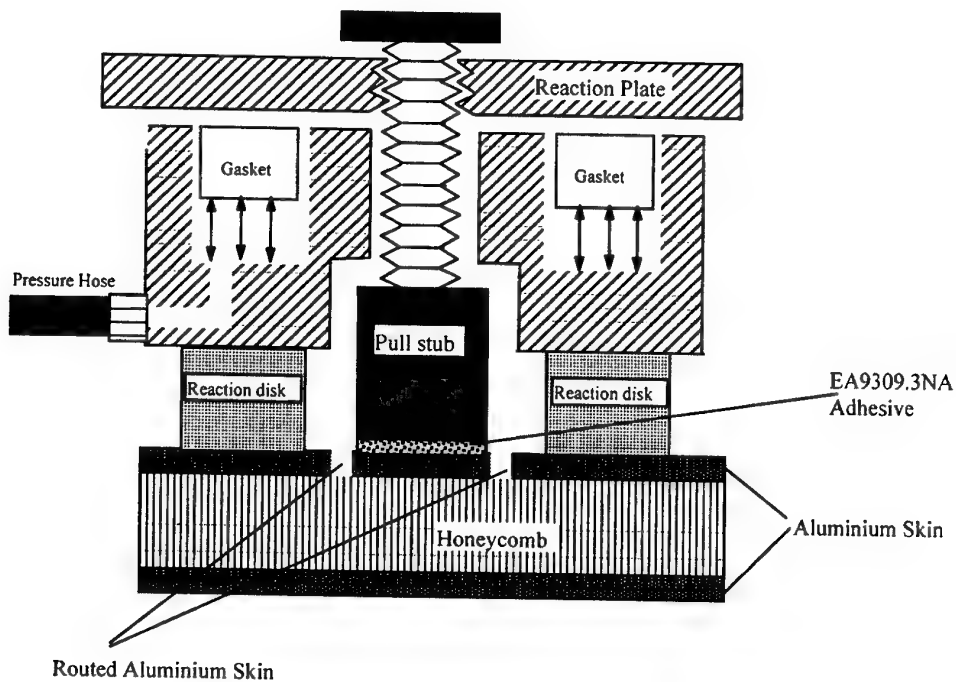
ASTM C 393-94 [7] was employed to determine the flexural stiffness properties of honeycomb sandwich panels. Specimens of dimension 51mm x 229mm were prepared and tested in 3 and 4 point bending mode. The load-span was 180mm and in the case of 4 point bending the quarter point load was 45mm. Load-deflection curves were recorded using an extensometer and cross-head displacement of 0.2mm/min.

Ultimate Load,  $P(N)$ , Core Shear Stress,  $\tau$  (MPa), Facing Bending Stress,  $\sigma$  (Mpa), Flexural Stiffness,  $D$  (N.mm<sup>2</sup>), Panel Shear Rigidity,  $U$  (N) and Core Shear Modulus,  $G$  (MPa) were determined as specified in ASTM C 393-94 [7].

Unless stated, all samples were manufactured with the ribbon direction running at a 90° angle relative to the length of the specimen. This is indicated in Figure 2.4. This honeycomb orientation enables maximum exposure of the node bonds to the environment.



Cross Section After Routing to Remove Aluminium Skin Around Bonded Pull-Stub



Cross Section Schematic of Piston Attached to Pull-Stub

**Figure 2.2** Elcometer and test arrangement.

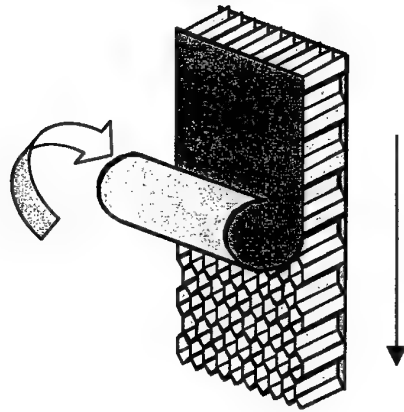


**Figure 2.3** Arrangement for peel testing of honeycomb sandwich panel.

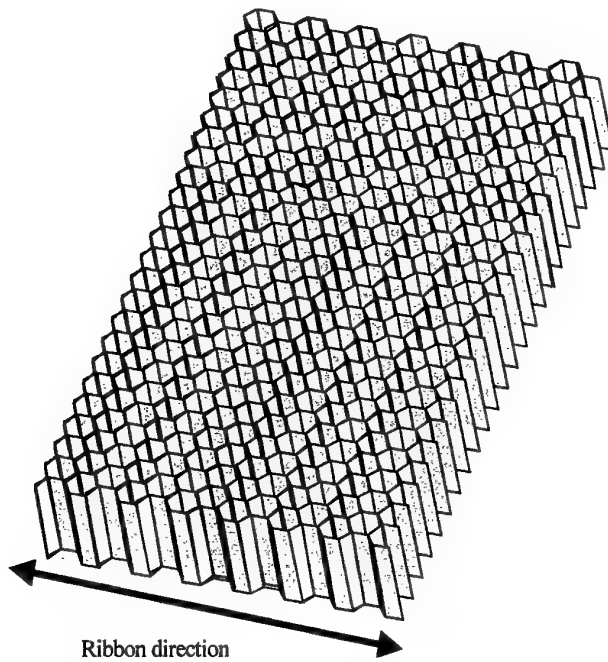


**Figure 2.4** Arrangement of honeycomb core for preparation of Beam samples

### 2.2.7 Node Bond Peel Testing

A simple method was developed to estimate honeycomb node bond peel strength. A single row of cells was peeled in an Instron as indicated in Figure 2.5, with a cross-head displacement of 25mm/min. Good reproducibility was achieved if the first cell was rejected from the measurement, which includes 5 cells, with the measurement being repeated for 5 samples. The width of the ribbon was dictated by core thickness and is specified in Table 1.

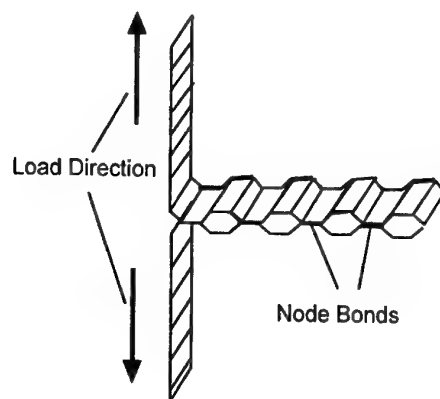


**Figure 2.5** *Schematic representation of node bond peel strength measurement*

### 2.2.8 Fracture Analysis and Surface Characterisation Studies

Surface characterisation studies employed a variety of spectroscopic techniques including Fourier-Transform Infrared Spectroscopy (FT-IR) [8], X-ray Photoelectron Spectroscopy (XPS) [9] and Auger Electron Spectroscopy (AES) [9]. Details of these techniques can be found in the references provided, however, briefly, the techniques can be used to chemically characterise the honeycomb core or honeycomb metal sandwich fracture surfaces. In the case of FT-IR, spectra revealed molecular information about the outer 1µm of the surface, whereas, XPS and AES provided elemental information from the first 5-10nm of the surface.

In a series of experiments XPS and AES spectra were recorded as a function of depth through the use of an Argon Ion Gun. Argon ions directed at the surface with 5kV potential eroded or etched the surface material at a rate of approximately 5nm/min. AES and XPS spectra recorded during the etching gave a depth profile concentration of the elemental species in the surface layers.

### 2.2.9 Honeycomb Sandwich Water Diffusion Studies

Moisture ingress into metal honeycomb sandwich panels was monitored via water mass uptake and radiographic measurements. Sandwich panels of 50mmx50mm were immersed in 70°C water and withdrawn, dried with high-pressure air and mass uptake of water was measured gravimetrically.

Radiographic images of panels immersed in 50% w/w Cerium Nitrate solution held at 70°C were taken over a 10 day period. Cerium nitrate was used as a radio opaque dye for highlighting moisture ingress paths into the honeycomb sandwich. A 225kV Balteau X-ray source was run at 50-60kV and between 12 and 36mAmin using KodakM, Fuji IX80 and AgfaD2 film. Radiographs were recorded normal and parallel to the sandwich skin and converted to digital format with a high resolution drum scanner.

## 2.2.10 Honeycomb Sandwich Panel Failure Modes

Honeycomb sandwich panels may fail in a variety of ways dependent on the weakest link in the structure. In order to provide some indication of the expected failure modes, based on previous experience[10], Figure 2.6 indicates five typically observed failure modes for metal honeycomb sandwich construction. The modes described are:

- (A) cohesive failure of the fillet adhesive, which typically represents fracture in a dry undegraded adhesive bond
- (B) skin to adhesive disbond, which indicates degradation of the interfacial bond between the adhesive and the metal skin. This is one type of adhesive failure mode.
- (C) fillet bond pull-out, which represents failure of the interfacial bond between the honeycomb core and the adhesive fillet. This is the second type of adhesive failure mode.
- (D) core node bond failure, which represents failure of the of the adhesive bond of the honeycomb core nodes. This failure may be adhesive, at the node bond adhesive and honeycomb foil interface, or cohesive, within the node bond adhesive layer.
- (E) core corrosion failure, which represents failure of the core foil material as a result of corrosion degrading the foil.

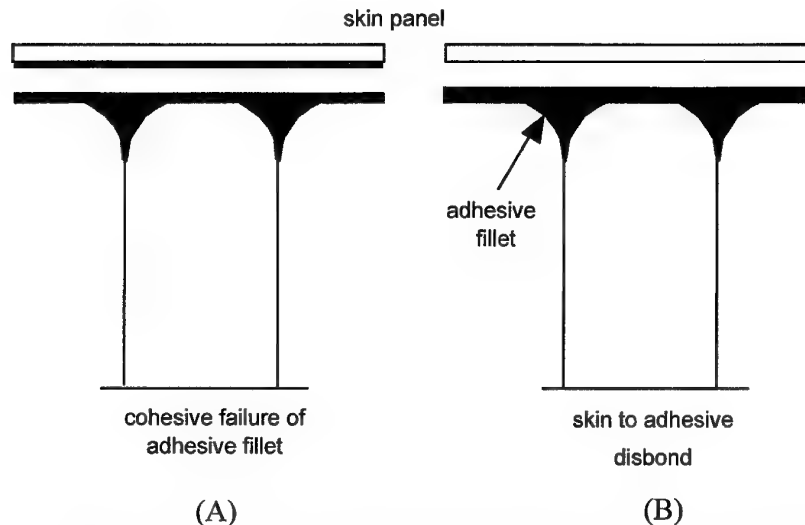


**Figure 2.6** Common failure modes observed for metal honeycomb sandwich construction.



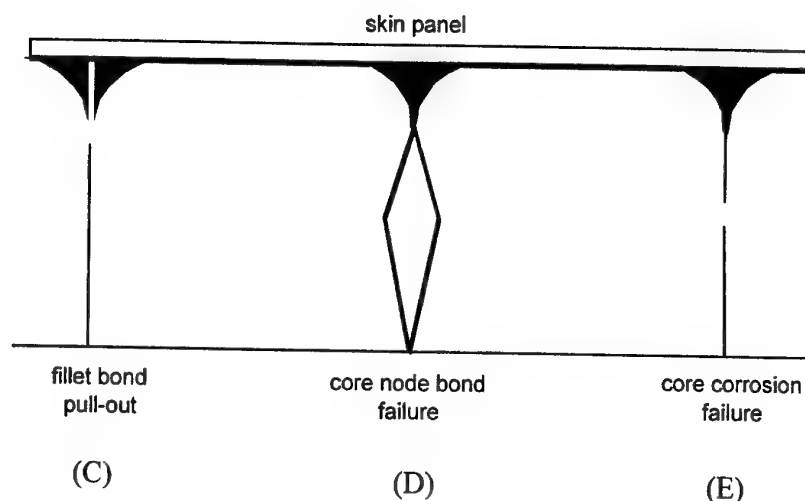


**Figure 2.6 con't.**      *Common failure modes observed for metal honeycomb sandwich construction.*

#### 2.2.11 FM-300 and FM-300-2K Water Diffusion Studies

Moisture diffusion in FM-300 and FM-300-2K was assessed by monitoring the mass uptake of a 1" diameter disk of FM-300 that had been cured at 177°C and 120°C, respectively, for 1 hour. Diffusion rates were assessed at 50°C, 70°C and 95°C in distilled water and at 70°C in a 100% relative humidity environment. Individual experiments used at least 6 disks for measuring the weight uptake of the adhesive. The rate of drying of the same adhesive disks was assessed by monitoring their weight loss as a function of drying time in a 80°C isothermal oven

### 3. Honeycomb Characterisation

#### 3.1 Hexcel CR3 Honeycomb

FT-IR analysis of the honeycomb indicated that the node bond adhesive was a nitrile rubber (acrylonitrile butadiene) modified phenolic. The scanning electron microscopy (SEM) data showed that the node bond adhesive was discontinuous in places and covered approximately 72% of the coated area in samples investigated. This offers potential paths for moisture ingress. Images of the node bond adhesive are shown in Figure 3.1 and 3.2. Figure 3.2 indicates the node bond adhesive appears to be nodular in shape. Cross-sectional SEM measurements indicated that the node bond adhesive was 3.5µm thick.

XPS Depth profile analysis of the coating in Figure 3.3 indicates a chromium rich layer. FT-IR analysis failed to detect any significant evidence of organic species on the honeycomb surface, suggesting the coating is predominantly inorganic in nature. This is consistent with the XPS data which showed a rapid drop in the carbon level after only a short period of etching. Microscopic analysis from SF (the Swiss Aircraft and Systems Company) [11], indicated that a

thin topcoat was evident on the CR3 coating with a thickness of  $0.05\mu\text{m}$  to  $0.2\mu\text{m}$ . The chromium coating was reported to have a thickness of  $0.2\mu\text{m}$  to  $0.9\mu\text{m}$ .

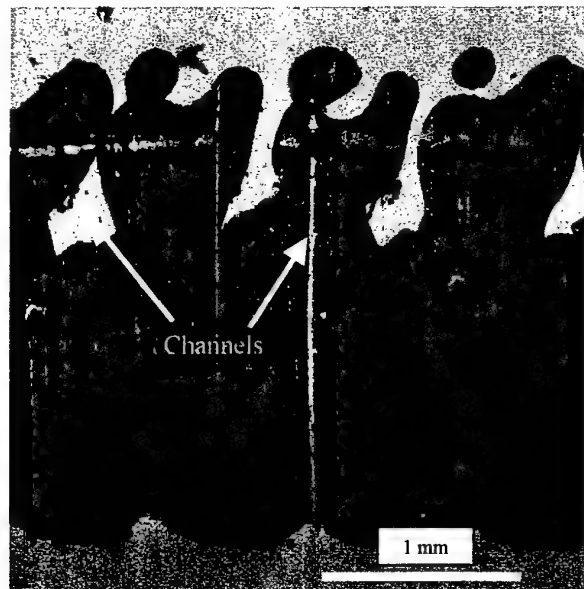


**Figure 3.1** *Backscattered image of Hexcel CR3 3/16" honeycomb node bond area. Black areas indicate adhesive.*

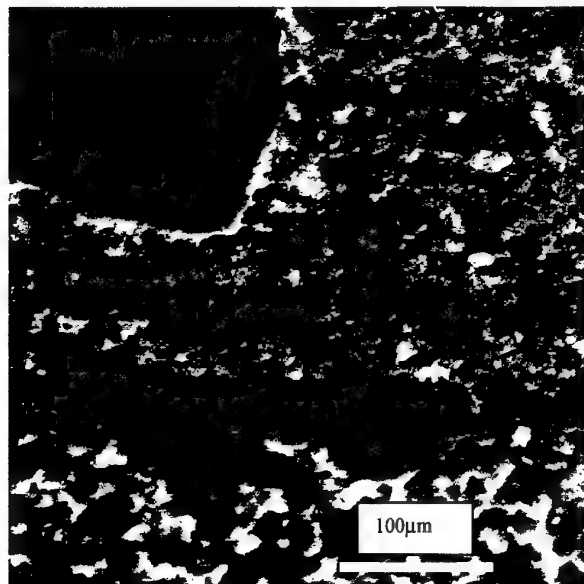


**Figure 3.2** *Hexcel CR III 3/16" honeycomb node bond area enlarged*

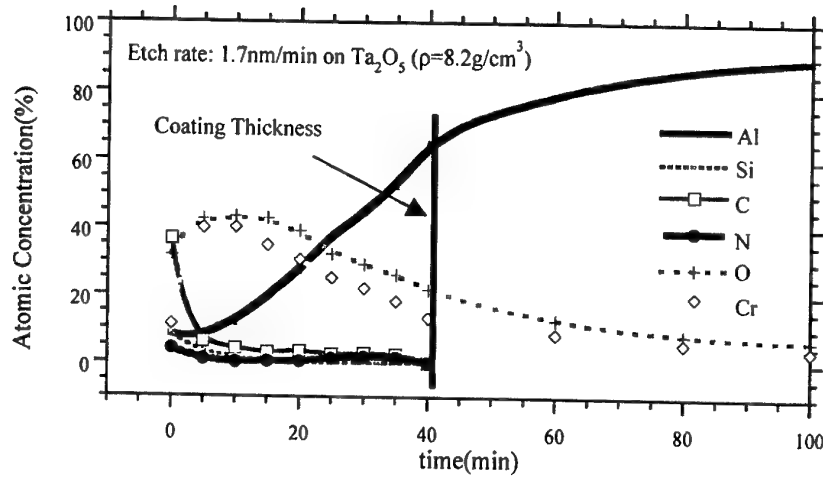


**Figure 3.3** XPS Depth Profile analysis of Hexcel CR3 honeycomb coating.

### 3.2 Alcore Dura-Core Honeycomb

FT-IR analysis of the honeycomb indicated that the node bond adhesive was a polyamide. The SEM data showed that the node bond adhesive was also discontinuous for the samples investigated. Figure 3.4 indicates the discontinuous nature of the honeycomb node bond adhesive. This offers more potential paths for moisture ingress in comparison with the Hexcel CR3 honeycomb, refer Figure 3.1.

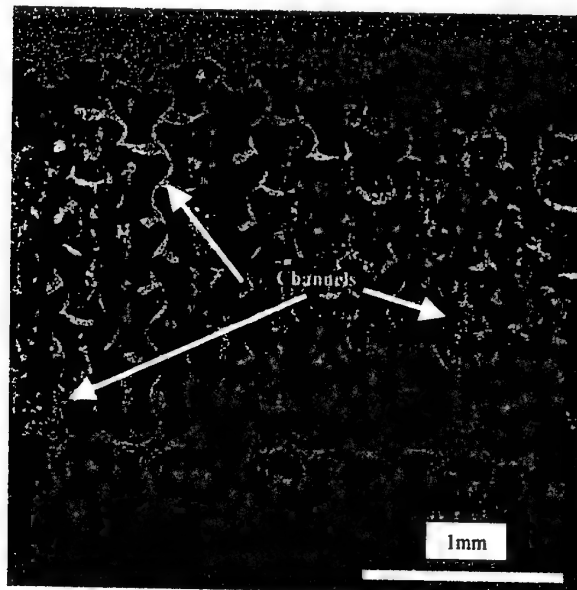


**Figure 3.4** Backscattered image of Alcore Dura-Core 3/16" honeycomb node bond area. Black areas indicate adhesive.

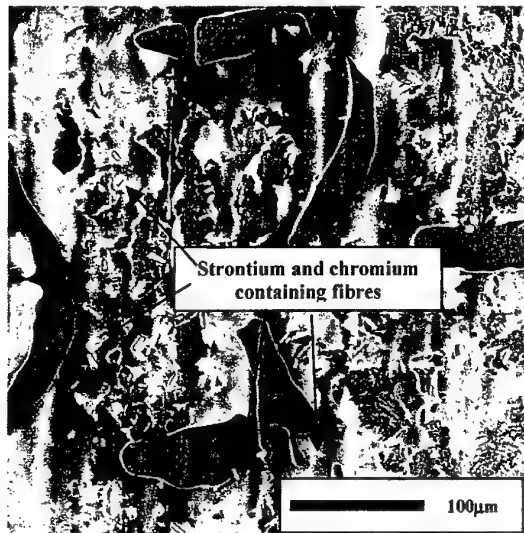


**Figure 3.5** Alcore Dura-Core 3/16" honeycomb node bond area enlarged

The node bond adhesive was 3.0µm thick and contained fibres of 10µm x 2µm diameter which consisted of strontium, chromium, carbon, oxygen and silicon, as indicated in Figure 3.5

XPS analysis indicated a chromium rich outer layer. A depth profile of the honeycomb coating is shown in Figure 3.6. As with the Hexcel CR3 honeycomb, FT-IR failed to detect any organic species on the honeycomb surface. The depth profile data in Figure 3.6 is consistent with the FT-IR analysis. The carbon concentration drops very quickly, and is initially at a low level typical of adventitious contaminant species from the atmosphere, suggesting that the outer surface is only chromium oxide. Binding energy data for the chromium and oxygen species possibly indicate the film is  $\text{CrO}_2$ . The etch rate is about 100nm/hour on  $\text{Ta}_2\text{O}_5$ , with a density of 8.2g/cm<sup>3</sup>. Chromium oxide has a density ranging from 2.7 to 5.2g/cm<sup>3</sup>, depending on the oxidation state. Based on this approximate calibration, the chromium layer would be expected to be between 50nm and 120nm.

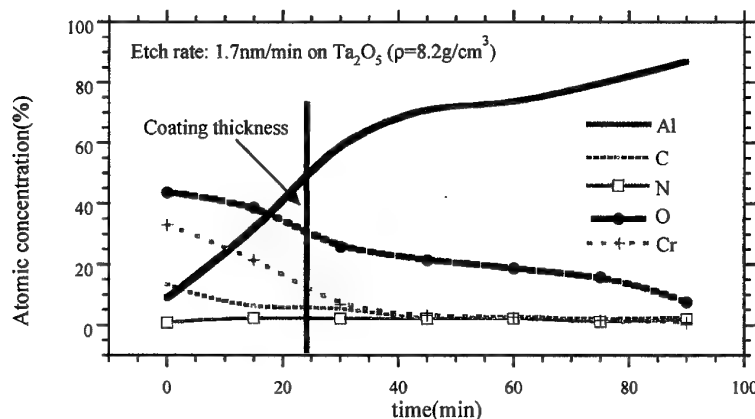


**Figure 3.6** XPS depth profile of Alcore Dura-Core Honeycomb coating.

### 3.3 Hexcel PAA Honeycomb

Analysis of the Hexcel phosphoric acid anodised (PAA) honeycomb core by SF [11] indicates the anodic oxide is about  $0.14\mu\text{m}$  thick, with a top coat that is about  $0.28\mu\text{m}$  thick. The top-coat is substantially thicker than that reported for the Hexcel CR3 product.

### 3.4 Alcore 5056 PAA Honeycomb

FT-IR analysis of the surface layer of the Alcore PAA honeycomb indicated that a coating which was similar to the node bond adhesive existed, ie. polyamide. However, the polyamide on the honeycomb surface had a higher concentration of either phenolic or epoxy species. Infrared analysis suggested a thick topcoat exists on the honeycomb surface and was consistent with the SF analysis of the Hexcel PAA product [11].

XPS depth profile analysis, shown in Figure 3.7 suggests a thick organic coating exists on the surface of the honeycomb metal. The carbon and nitrogen levels are consistent with the FT-IR analysis. The depth calibration would suggest that the coating is thicker than  $500\text{nm}$ . Given the calibration was performed on  $\text{Ta}_2\text{O}_5$ , which has a density of  $8.3\text{g}/\text{cm}^3$ , and most organic coatings have a density of  $1\text{g}/\text{cm}^3$ , the thickness is more likely to be several microns.

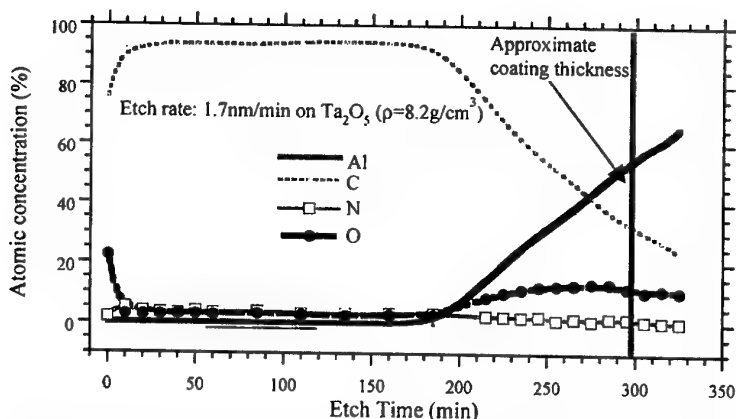


**Figure 3.7** XPS depth profile analysis of Alcore 5056 PAA honeycomb coating.

## 4. Results

### 4.1 Flatwise Tension Testing

#### 4.1.1 FM-300, Hexcel CR3 Honeycomb, Strength versus Adhesion Area

Figure 4.1.1 indicates the flatwise tension (FWT) strength as a function of bonded area. The area percentage of one skin bonded to the honeycomb core was reduced by increasing the width of teflon tape around the perimeter of the bonded sandwich sample. The data indicates a linear response in FWT strength as a function of adhesion area.

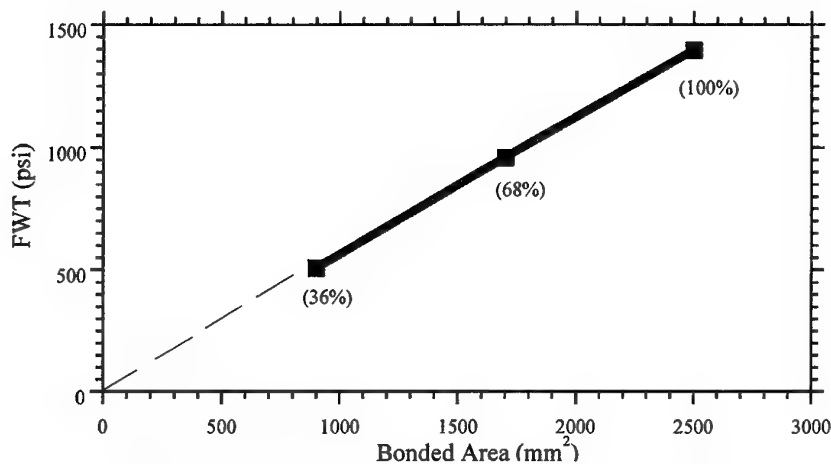


**Figure 4.1.1** Flatwise tension Strength as a Function of Adhesion Area

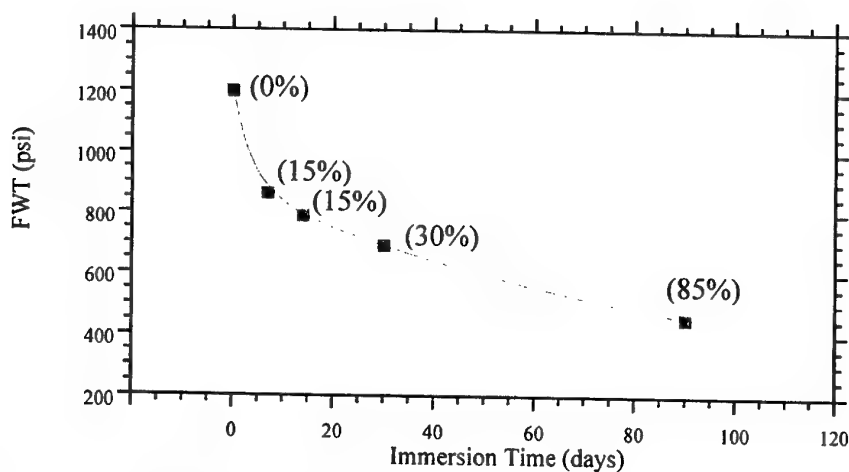
#### 4.1.2 FM-300, Hexcel CR3 Honeycomb, 95°C humid exposure

Figure 4.1.2 indicates that the FWT strength degrades to a value approaching 400psi for Hexcel CR3 honeycomb immersed in 95°C water. The FWT blocks were bonded to the honeycomb sandwich skins with FM-73 at 80°C for 16 hours. The percentage values in brackets provide an indication of adhesional failure area i.e. failure percentage that has occurred between the adhesive and honeycomb layer. The area of adhesion failure of 85% occurs for a FWT value of about 500psi, which only represents a 60% reduction in FWT strength.

Figure 4.1.3 indicates the FWT strength of single sided (only one skin bonded) Hexcel CR3 sandwich samples immersed in 95°C water. The samples were tested after bonding a second skin to the side of exposed honeycomb core, after removal from the water. The second skin and blocks were bonded with FM-73 for 16 hours at 80°C. The data suggests an inconsistent response to the conditioning environment, in contrast to that observed in Figure 4.1.2. The adhesional failure percentages are consistent with the values reported in Figure 4.1.2 and show a relationship between the FWT strength and adhesional failure area.

#### 4.1.3 Dry Recovery Experiments for FM-300 and Hexcel CR3 Honeycomb.

The inconsistent trend in data reported in Figure 4.1.3, suggested that some recovery of the FWT strength may have been occurring as a result of the procedure employed to bond the second skin to the conditioned honeycomb sample. A number of core drying experiments were carried out in a vacuum oven at a pressure of 100mTorr (Torr=1mmHg) and 90°C. Single sided samples which were immersed in 95°C water for 7 days were dried for 2 weeks prior to testing. All strength values were between 1100 and 1400psi, compared with values between 1400 and 1600 psi for the control samples. Notably, failure occurred cohesively within the fillet adhesive, suggesting that the drying procedure could recover the strength of adhesive bonds between the honeycomb core and the adhesive, but that some irreversible plasticisation\* of the resin had occurred, reducing the mechanical strength by approximately 20%. A similar experiment was performed on the double skinned samples immersed in 95°C water, producing a similar recovery strength. Whilst the experiments indicate recovery through drying is possible, shorter drying periods should be examined to assess the period required to achieve maximum recovery of FWT strength. Work in this area has been reported in other AMRL research [12].



**Figure 4.1.2** *FWT strength as a function of immersion time in 95°C water for Hexcel CR3 honeycomb. Sandwich sample was immersed in water with both skins bonded.*

\* Adhesive plasticisation describes a process in which water absorption effectively reduces the dry glass transition temperature,  $T_g$ , of the adhesive making it more flexible or rubbery. This may occur as a result of hydrolysis of the cross-linked polymer units or water absorption altering chain interactions in the adhesive. The former will be irreversible and the latter reversible.

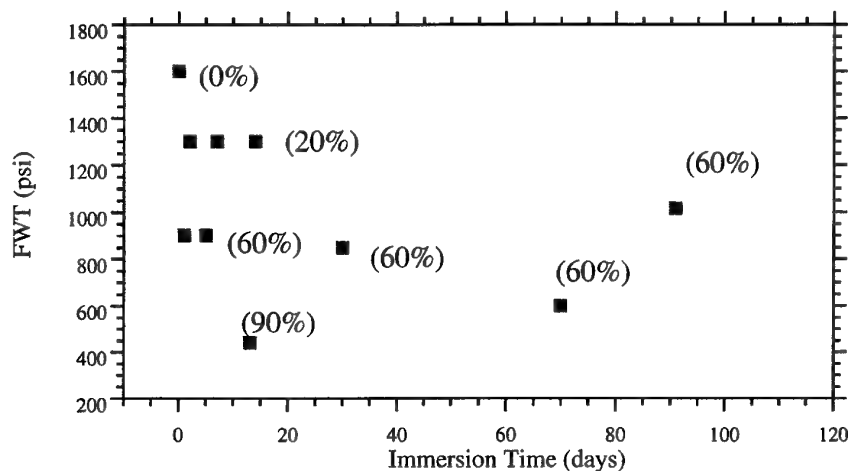


**Figure 4.1.3** FWT strength as a function of immersion time in 95°C water for Hexcel CR3 honeycomb. Sandwich sample was immersed in water with only one skin bonded.

#### 4.1.4 FM-300, Hexcel CR3 and Alcore Honeycomb, 95°C humid exposure

Figure 4.1.4 indicates the trend in FWT strength for the Hexcel honeycomb in comparison with three types of Alcore honeycomb product for double skinned samples. Surprisingly, the Alcore 5056 untreated honeycomb offers similar durability at extended exposure to the Alcore 5052 PAA treated honeycomb. The Alcore 5056 PAA and Hexcel CR3 offer similar durability, with both being considerably worse than the Alcore 5056 untreated and 5052 PAA honeycomb samples. The approximate area of adhesion failure is indicated by percentage values in brackets at the three month exposure time for comparison. The adhesion failure percentages correlate with the FWT values obtained in Figures 4.2 and 4.3 for the Hexcel samples.

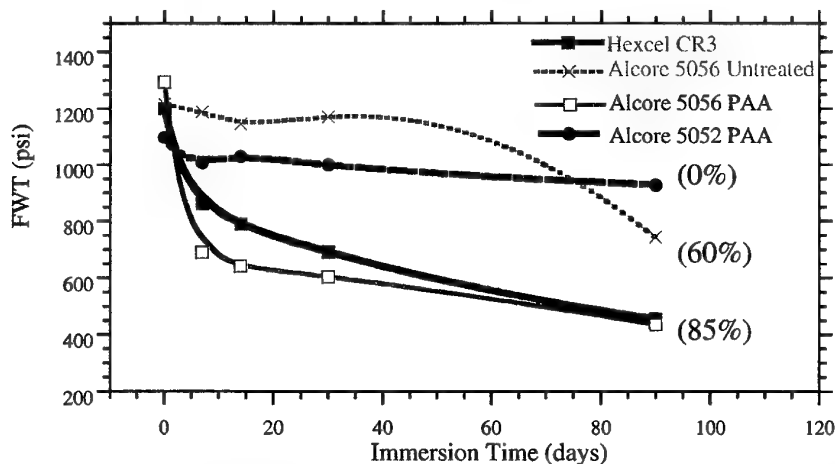


**Figure 4.1.4** FWT strength as a function of immersion time in 95°C water for double skinned Alcore and Hexcel honeycomb sandwiches bonded with FM-300.



#### 4.1.5 FM-300 Hexcel CR3 and Alcore Honeycomb, 50°C and 70°C humid exposure

Figure 4.1.5 indicates the effect of exposure of Hexcel CR3 bonded metal skin sandwiches to 50°C and 70°C environments of 95% relative humidity. Single skin samples were exposed to the humid environments and the second skin bonded at 80°C for 16 hours with FM-73 adhesive. The data indicates very minimal reduction in FWT strength. Some failures occurred in the second skin bonded with FM-73 after conditioning. This failure mode also suggests a minimal reduction in FWT strength of the fillet bond. All other failure modes were cohesive failure of the fillet bond adhesive. The data suggests that the environment has no effect on the strength of the honeycomb sandwich specimens. Once again, there is a possibility that the procedure used to bond the second skin, after exposure to the conditioning environment, may have resulted in some drying of the sandwich specimen and therefore some recovery of bond strength.

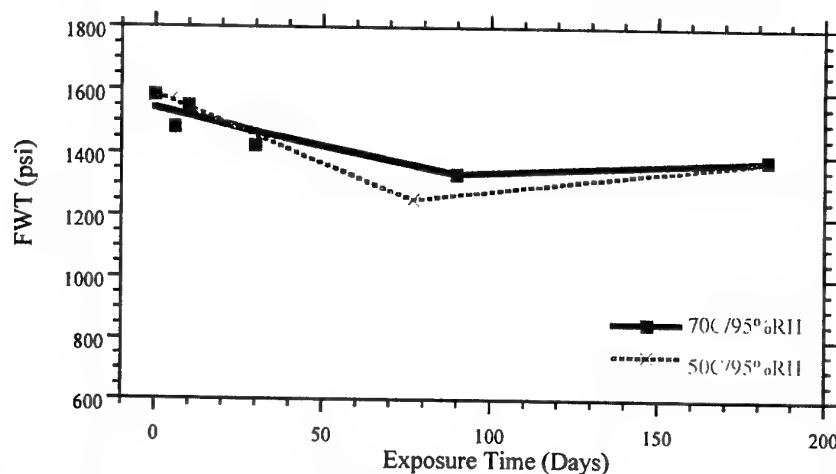
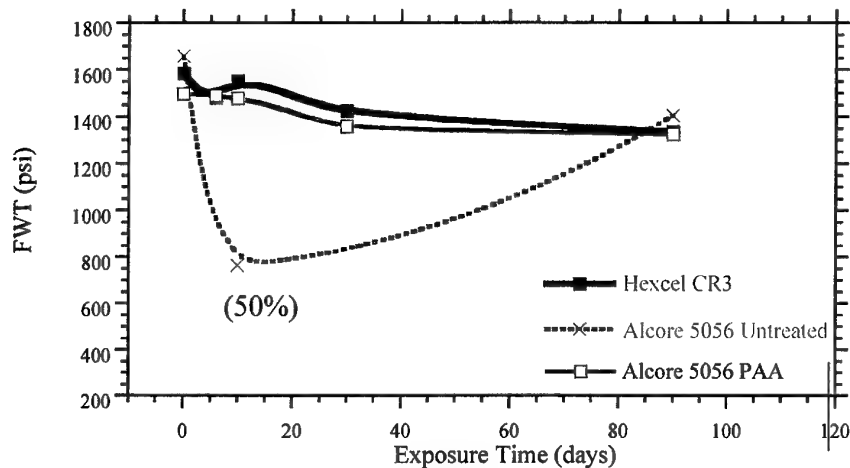


**Figure 4.1.5** Effect of 50°C and 70°C exposure at 95% relative humidity (R. H. ) on FWT strength of Hexcel CR3 honeycomb-metal sandwiches bonded with FM-300.

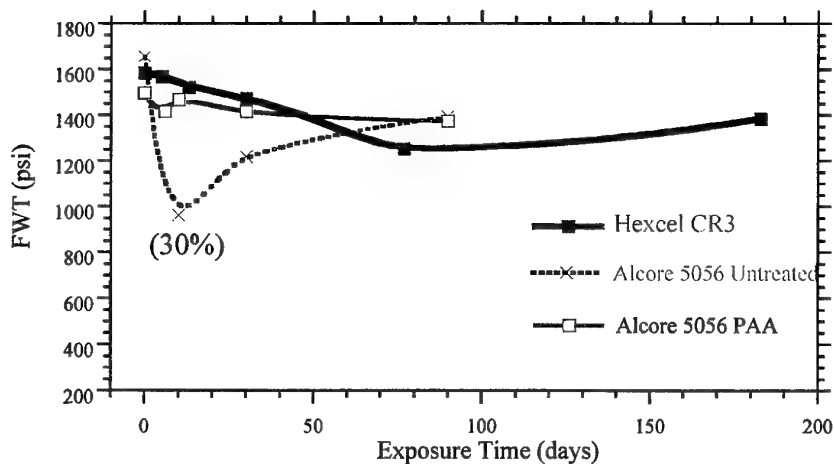
Figure 4.1.6 provides a comparison of the Hexcel CR3 metal skin sandwiches bonded with FM-300 with the 5056 untreated and 5056 PAA Alcore honeycomb samples. Exposure was at 70°C and 95% R.H. The data is different from the 95°C exposure in that the untreated Alcore sample provides worse durability than the Hexcel CR3 or Alcore 5056 PAA samples. In the 95°C immersion case the reverse trend was observed. The only example of adhesional failure was observed for the Alcore untreated sample exposed for 10 days, as indicated in brackets.

Figure 4.1.7 indicates the response of FWT strength for the Hexcel CR3 samples exposed to 50°C and 95% R. H., in comparison with the Alcore 5056 untreated and PAA honeycomb samples. The data is similar to the 70°C case shown in Figure 4.6, with the untreated honeycomb showing a reduction in strength at about 10 days exposure, however, the reduction in strength is not as marked as in the 70°C case. The adhesional failure is approximately 30% at the 10 day exposure for the untreated honeycomb sample, as indicated in brackets. Apart from the untreated honeycomb samples, the data indicates insensitivity to the 50°C humid environment, as in the 70°C case. Once again, the scatter associated with the data shown in Figure 4.1.3 may also be affecting the durability response, with post conditioning bonding of the second skin drying the specimen and recovering the majority of dry strength. The recovery of

FWT strength for the untreated samples after the 10 day exposure period for both conditioning environments is unexpected and suggests that some physical changes of the fillet bond adhesion may be occurring.



**Figure 4.1.6** The relative effect of 70°C/95% R. H. environment on Hexcel CR3 and Alcore PAA and untreated honeycomb-FM-300 single metal skin honeycomb sandwiches.



**Figure 4.1.7** The relative effect of 50°C/95% R. H. environment on Hexcel CR3 and Alcore 5056 PAA and untreated honeycomb/FM-300 single metal skin honeycomb sandwiches.

## 4.2 Pull-Off Tension (Elcometer) results

Single skin experiments conducted in section 4.1, in which the honeycomb sample was exposed to the conditioning environment prior to bonding a second skin with FM-73 at 80°C for 16 hours, suggested that some drying of the samples was occurring and that a partial recovery in flat-wise tension (FWT) strength may have resulted. In order to examine the possible effect of moisture ingress on the FWT strength an Elcometer test was employed, as described in section 2.2.4. The benefit of this test is that a second skin may be bonded with paste adhesive at room temperature to the pre-conditioned sample prior to testing the pull-off strength, without the problem of the second skin failing during the test, as was occurring on a regular basis for the FWT experiments. Whilst bonding the second skin with the FM-73 adhesive at 80°C for 16 hours produced a strong bond, the process may also have resulted in sample drying. Additionally, the Elcometer test can be adapted for use in field measurements of panel strength due to its portability and results from these experiments will provide essential reference data for in-situ applications such as the F-111 Teardown task.

### 4.2.1 FM-300 and FM-300-2K, Hexcel CR3 Honeycomb, 95°C humid exposure

Figure 4.2.1 indicates the decrease in pull-off tension for Hexcel CR3 honeycomb bonded to FM-300 and FM-300-2K adhesive as a function of immersion time in 95°C water. In contrast with the single skin experiments shown for the FWT work in Figure 4.1.3, the data indicates a rapid loss in strength after only one day of immersion for the FM-300 sample. The value after 1 day, which is approximately 400 psi, remains at about this level for extended exposure times. The failure was predominantly fillet bond pull-out. The rate of degradation for the FM-300-2K sample is slower in comparison with the FM-300 sample and the plateau value at extended exposure time is also higher. This suggests the FM-300-2K and Hexcel CR3 bond is more durable than the Hexcel CR3 and FM-300 bond.

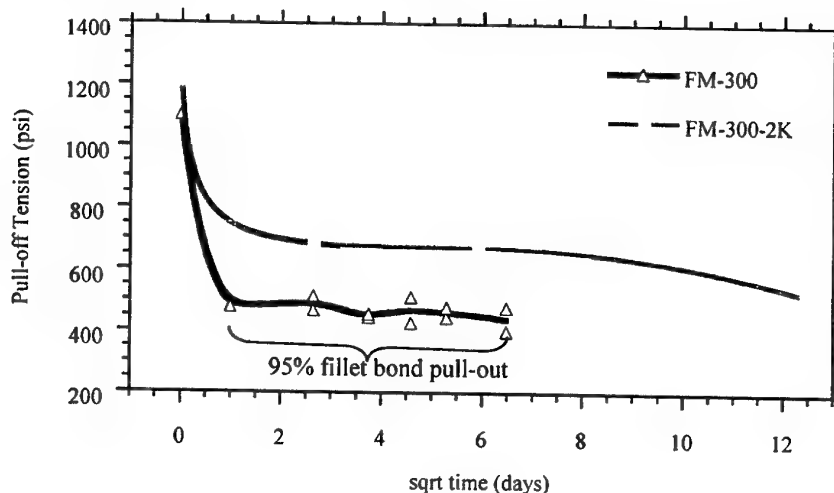


**Figure 4.2.1** Pull-off tension as a function of immersion in 95°C water for Hexcel CR3 honeycomb bonded to FM-300 and FM-300-2K.

#### 4.2.2 FM-300, Hexcel CR3 and Alcore Honeycomb, 70°C humid exposure

Figures 4.2.2 and 4.2.3 compare Hexcel and Alcore Honeycomb sandwich samples bonded with FM-300 and exposed to 70°C humid environments.

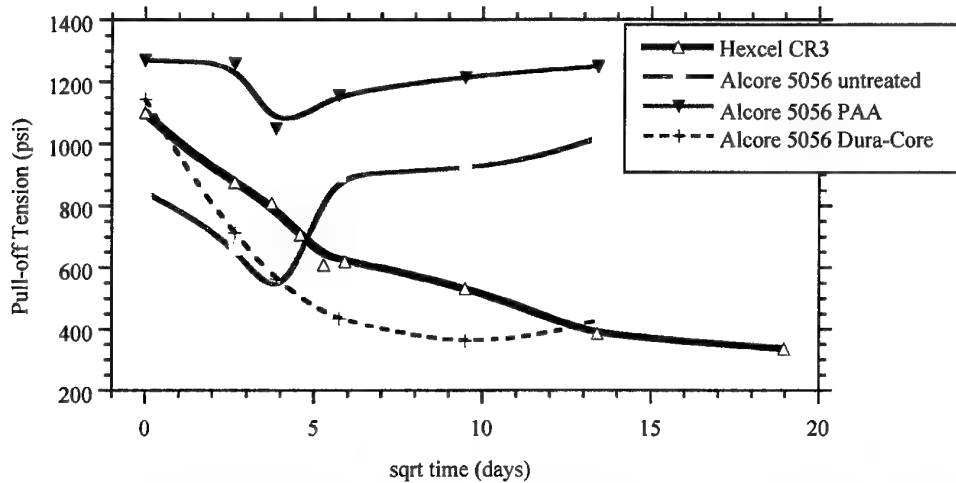


**Figure 4.2.2** Pull-off tension as a function of immersion in 70°C water for Hexcel CR3, Alcore 5056 untreated, Dura-Core and PAA honeycomb bonded to FM-300.

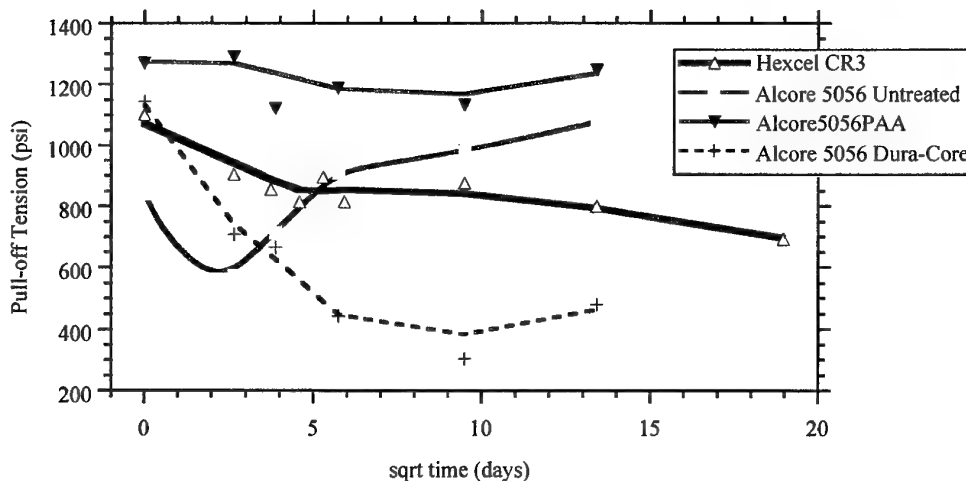


**Figure 4.2.3** Pull-off tension as a function of exposure to 70°C/100% R.H. for Hexcel CR3, Alcore 5056 untreated, Dura-Core and PAA honeycomb bonded to FM-300.

The data in Figures 4.2.2 and 4.2.3 indicate the same general trend in the reduction in pull-off tension for the different honeycomb samples. The 70°C/100% R.H. environment, however, does not degrade the bond strength at the same rate as in the water immersion conditioning case. The data suggests the Alcore 5056 PAA honeycomb offers the best durability, with the Alcore Dura-

Core honeycomb providing the worst results. The Elcometer results show a similar trend in the pull-off tension for the Alcore 5056 untreated honeycomb, as was observed in the flat-wise tension testing, refer Figure 4.1.6. The unusual result sees the initial degradation in pull-off tension strength for the untreated honeycomb sample, at about 10 days, recover to a value similar or slightly better than the dry strength value after 30 days. The reproducibility of this result suggests that some physical change is occurring to the untreated honeycomb sample as a result of the conditioning environment. Given this is not observed for the other treatments, it suggests that the change may be caused by the fillet bond adhesion ie. some change occurring between the physical nature of the adhesive to honeycomb bond due to the presence of moisture.

#### 4.2.3 FM-300, Hexcel CR3 Honeycomb, Double versus Single Skin Exposure

Figure 4.2.4 indicates the response of FM-300 and Hexcel CR3 honeycomb samples to 70°C humid environment. The double skin samples indicate similar insensitivity to either full immersion or high humidity. The single skin samples, in which water has direct access to the honeycomb and fillet bonds, indicate a greater reduction in pull-off tension, with the full immersion environment being notably harsher.

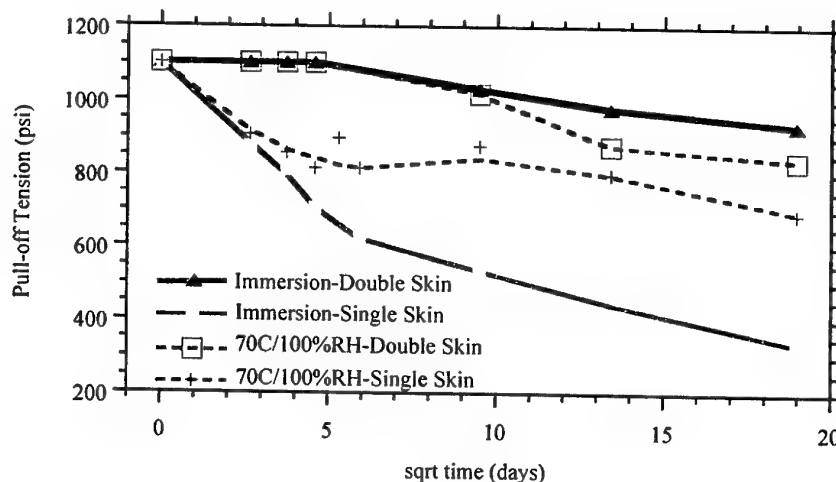


**Figure 4.2.4** Change in pull-off tension strength for Hexcel CR3 honeycomb and FM-300 panels exposed to a 70°C humid environment. Double and Single skin exposure data indicated.

#### 4.2.4 FM-300-2K, Hexcel CR3 and Alcore Honeycomb, 70°C humid exposure

Figures 4.2.5 and 4.2.6 both indicate the change in pull-off tension for Alcore and Hexcel honeycomb panels bonded with FM-300-2K adhesive. The two figures show different response, dependent on the exposure environment. The immersion in 70°C water results in a more rapid strength degradation for the Hexcel honeycomb samples, but similar response in both environments was observed for the Alcore Dura-Core sample. In both environments the Hexcel CR3 honeycomb produced the best durability and the Alcore Dura-Core sample the worst. The interesting change in durability for the untreated Alcore sample that has occurred in these experiments also indicates that the untreated honeycomb sample's initial strength reduces and

recovers at intermediate exposure times for the immersion environment, before deteriorating again at the extended exposure time. In the humid environment, the poor initial strength of the untreated honeycomb sample actually increases as a function of exposure time.

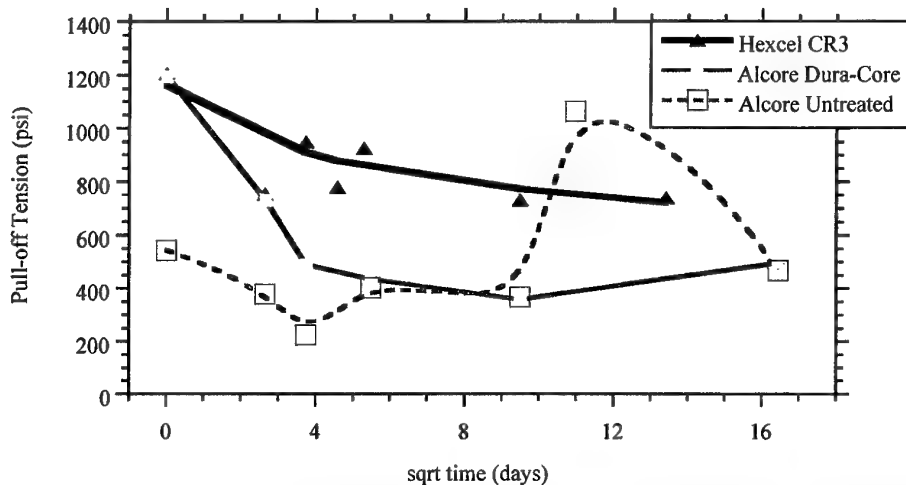


**Figure 4.2.5** Hexcel and Alcore honeycomb bonded to FM-300-2K adhesive and immersed in 70°C water. Pull-off tension as a function of immersion time is indicated.

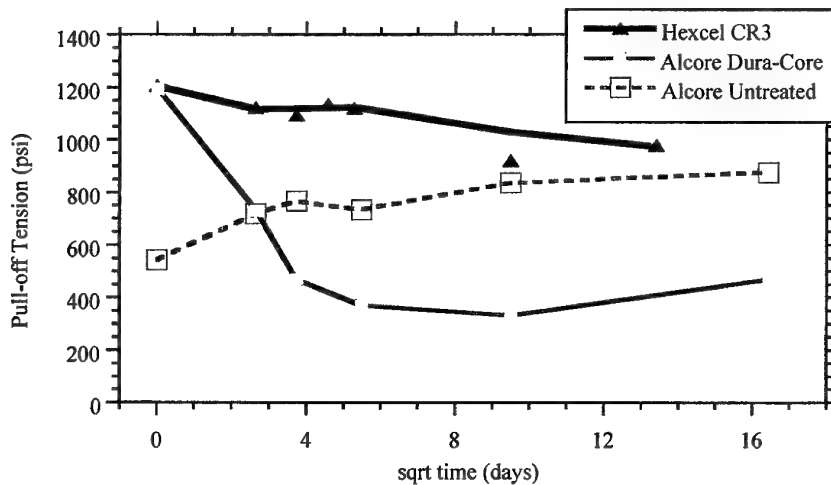


**Figure 4.2.6** Hexcel and Alcore honeycomb bonded to FM-300-2K adhesive and exposed to 70°C/100% R.H. Pull-off tension as a function of immersion time is indicated.

#### 4.2.5 Adhesional Failure as a Function of Pull-Off Tension

The percentage of adhesional failure was plotted as a function of the measured pull-off tension for all the samples tested in section 4.2, and is indicated in Figure 4.2.7. In all cases adhesional failure was associated with fillet bond pull-out. The plot suggests a linear relationship exists for the samples examined, as expected from the relationship established in section 4.1.1. for the

flatwise tension work. A 100% adhesion failure area occurs at approximately 200 psi and 100% cohesive failure area occurs for values of approximately 1000 psi or greater. This data is consistent with the flatwise tension work performed for the Hexcel CR3 honeycomb samples immersed in 95°C water, refer Figure 4.1.2. The data in Figure 4.2.6 also suggests that some flatwise tension strength is still retained in the honeycomb sandwich even at the stage when 100% adhesion failure area occurs. The large scatter in data of the fully cohesive failure mode is indicative of brittle fracture which is unstable and leads to variation in the measured strength.

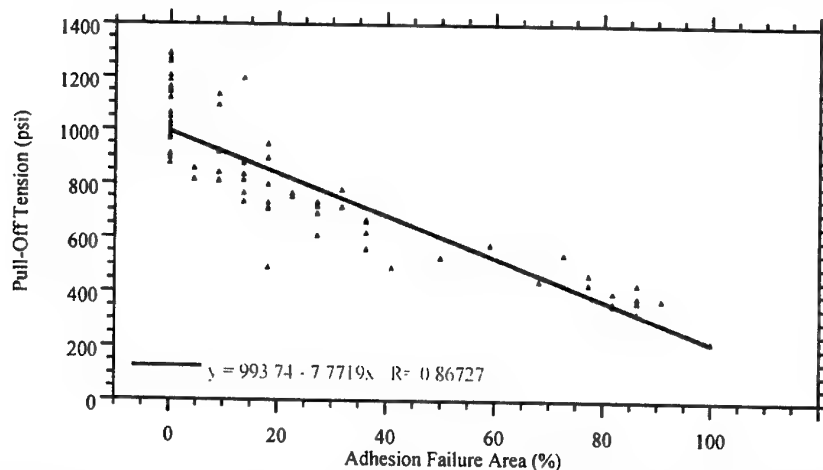


**Figure 4.2.7** Percentage Adhesional Failure as a function of Pull-Off tension (psi) for Honeycomb samples tested in section 4.2 using the Elcometer method.

### 4.3 Peel Results

#### 4.3.1 FM-300, Hexcel CR3 and Alcore Honeycomb, 70°C and 95°C humid exposure

Figure 4.3.1 indicates the peel torque values measured as a function of exposure to a 70°C/100% R.H. environment for Hexcel CR3 and Alcore honeycomb samples bonded with FM-300. The trend in data is similar to that observed in Figure 4.2.3 for the pull-off tension values measured using the Elcometer test. The peel data, however, suggests the environment more rapidly degrades the peel torque than the pull-off tension. The difference in the relative performance of the Alcore Dura-Core and Hexcel CR3 samples is less marked than for the pull-off tension data, with both samples showing a rapid decrease in dry strength values. The Alcore PAA sample shows excellent durability with a slight initial increase in the measured dry strength value. The reason for this increase is unclear. The untreated Alcore sample once again shows the unusual characteristic of re-establishing peel torque values that are similar to the control values at extended exposure times, after a significant drop after 1 week of conditioning. Decreases in peel torque for the Hexcel CR3 and Alcore Dura-Core and Untreated honeycomb samples exhibited increased percentages of fillet bond pull-out.

A double skinned Hexcel CR3 sample was also immersed in 95°C water to provide a base line comparison with the 95°C work performed in sections 4.1 and 4.2. The value of peel torque after 6 months of immersion is indicated in Figure 4.3.1 by the symbol "O". The 6 month value in 95°C water appears to correspond with a plateau value of about 1.5mm.kg/mm of peel torque

measured at extended exposure for the Hexcel CR3 70°C/100%R.H. exposure sample. This value would appear to represent the minimum value expected for 100% fillet-bond pull-out. The other point of interest is the mixed failure modes observed for the 6 month conditioned Alcore untreated and PAA samples. Both these samples show a small decrease in their maximum peel strength values. The untreated sample exhibited more than 50% failure at the skin to adhesive interface, whereas the PAA sample indicated almost 10% skin to adhesive failure near the end of the sample, where both skin edges are directly exposed to the environment.

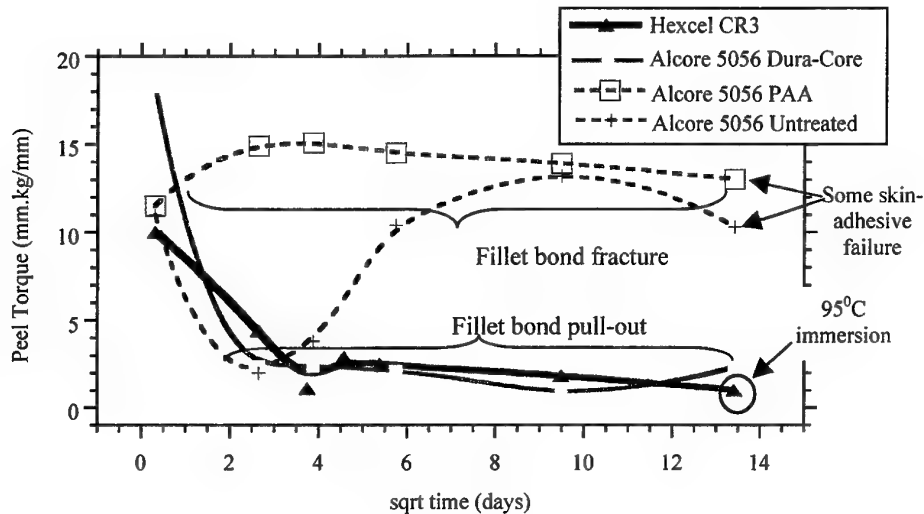


**Figure 4.3.1** Peel torque values measured as a function of exposure to a 70°C/100%R.H. environment for Hexcel and Alcore honeycomb samples bonded with FM-300.

#### 4.3.2 FM-300-2K, Hexcel CR3 and Alcore Honeycomb, 70°C humid exposure

Figure 4.3.2 indicates the peel torque for Alcore and Hexcel honeycomb bonded with FM-300-2K and exposed to a 70°C/100%R.H. environment. The Hexcel CR3 honeycomb indicates significantly improved durability for the FM-300-2K samples relative to the FM-300 samples. After 90 days exposure, the peel torque for the Hexcel CR3 sample has only dropped to about 6 mm.kg/mm, refer Figure 4.3.2, in comparison with a value around 2mmkg/mm for the equivalently conditioned FM-300 sample, refer Figure 4.3.1. After 6 months conditioning, the Hexcel CR3 sample indicates a value that approaches the plateau value observed in Figure 4.3.2. Notably, the failure mode for the Hexcel CR3 and FM-300-2K sample for the 6 month exposure was at the skin to adhesive interface compared to fillet bond pull-out for the FM-300 sample. In the FM-300-2K and Hexcel CR3 case degradation in peel torque corresponds with an increase in the skin to adhesive interfacial failure area. The Alcore Dura-Core sample indicates similar peel torque values as a function of humid exposure for both adhesive systems shown in Figures 4.3.1 and 4.3.2.

The trend in peel torque for the Alcore untreated honeycomb bonded with FM-300-2K, Figure 4.3.2, is very inconsistent in comparison with the Alcore untreated honeycomb samples bonded with FM-300, Figure 4.3.1. The greatest scatter in the data occurs at three weeks exposure time,



which is similar to the time observed for the significant increase in peel torque observed for the untreated honeycomb sample bonded with FM-300. The initial peel torque value for the FM-300-2K and untreated honeycomb sample for zero exposure time is also noticeably lower than in the equivalent FM-300 sample, refer Figure 4.3.1. The reduction in dry strength value for the untreated honeycomb and FM-300-2K sample may suggest that surface contamination effects are present. Contaminant present between the adhesive and honeycomb surface will affect bonding and possibly influence the processes occurring at the interface when water migrates to this region during the high humidity exposure [13]. The 3 and 6 months conditioned sample indicated a large percentage of skin-adhesive interfacial failure, as observed with the Hexcel CR3 sample.

The failure modes observed for the FM-300-2K and FM-300 samples indicates subtle differences in the nature of the bonds formed between the aluminium skin and the different honeycomb surfaces and the FM-300 and FM-300-2K adhesives. Interestingly, despite the different modes of failure for the Hexcel CR3 and FM-300-2K and FM-300 adhesive samples, the peel torque for both samples was similar for the 100% adhesive failure area condition.

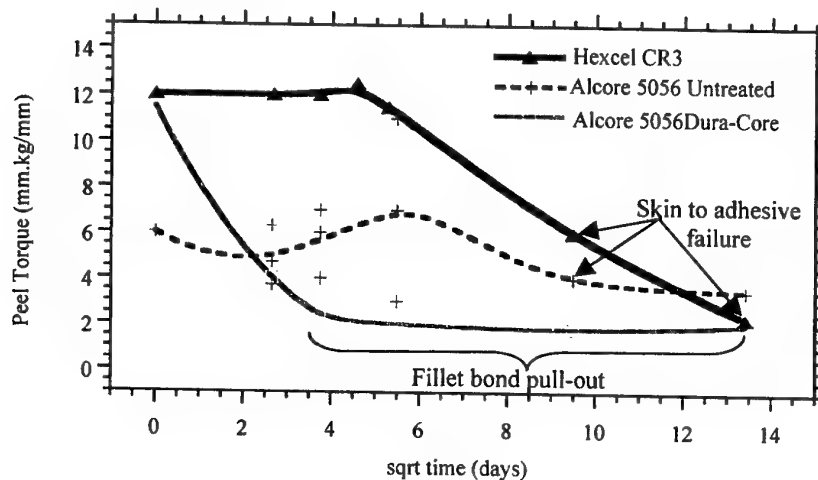


**Figure 4.3.2** Peel torque for Alcore and Hexcel honeycomb bonded with FM-300-2K and exposed to a 70°C/100% R.H. environment.

#### 4.3.3 Adhesional Failure as a Function of Peel Torque

Figure 4.3.3 indicates the peel torque of the honeycomb samples tested in section 4.3.1 as a function of the adhesion failure area, which was estimated visually. The adhesional failure represents fillet-bond pullout, or failure between the adhesive and honeycomb metal surfaces. As with Figure 4.2.7, for the Elcometer failure data, there is an approximate linear relationship between the percentage of adhesion failure area and the measured peel torque.

The case for 100% cohesion failure area within the fillet bond adhesive layer produced values of 12 mm.kg/mm of peel torque or greater and 100% adhesion failure area produced a peel torque value of approximately 1 mm.kg/mm. The percentage change in peel torque between 100% cohesion failure area and 100% adhesion failure area was approximately 90%. In the case of the

equivalent percentage change for the pull-off tension samples, this value was approximately 80%, refer Figure 4.2.7.

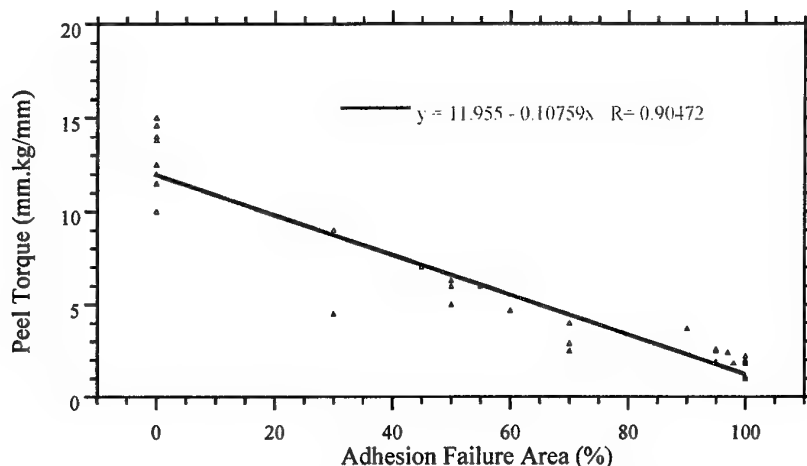


**Figure 4.3.3** Percentage adhesional failure as a function of peel torque (mm.kg/mm) for honeycomb samples tested in section 4.3.1.

#### 4.4 Fracture Analysis

X-ray photoelectron spectroscopy (XPS) was used in conjunction with Auger Electron Spectroscopy (AES) to analyse the adhesion failure surfaces of representative flatwise tension, Elcometer and peel samples. XPS and AES was performed using a Kratos XSAM-800 model spectrometer operating in FRR mode with a retard ratio of 53 and 150W flux of  $AlK\alpha$  radiation or 10kV electrons producing  $2nA/cm^2$  of specimen current. The ion etching was performed with an Argon ion gun operating at 2.5kV. The calibrated etch rate was 1.7nm/min on  $Ta_2O_5$ . Small spot analysis of the honeycomb failure surfaces was performed by Dr. Brack at La Trobe University Physics Department using a Kratos Axis Ultra Imaging XPS system with monochromatic  $AlK\alpha$  radiation.

##### 4.4.1 Flatwise Tension Failure Analysis of FM-300, Hexcel CR3 Honeycomb

A Hexcel Chromium coated honeycomb sample bonded with FM-300 was immersed in 95°C water for 75 days and produced a flatwise tension strength of 853 psi. Figure 4.4.1 indicates the complementary fracture surfaces resulting from the failed sample. Figure 4.4.1 indicates that the majority of failure has occurred within the FM-300 layer bonding the skin and honeycomb, however, some fillet bond pullout is also observed where failure has occurred near the FM-300 to honeycomb interface. Surface analysis using XPS was performed on the complementary fracture surfaces where fillet bond pullout had occurred.

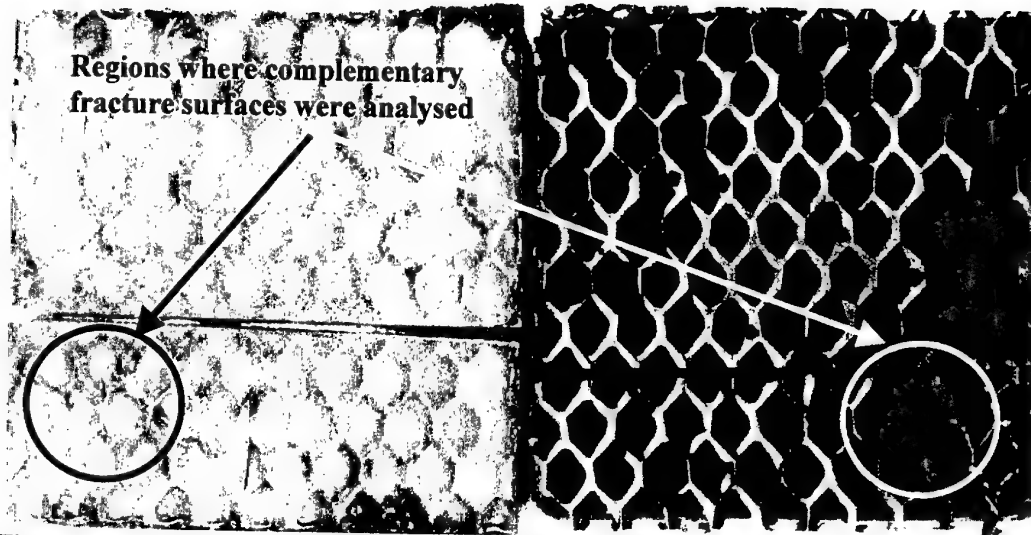


**Figure 4.4.1** Failure surfaces resulting from flatwise tension testing of Hexcel CR3 honeycomb bonded to aluminium and immersed in 95°C water for 75 days.

The honeycomb cell was analysed in two positions, as indicated in Figure 4.4.2. The top of the honeycomb cell is approximately 50µm wide and the fillet bond failure region, where adhesion failure has occurred between the FM-300 and honeycomb interface is approximately 0.5mm in width.

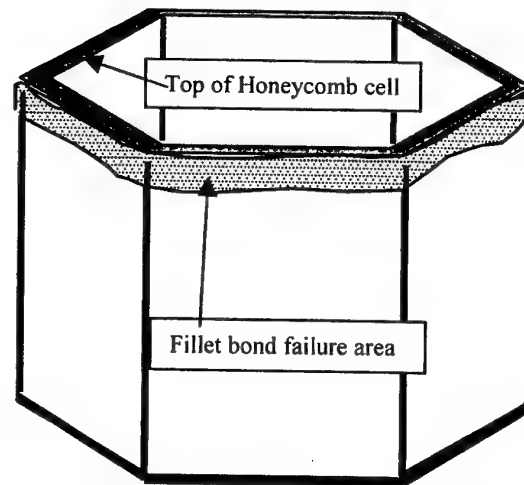


**Figure 4.4.2** The two regions of honeycomb examined using surface analysis

Table 4.4.1 indicates the surface concentrations of elements present on the top of the honeycomb cell, refer Figure 4.4.2, in the fillet bond pullout region.

**Table 4.4.1** *Elemental concentration of the top of the honeycomb cell in the fillet bond pullout region. Area 2 was also etched to remove the surface contaminant layers.*

Area on top of Honeycomb Cell Wall	%O	%N	%C	%Br	%Al
Area 1	20.7	10.7	67.9	0.7	---
Area 2	23.3	6.0	69.0	---	1.7
Area 2 (5minute etch)	26.6	5.8	63.2	---	4.4
Area 2 (30minute etch)	25.7	5.0	62.8	---	6.5

Figure 4.4.3 shows a series of XPS maps taken on the top of the cell wall (A) before and (B) after etching, indicating the distribution of the surface elements.

Table 4.4.2 indicates the surface concentration of elements present in the failed fillet bond region on the honeycomb cell wall, as indicated in Figure 4.4.2.

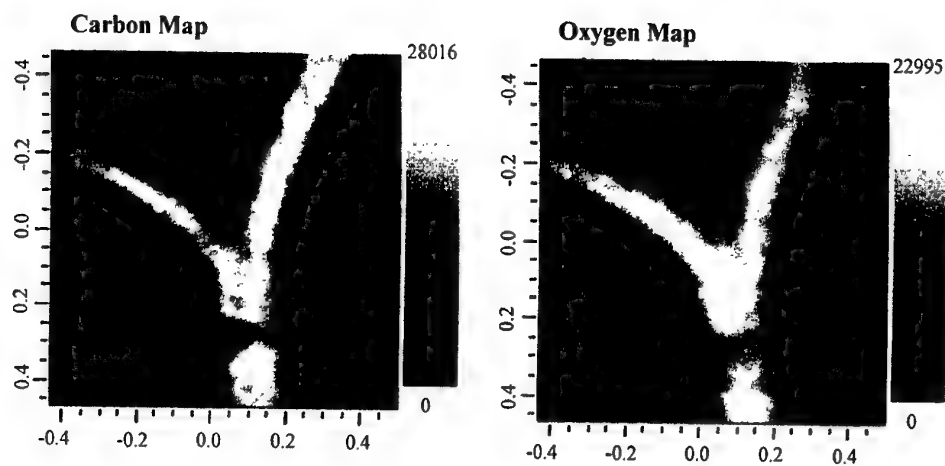
**Table 4.4.2** *Composition of the honeycomb surface in the region of the fillet bond failure at four different locations.*

Position No.	%Cr	%O	%N	%C	%Cl	%Si	%Br
1	1.8	21.8	8.6	64.4	1.0	2.4	0.2
2	1.3	21.0	10.7	63.6	1.4	1.8	0.2
3	1.3	19.5	12.7	63.3	1.4	1.6	0.3
4	1.2	19.9	11.9	63.7	1.3	1.8	0.2

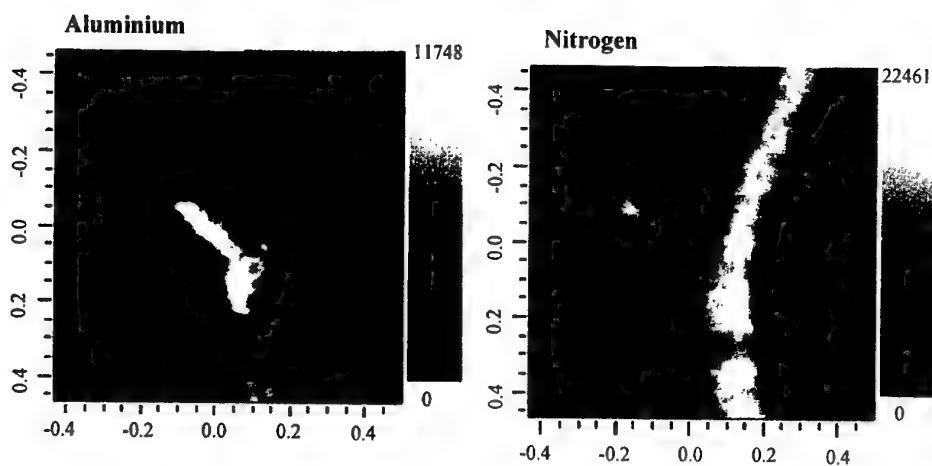
The fillet bond FM-300 surface was also analysed from the complementary fracture region analysed on the honeycomb cell wall to determine the locus of fracture. The surface composition of the fillet FM-300 surface is shown in Table 4.4.3.

**Table 4.4.3** *Composition of the FWT FM-300 failure surface in the fillet bond region at two different locations.*

Position No.	%O	%N	%C	%Si	%Al	%Br	%Na
1	23.8	7.3	64.8	2.8	0.4	0.4	0.5
2	35.8	1.2	52.6	---	10.4	---	---



**Figure 4.4.3(A)** *XPS maps taken on the top of the failed FWT honeycomb cell prior to argon ion etching*



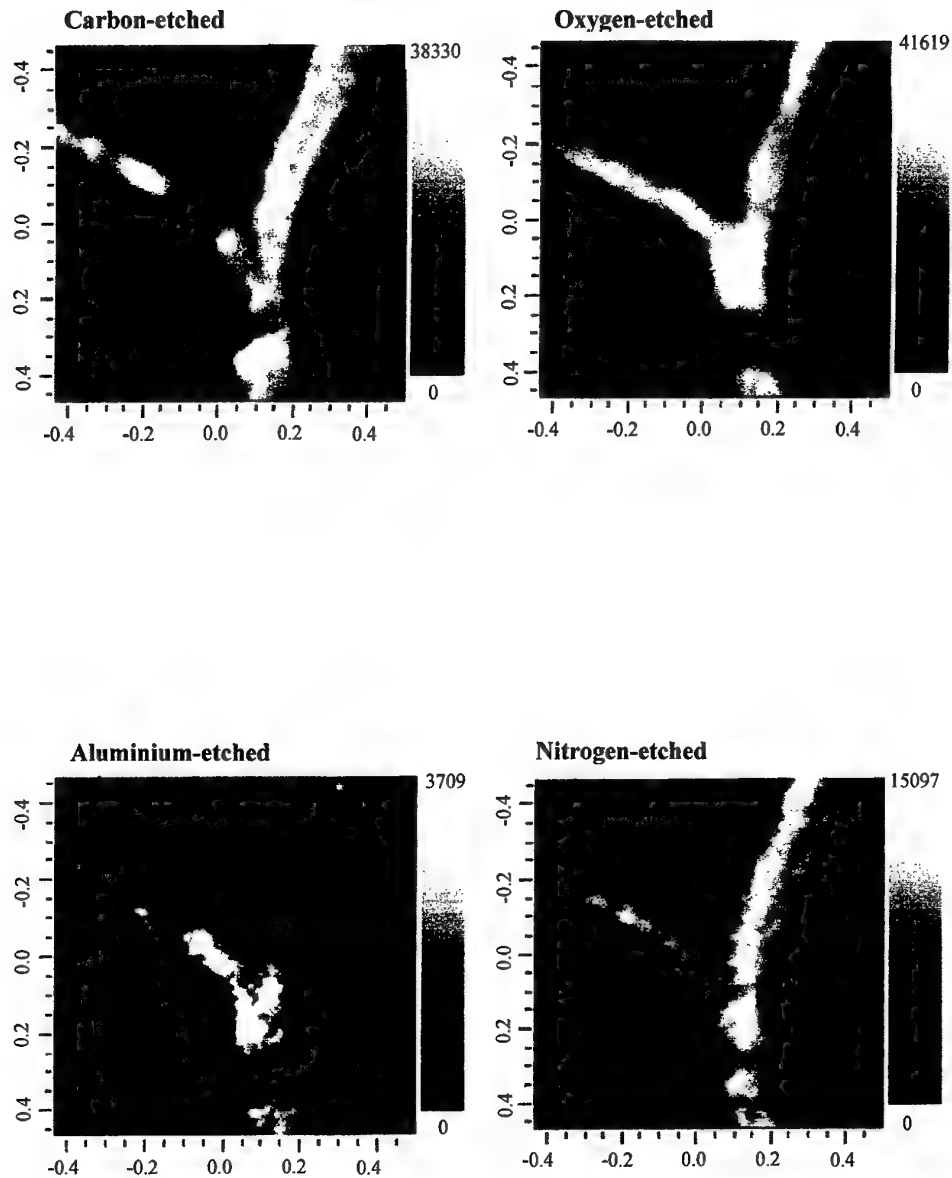


**Figure 4.4.3(B)** XPS maps taken on the top of the failed FWT honeycomb cell after a 30 minute Argon ion etch.

The fracture analysis data suggests that a thin FM-300 layer remains on the top of the honeycomb cell. Evidence for this conclusion is provided by the high carbon concentration, together with a nitrogen signal, which is typical of the chemical character of the FM-300, refer Table 4.4.1. Importantly, bromine is detected in the surface layer which is an element only present in the FM-300, hence, this acts as a marker for the presence of FM-300. The aluminium level is also quite low and the maps of the elemental distributions, refer Figures 4.4.3(A) and

(B), suggest that the aluminium signal was produced from a small area of the surface only after etching removed a thin layer of FM-300.

Analysis of the fillet bond failure region indicates that the honeycomb surface has a chemical character similar to that observed for the Hexcel CR3 honeycomb which was depth profiled in section 3.1, Figure 3.1. Silicon, nitrogen, oxygen, chromium and carbon levels are at similar levels to the as received honeycomb material, refer Table 4.4.2. However, no aluminium signal was observed, suggesting that some failure in the fillet bond area has occurred in the epoxy resin layer, near the coating to FM-300 interface. The presence of Bromine suggests that some FM-300 is present on the surface layer and supports this conclusion.

Analysis of the FM-300 surface in the fillet bond region does not provide a straightforward interpretation. In the case of position 1 analysis, refer Table 4.4.3, the data is consistent with the interfacial failure near the honeycomb to FM-300 interface, described above. This failure locus is supported by the concentrations of carbon, oxygen, nitrogen and bromine typical of the FM-300. The source of silicon is not clear, given both the coating and the FM-300 have levels similar to that indicated in Table 4.4.3. Position 1 provides an example of the commonly observed fracture surface for a number of analyses on separate regions.

Position 2 analysis in Table 4.4.3 indicates that the aluminium level has increased to 10 atomic percent. This increase suggests that the locus of failure is not solely near the FM-300 to honeycomb interfacial region. The higher aluminium concentration suggests some regions exist where the fracture path has propagated into the aluminium layer. The increase in oxygen concentration associated with the increased aluminium level suggests that the oxide may be hydrated. Failure through a hydrated oxide layer has previously been reported for aluminium-epoxy systems exposed to a humid environment [13]. Position 2 surface composition was not typically observed for the analyses performed on the fillet bond FM-300 surface, and suggests that failure in the oxide layer was not the dominant failure mechanism. This is supported by the absence of aluminium on the honeycomb fillet bond failure surfaces examined in Table 4.4.2.

Figure 4.4.4 indicates the proposed locus of fracture of the adhesive failure regions for the Hexcel CR3 and FM-300 FWT honeycomb sample immersed in 95°C water for 75 days. This fracture path represents the dominant mode of failure in the adhesive failure zones and does not include the unusual fracture observed for position 2 analysis in Table 4.4.3.

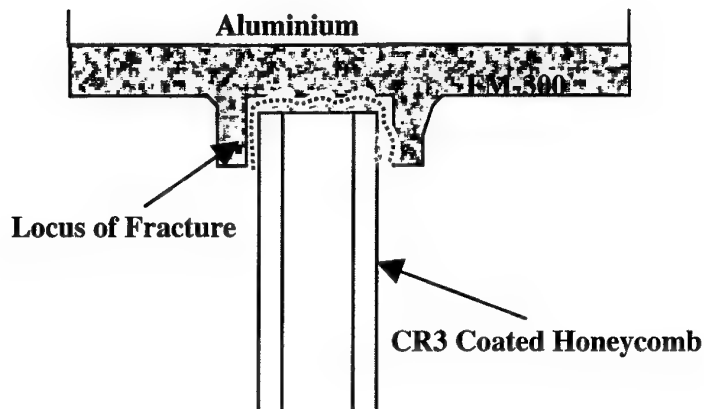


**Figure 4.4.4** Cross-sectional representation of the Hexcel CR3 honeycomb bonded to aluminium with FM-300. The dominant locus of fracture for the FWT sample in the adhesive failure zones tested after 75 days immersion in 95°C water is proposed.

#### 4.4.2 Peel Failure Analysis of FM-300, Hexcel CR3 Honeycomb

A Hexcel Chromium coated honeycomb sample bonded with FM-300 was exposed to 70°C/100%R.H. environment for 14 days and produced a peel torque of 1.5 mm.kg/mm. Figure 4.4.5 indicates the complementary fracture surfaces resulting from the failed sample showing failure is fillet bond pullout i.e. where failure has occurred near the adhesive-honeycomb interface. Surface analysis using XPS was performed on the complementary fracture surfaces.

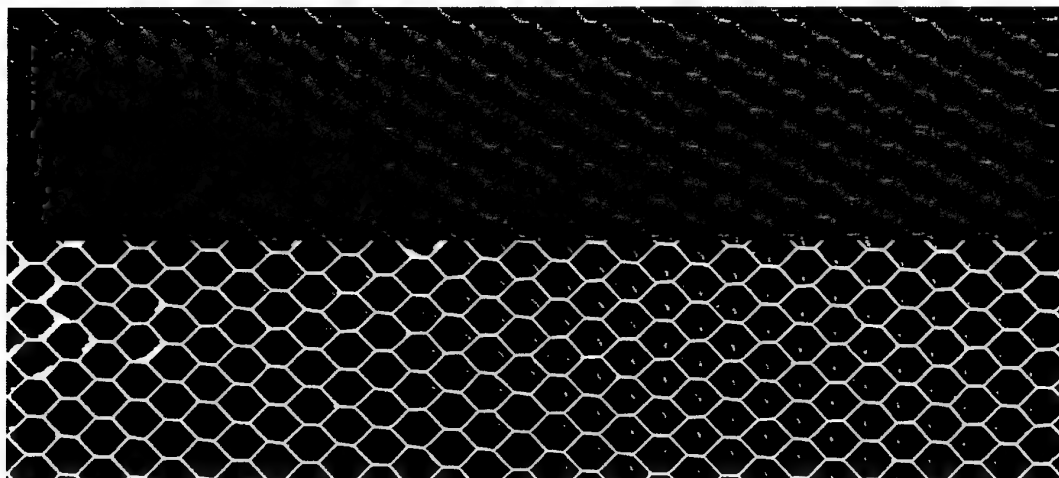


**Figure 4.4.5** Failure surfaces resulting from peel testing of Hexcel CR3 honeycomb bonded to aluminium and exposed to 70°C/100%R.H. environment for 14 days .



The honeycomb cell was analysed in two positions, as indicated previously in Figure 4.4.2. Table 4.4.4 indicates the atomic concentration on the top of the honeycomb cell before and after light etching.

**Table 4.4.4** *Elemental concentration on the top of the honeycomb cell for fillet bond pullout of the Hexcel CR3 peel sample exposed for 14 days at 70°C/100%R.H.. Etching to remove the surface contaminant layers was also performed.*

Area on top of Honeycomb Cell Wall	%O	%N	%C	%Si	%Al
Area Before Etch	42.5	4.7	43.4	1.8	7.5
Area After Etch (5 minute etch)	53.1	2.5	22.9	---	21.5

Table 4.4.5 indicates the surface concentration of elements present in the failed fillet bond region on the honeycomb cell wall, as indicated in Figure 4.4.2.

**Table 4.4.5** *Composition of the honeycomb surface in the region of the fillet bond failure before and after etching.*

Atomic (%)	%Cr	%O	%N	%C	%Na	%Si	%Al
Before Etch	1.9	25.6	7.2	61.5	0.9	3.0	---
5 min. etching	9.8	28.2	3.0	54.9	0.6	2.7	0.8
10 min. etching	15.4	36.6	2.1	41.2	0.9	2.5	1.4

A comparison between the fillet bond failure region on the honeycomb wall and the same piece of honeycomb below the fillet bond region, which had been exposed to the humid environment, was also undertaken. Table 4.4.6 indicates the surface composition of the honeycomb wall before and after etching.

**Table 4.4.6** *Composition of the honeycomb surface in the region below the fillet bond failure before and after etching.*

Atomic (%)	%Cr	%O	%N	%C	%Na	%Si	%Al
Before Etch	0.6	22.1	10.3	63.1	0.4	3.5	---
5 min. etching	12.9	39.6	3.7	35.8	0.5	6.7	0.8
10 min. etching	16.4	42.1	2.4	32.4	0.3	4.3	2.1

The surface of the FM-300 in the fillet bond region was also analysed, from the complementary fracture region analysed on the honeycomb cell wall. The surface composition of the FM-300 fillet bond surface is shown in Table 4.4.7.

**Table 4.4.7** *Composition of the FM-300 failure surface in the fillet bond region at five different locations.*

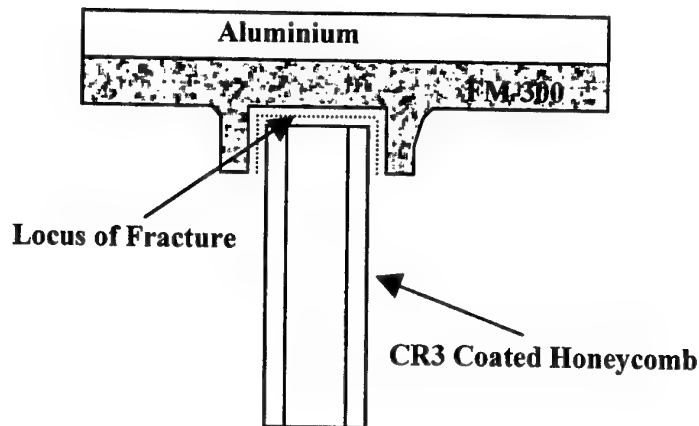
Position No.	%O	%N	%C	%Si	%Br	%Na	%Cr
1	18.3	4.3	74.7	2.1	0.3	0.3	---
2	20.0	5.9	71.8	1.4	0.4	0.5	---
3	20.5	4.9	71.8	2.1	0.3	0.2	0.3
4	21.5	7.1	68.3	2.6	0.1	0.1	0.3
5	20.1	5.3	71.6	2.8	0.1	---	---

Analysis of the fracture surfaces from the failed peel sample reveal subtle differences with the flat-wise tension (FWT) specimen analysed in section 4.4.1. The top of the honeycomb cell indicated that the carbon level was reduced to about 20% after a brief etch, refer Table 4.4.4. The aluminium signal also increased to 20% after the initial etch. In contrast, the carbon level remained high after etching for the equivalent analysis on the FWT sample. This suggests that the failure on the top of the honeycomb cell occurs very close to the honeycomb metal and FM-300 interface for the failed peel sample, which contrasts with failure within the adhesive layer for the FWT sample.

Analysis of the fillet bond failure region on the honeycomb cell wall surface, Table 4.4.5, indicates a similarity with the surface of the exposed honeycomb wall surface, Table 4.4.6. Similar trends in atomic concentrations during etching, suggest the fillet bond failure occurs very close to the honeycomb surface and FM-300 interface. In comparison with the fillet bond failure on the FWT sample, refer Table 4.4.2, similar surface elemental concentrations exist, however, bromine was not detected for the peel failure surfaces. This may suggest the failure is more interfacial than in the FWT case.

The interfacial failure mode for the fillet bond failure region of the honeycomb wall is supported by analysis of the complementary FM-300 surface, refer Table 4.4.7. The adhesive failure surface concentration is similar to that observed for FM-300 and indicates the presence of bromine, only seen in the FM-300. Two regions analysed indicate trace concentrations of chromium on the fillet adhesive surface, which may suggest that some failure has propagated into the honeycomb coating layer. The very low concentrations of chromium suggest this mode of failure only makes up a small percentage of the total locus of fracture, which appears to predominantly occur in the adhesive honeycomb surface interfacial region. The proposed locus of fracture is indicated in Figure 4.4.6.

**Figure 4.4.6** *Cross-sectional representation of the Hexcel CR3 honeycomb bonded to aluminium with FM-300. The dominant locus of fracture for the peel sample tested after 14 days exposure to 70°C/100%R.H. is proposed.*

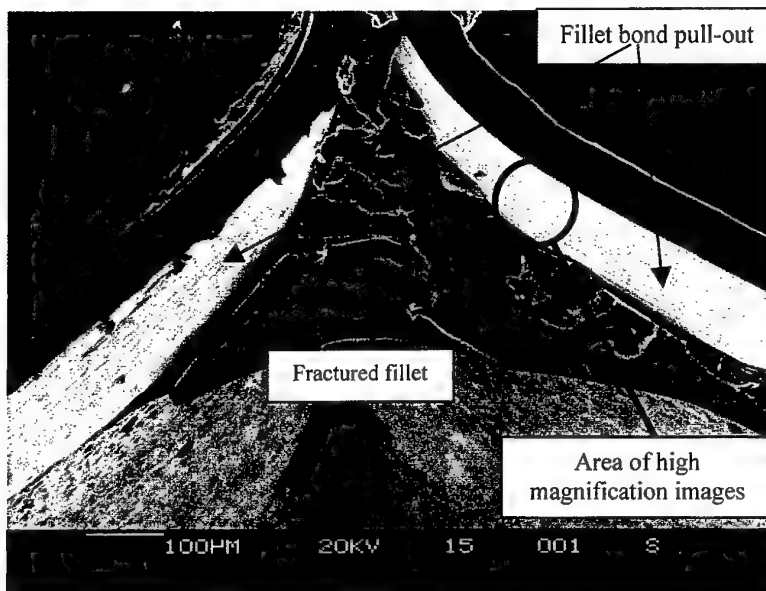


#### 4.4.3 Peel Failure Analysis of FM-300, Alcore Untreated Honeycomb

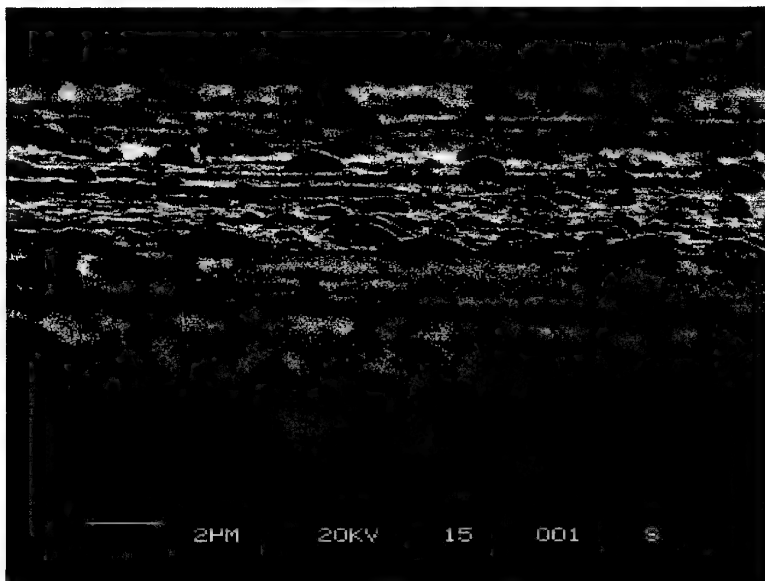
Fracture analysis of two Alcore untreated honeycomb samples bonded to FM-300 and conditioned in a 70°C/100%RH environment for 3 and 6 months was performed with SEM. These samples failed predominantly by cohesive failure of the fillet bond i.e. fillet bond fracture. In order to interrogate the fracture region, the failed adhesive fillet bond surface was ultramilled until the top of the honeycomb cells could be observed. Small areas indicated a mixture of fillet bond fracture and pull-out had occurred. Micrographs were then taken in these regions.

Figure 4.4.7 indicates a low magnification image of the failed peel sample that had been conditioned for 6 months in the 70°C/100%RH environment. The image indicates a region where fillet bond fracture and fillet bond failure has occurred. The high magnification image shown in Figure 4.4.8 indicates the surface of the fillet bond pull-out region has a high number of circular protrusions growing on the honeycomb surface. These areas represent regions where moisture has diffused along the adhesive-honeycomb interface and subsequently reacted with the aluminium, producing islands of hydrated aluminium oxide.

Figure 4.4.9 indicates a low magnification image of the failed peel sample that had been conditioned for 3 months in the 70°C/100%RH environment. Unlike the fillet bond pull-out region shown in Figure 4.4.8, there appears to be a lower density of hydrated oxide protrusions. The high magnification image in Figure 4.4.10 indicates that the hydrated oxide growth under the adhesive film has not progressed to the same extent after 3 months as it has for the 6 months of conditioning, refer to Figure 4.4.9.



**Figure 4.4.7** SEM image of the fracture surface from Alcore untreated honeycomb bonded to FM-300 and conditioned 6 months at 70°C/100%RH



**Figure 4.4.8** High magnification SEM image of the fillet bond pull-out fracture surface from Alcore untreated honeycomb bonded to FM-300 and conditioned 6 months at 70°C/100%RH.

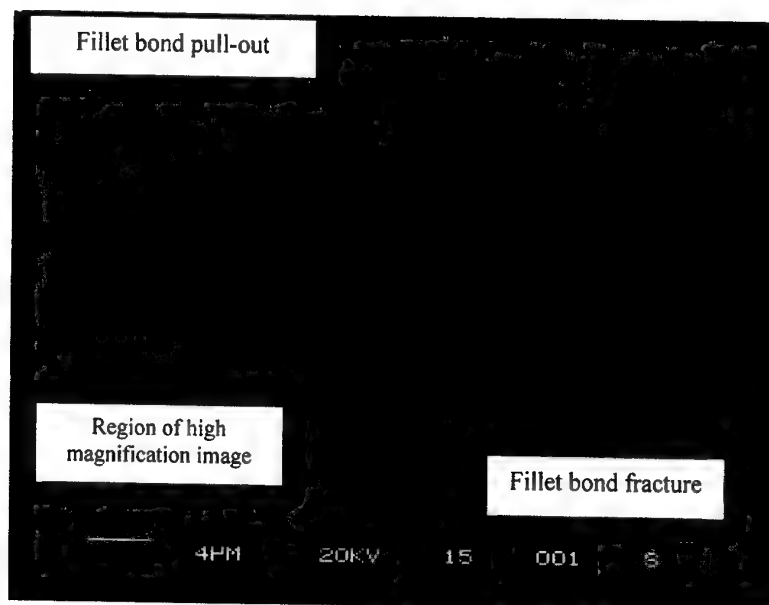


**Figure 4.4.9** SEM image of the fracture surface from Alcore untreated honeycomb bonded to FM-300 and conditioned 3 months at 70°C/100%RH.

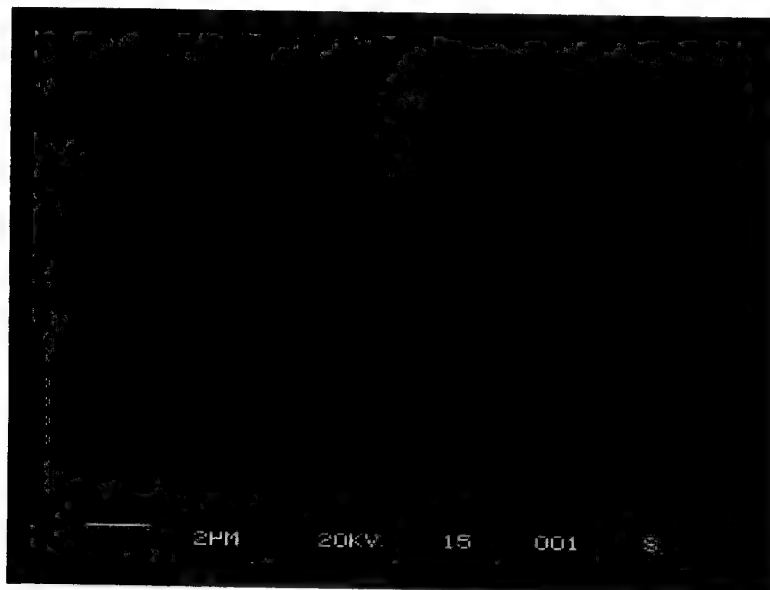


**Figure 4.4.10** High magnification SEM image of the fillet bond pull-out fracture surface from Alcore untreated honeycomb bonded to FM-300 and conditioned 3 months at 70°C/100%RH.

#### 4.4.4 Elcometer Failure Analysis of FM-300, Hexcel CR3 Honeycomb

A Hexcel Chromium coated honeycomb sample bonded with FM-300 was immersed in 70°C water for 6 months and produced a pull-off tension of 386 psi. Figure 4.4.11 indicates the complementary fracture surfaces resulting from the failed sample.

Figure 4.4.11 indicates that the majority of the failure is fillet bond pullout i.e. where failure has occurred near the adhesive-honeycomb interface. Surface analysis using XPS was performed on the complementary fracture surfaces.

The honeycomb cell was analysed in two positions, as indicated previously in Figure 4.4.2. Table 4.4.8 indicates the atomic concentration on the top of the honeycomb cell before and after light etching.

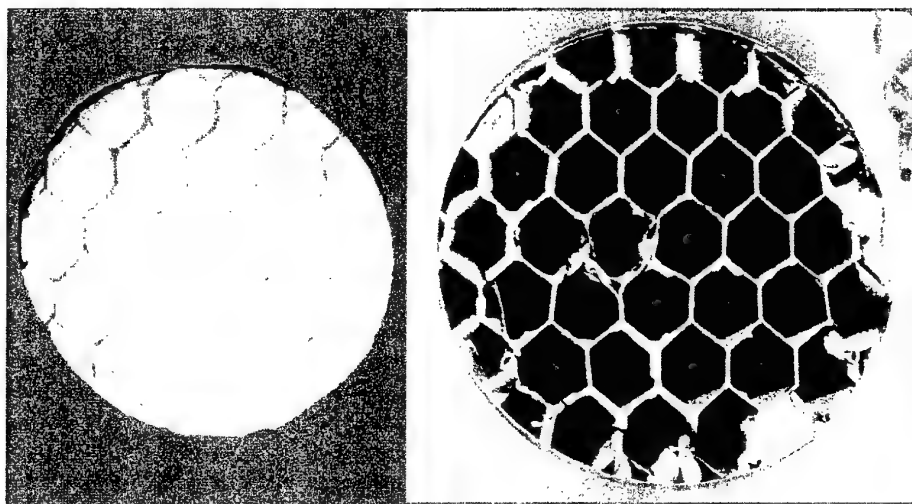


**Figure 4.4.11** Failure surfaces resulting from Elcometer testing of Hexcel CR3 honeycomb bonded to aluminium and immersed in 70°C water for 6 months.

**Table 4.4.8** Elemental concentration on the top of the honeycomb cell for fillet bond pullout of the Hexcel CR3 sample immersed in 70°C water for 6 months. Etching to remove the surface layers was also performed.

Area on top of Honeycomb Cell Wall	%O	%N	%C	%Al
Area 1 Before Etch	35.7	2.1	55.9	6.2
Area 1 After Etch (5minute etch)	51.1	2.5	31.5	17.5
Area 2	35.3	2.8	54.8	7.0

Table 4.4.9 indicates the surface concentration of elements present in the failed fillet bond region on the honeycomb cell wall, as indicated in Figure 4.4.2.

A comparison between the fillet bond failure region on the honeycomb wall and the same piece of honeycomb below the fillet bond region, which had been exposed to the humid environment was also undertaken. Table 4.4.10 indicates the surface composition of the honeycomb wall before and after etching for two locations.

The surface of the FM-300 fillet bond region was also analysed, from the complementary fracture region analysed on the honeycomb cell wall. The surface composition of the FM-300 fillet bond surface is shown in Table 4.4.11.

**Table 4.4.9** *Composition of the honeycomb surface in the region of the fillet bond failure before and after etching.*

Atomic (%)	%Cr	%O	%N	%C	%Si	%Al
Before Etch (Area 1)	3.3	34.8	2.7	53.9	1.7	3.7
5 min. etching (Area 1)	15.4	38.1	0.5	41.3	0.9	3.8
Before Etch (Area 2)	3.0	29.3	2.1	61.2	2.0	2.4
5 min. etching (Area 2)	9.5	25.8	0.1	61.4	0.8	2.8

**Table 4.4.10** *Composition of the honeycomb surface in the region below the fillet bond failure before and after etching.*

Atomic (%)	%Cr	%O	%N	%C	%Al
Before Etch (Area 1)	2.3	43.5	1.6	38.0	14.6
5 min. etching (Area 1)	7.4	42.4	---	31.8	18.4

**Table 4.4.11** *Composition of the FM-300 failure surface in the fillet bond region at three different locations.*

Position No.	%O	%N	%C	%Si	%Br	%Al	%Cr
1	17.5	2.0	77.6	1.6	0.3	0.8	0.2
2	16.9	2.7	77.3	1.9	0.3	0.6	0.4
3	15.2	1.7	80.9	1.8	0.2	0.2	0.2

Analysis of the failure surfaces resulting from the Elcometer sample immersed for 6 months in 70°C water indicates similarities with the peel failure analysis in section 4.4.2. The top of the honeycomb cell suggests that failure is very close to the FM-300 and honeycomb interface. The carbon signal drops notably with the complimentary rise in aluminium signal after the five minute etch, refer Table 4.4.8. This trend was similar to that observed in the peel failure analysis, refer Table 4.4.5.

The fillet bond failure on the side of the cell wall, refer Table 4.4.9, also appears to be similar to that observed for the peel failure. The presence of chromium, silicon and nitrogen is typical of the coating surface on the honeycomb. High levels of carbon and the presence of bromine on the FM-300 failure surface, refer Table 4.4.11, suggest failure in this region is near the FM-300 honeycomb coating interface. One change observed, in comparison with the peel sample, is the small increase in aluminium observed on both fracture faces. This may suggest that, whilst the failure is close to the FM-300 and coating interface, some fracture has propagated into the coating layer and to the aluminium layer beneath the coating. This mode of failure would occur if the moisture ingress was able to hydrate the coating on the honeycomb in some areas. The relatively low percentages of chromium and aluminium suggest this mode of failure is far less common than the interfacial failure.

Analysis of the honeycomb surface immersed in the 70°C water for 6 months suggests that the hydration process described above has progressed to a much greater extent in the region not covered by the adhesive layer, refer Table 4.4.10. The increase in aluminium, and decrease in carbon and chromium, suggests that moisture has reacted with the coating, resulting in substantial dissolution of the chromium layer and subsequent hydrolysis of the underlying aluminium layer.

The proposed locus of fracture for the Elcometer sample is shown in Figure 4.4.8. Whilst the locus of failure is represented as being similar to the peel sample, there is probably some small degree of failure which has propagated into the region of the interface where the coating has hydrated. The difference between the failure observed for the FWT sample in Figure 4.4.3 and that shown in Figure 4.4.12 is also noteworthy. The FWT sample exhibited a greater degree of cohesive failure in the adhesive layer for the region on top of the honeycomb cell. This may provide further evidence to support the process of moisture removal from the conditioned samples as a result of the bonding procedure employed for the FWT samples.



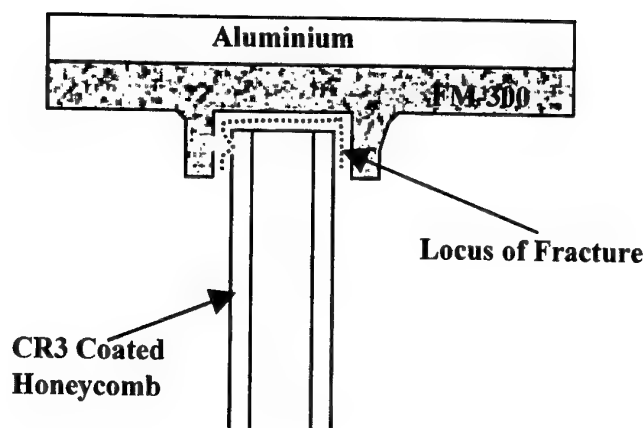


**Figure 4.4.12** Cross-sectional representation of the Hexcel CR3 honeycomb bonded to aluminium with FM-300. The dominant locus of fracture for the Elcometer sample tested after 6 months immersion in 70°C water is proposed.

## 4.5 Three and four Point Bending results

### 4.5.1 Hexcel CR3 Honeycomb, Strength versus Adhesion Area

The response of beam flexural stiffness to the percentage of honeycomb to skin fillet bond adhesion was investigated in an initial experiment to determine the expected changes in beam stiffness which may occur as a result of fillet bond degradation in a humid environment. The ultimate load for 3 and 4 point bending experiments performed on Hexcel CR3 honeycomb bonded to 0.5mm aluminium skins with FM-300 adhesive was performed where the area of adhesion between the honeycomb and metal skin was reduced. Figure 4.5.1 provides a diagrammatic representation of the perimeter area masked off and the percentage reduction in adhesion area. Figure 4.5.2 indicates the ultimate load measured for the 3 and 4 point bending tests as a function of adhesion area.

The data suggests that the four point bending provides a more even response in loading. The broken line may underestimate the actual load for a zero adhesion case. The value is for the case of no adhesive layer between the skin and honeycomb. Higher values may be achieved for exposure conditions which would produce 100% fillet bond pull-out in equivalent FWT and peel testing. In these situations the mechanical link between the adhesive fillet and honeycomb may be sufficient to retain some stiffness.

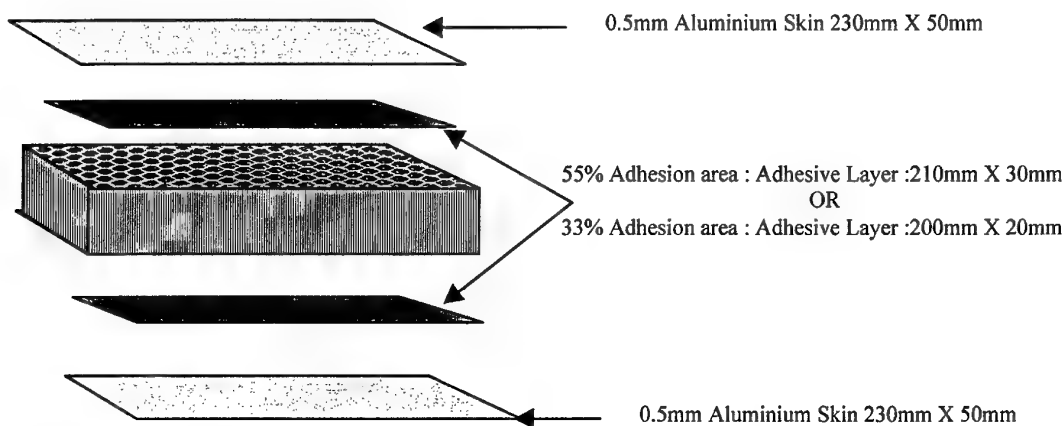


**Figure 4.5.1** Diagrammatic representation of the Beam samples produced for studies on the effect of fillet adhesion area on ultimate load in 3 and 4 point bending tests.

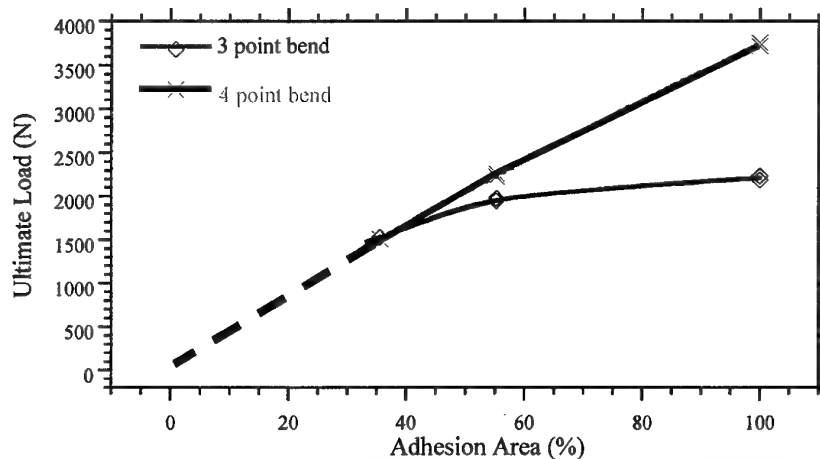


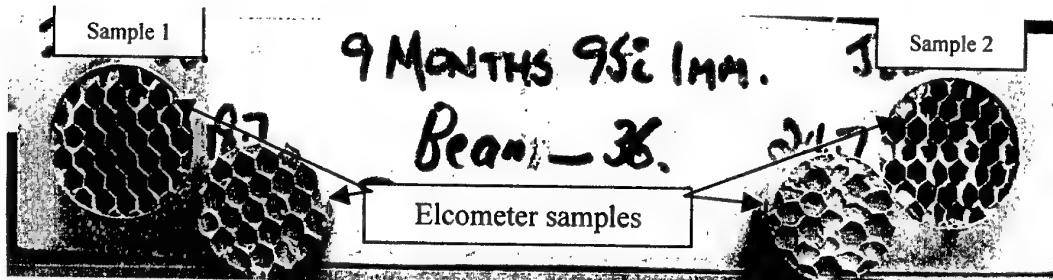
**Figure 4.5.2** Ultimate load as a function of fillet bond adhesive area for Hexcel CR3 honeycomb bonded to FM-300 adhesive for 3 and 4 point bending.

#### 4.5.2 Hexcel CR3 Honeycomb, 95°C humid exposure

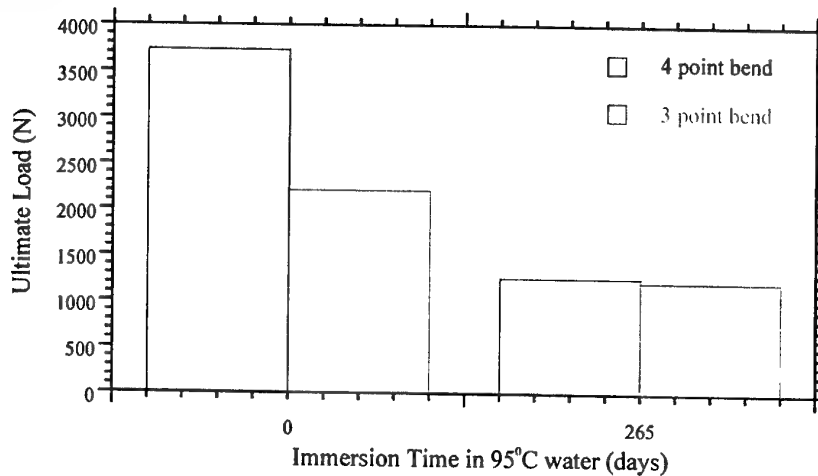
Two beam specimens constructed from FM-300 adhesive, Hexcel CR3 honeycomb and 0.5mm thick aluminium skins were immersed for 265 days in 95°C water in order to identify a likely plateau value in load for a fully degraded sandwich panel.

Figure 4.5.3 shows one of the failed beam samples and the location of 2 Elcometer samples taken at either end of the beam. The ultimate load measured for the two samples is indicated in Figure 4.5.4, relative to the dry strength values for the 3 and 4 point loading modes. The data in Figure 4.5.4 indicates that the 265 day exposure reduces dry strength by 66% in the 4 point bending mode and 45% in the 3 point bending mode. The equivalent Elcometer strength

measured for two locations on the different beam samples are indicated in Table 4.5.1, together with the estimated fraction of fillet bond pull-out. Failure surfaces for Elcometer samples 1 and 2 taken from the 3 point bend test are also indicated in Figure 4.5.3.



**Figure 4.5.3** Failed Beam sample tested in 3 point bending mode, immersed 9½ months in 95°C water. Elcometer samples are also included.



**Figure 4.5.4** Ultimate load in 3 and 4 point bending modes for beam samples immersed 9½ months in 95°C water, relative to control samples.

**Table 4.5.1** Elcometer values measured for Beam samples immersed 265 days in 95°C water.

Elcometer Sample	Pull-Off tension (psi)	Failure(%)
3 point-Sample 1	380	100 adhesion of fillet
3 point- Sample 2	502	75 adhesion of fillet
4 point-Sample 1	158	50 adhesion of fillet and 50 core corrosion
4 point-Sample 2	184	50 adhesion of fillet and 50 core corrosion

The skins from the beam samples were peeled off manually and examined. A representative failure surface is shown in Figure 4.5.4. Over 90% of the surface indicates fillet bond pull-out i.e. adhesive failure between the fillet bond and honeycomb metal. The failure of the node bonds during the bend test is also indicated by the honeycomb core material which has remained on the skin. The degree of fillet bond pull-out, together with the pull-off tension values measured, refer Table 4.5.1, suggests the sample has reached the maximum degradation state observed for unstressed exposure to a humid environment, just prior to significant onset of core corrosion. Examination of the core material revealed evidence of core corrosion, however, the failure surfaces appeared to have failed predominantly through fillet bond pull-out.

Examination of the beam samples, prior to Elcometer testing and manual removal of the skin, indicated that at ultimate load node bond and fillet bond failure had occurred near the point where the upper rollers loaded the sample at the  $\frac{1}{4}$  load-span region in compression.

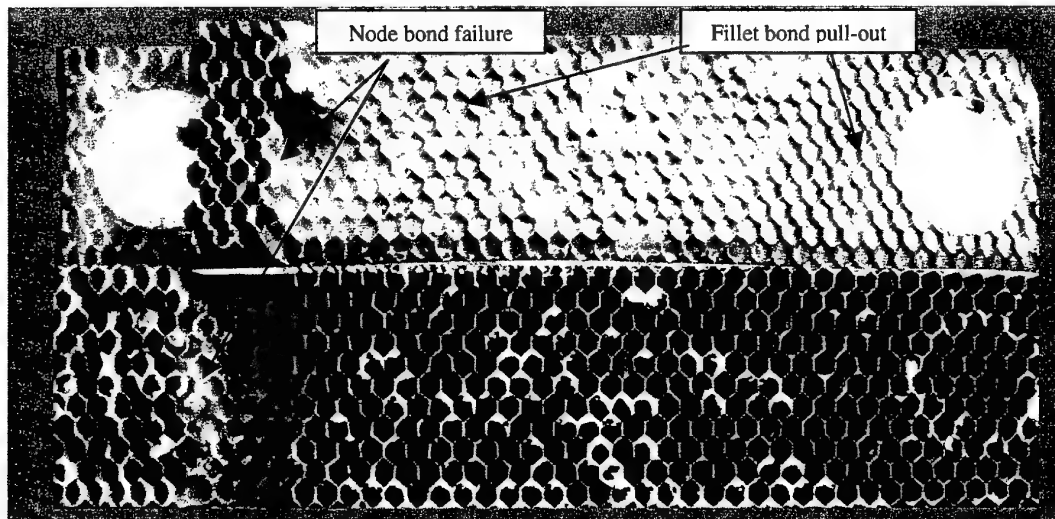


**Figure 4.5.4** Failure surfaces produced by manually peeling the skin from the failed beam sample immersed 265 days in 95°C water.

#### 4.5.3 Single Sided Beam Mechanical Properties

In order to examine the possibility accelerating the environmental conditioning procedure, single sided beam samples were manufactured in which one side was constructed from FM-300 adhesive and the second skin was bonded after exposure with EA9309.3NA paste adhesive, as with the peel and Elcometer experiments. The skin bonded with structural adhesive also had the bonding region reduced, as described in Figure 4.5.1, and the mechanical properties were measured from load-deflection curves. As with the above samples, the honeycomb ribbon ran in the width direction, as seen in Figure 4.5.4.

The Core Shear Stress,  $\tau$  (MPa), and Facing Bending Stress,  $\sigma$  (MPa) are plotted for all 3 and 4 point bending samples tested as a function of adhesion area in Figure 4.5.5 and 4.5.6. The equivalent bending loads were shown in Figure 4.5.2. The data shows some degree of scatter, however, all single sided samples in which the second skin was bonded with EA9309.3NA paste adhesive, fell within range of values observed for double sided samples, in which both skins were bonded with FM-300.

The Flexural Stiffness,  $D(\text{N}\cdot\text{mm}^2)$ , Core Shear Modulus,  $G(\text{MPa})$  and Panel Shear Rigidity,  $U(\text{N})$  values determined in the elastic zone are plotted for all 3 and 4 point bending samples tested as a function of adhesion area in Figures 4.5.7, 4.5.8 and 4.5.9. The data shows some degree of scatter, however, all single sided samples fell within the range of values observed for double skinned FM-300 samples.

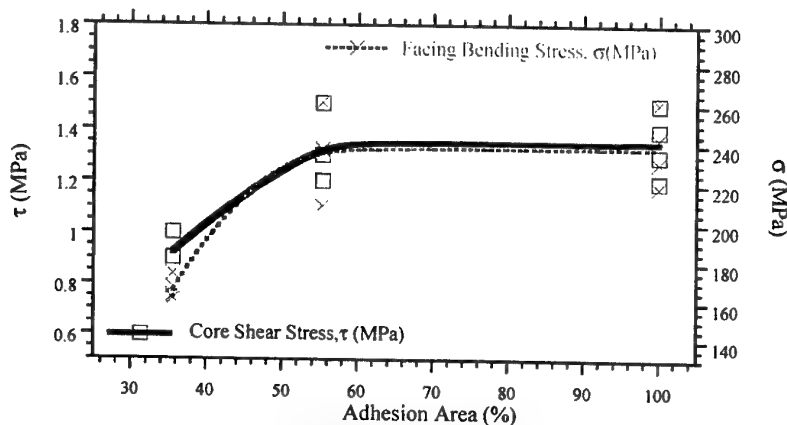


**Figure 4.5.5** Core Shear Stress,  $\tau$  (MPa), and Facing Bending Stress,  $\sigma$  (MPa) for 3 point bending of Hexcel CR3 honeycomb panels bonded with FM-300 as a function of adhesion area.

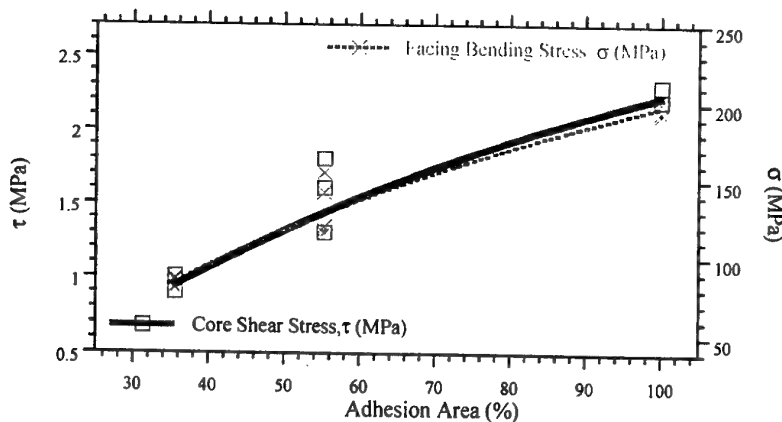


**Figure 4.5.6** Core Shear Stress,  $\tau$  (MPa), and Facing Bending Stress,  $\sigma$  (MPa) for 4 point bending of Hexcel CR3 honeycomb panels bonded with FM-300 as a function of adhesion area.

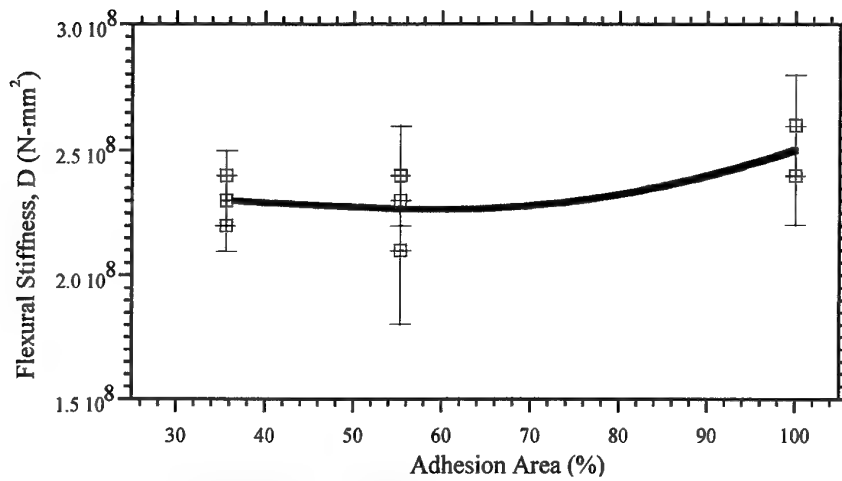


**Figure 4.5.7** Flexural Stiffness,  $D(N.mm^2)$ , for Hexcel CR3 honeycomb panels bonded with FM-300 as a function of adhesion area.

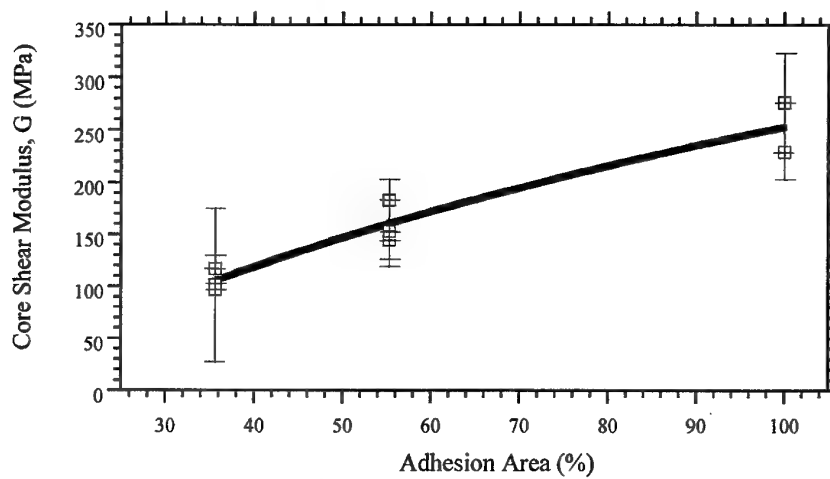


**Figure 4.5.8** Core Shear Modulus,  $G(MPa)$ , for Hexcel CR3 honeycomb panels bonded with FM-300 as a function of adhesion area.

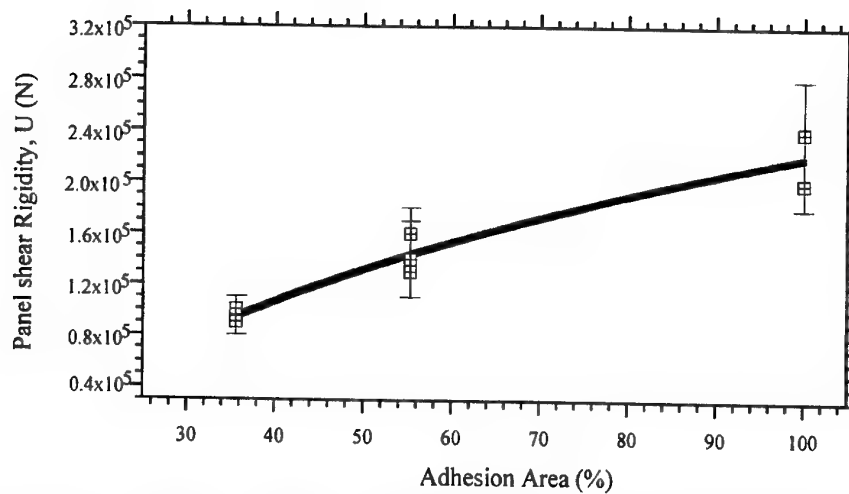


**Figure 4.5.9** Panel Shear Rigidity,  $U(N)$ , for Hexcel CR3 honeycomb panels bonded with FM-300 as a function of adhesion area.

The data shown in Figures 4.5.5 to 4.5.9 suggests that asymmetric beam samples can be manufactured, enabling conditioning in environments less severe than the 95°C water immersion environment. Changes in Flexural Stiffness properties monitored for asymmetric samples should be representative of equivalent changes in symmetrical samples.

The trend in Elastic properties of the beam samples as a function of adhesion area provide some interesting trends. The Core Shear Modulus,  $G$  (MPa) and Panel Shear Rigidity,  $U(N)$ , both appear to decrease as a function of adhesion area, allowing for the scatter in the data. In contrast, Flexural Stiffness,  $D(N \cdot mm^2)$ , did not appear to be sensitive to adhesion area changes in the elastic region, as would be expected.

It should be noted the flexural stiffness properties calculated in the elastic zone are particularly sensitive to errors in measured deflection as a function of load and the error bars indicated in the above plots indicate scatter, not absolute error measurements.

## 4.6 Node Bond results

The peel strength of Alcore and Hexcel node bonds from as received honeycomb core material was tested as described in section 2.2.7, Figure 2.5. The effect of temperature and moisture exposure on node bond strength was examined.

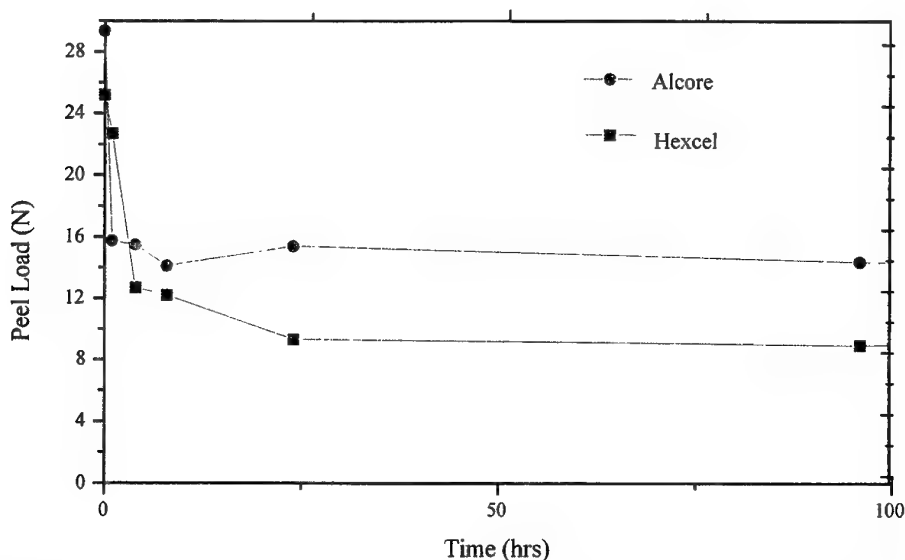
### 4.6.1 Hexcel and Alcore Node Bond Peel strength and humid exposure

Figure 4.6.1 indicates that immersion of Hexcel and Alcore honeycomb in 95°C water results in a substantial and rapid decrease in node bond strength. The nitrile rubber modified phenolic

adhesive of Hexcel node bonds appears to be weaker and less durable under the 95°C water immersion conditions than the polyamide node adhesive of the Alcore honeycomb.

Alcore and Hexcel honeycomb was also exposed to 70°C/100%R.H. and 80°C/95%R.H. for 7 days and node bond peel strength measured. Under 70°C/100%R.H. exposure conditions, Hexcel and Alcore products lost 53% and 37% of their original strength, respectively. Under 80°C/95%R.H. exposure conditions, Hexcel and Alcore products lost 37% and 27% of their original strength, respectively. The Alcore product appears to produce better results than the Hexcel product for humid exposure testing.

Strength recovery of the node bonds after environmental exposure was also investigated. Replicate samples of Alcore and Hexcel honeycomb were immersed in 95°C water for 24 hours and half were immediately tested, whilst the remaining samples were dried in a 60°C vacuum oven for 3 days prior to testing. Hexcel samples, which exhibited a 53% reduction in dry peel strength, recovered 100% of their original strength after vacuum drying. The Alcore sample lost 53% of its original peel strength after conditioning and recovered 95% of the original dry strength value after vacuum drying. The recovery in strength of both honeycomb types suggests that the reduction in strength is caused by plasticisation of the adhesive due to water absorption. Vacuum drying at 60°C for 3 days is sufficient to remove the moisture and almost fully recover the initial strength values.



**Figure 4.6.1** Node bond peel load as a function of time of immersion in 95°C water for Alcore and Hexcel honeycomb using the method shown in Figure 2.5.

Failure surfaces for the conditioned node bond samples were also analysed. The Hexcel samples all exhibited substantial amounts of adhesive failure after humid exposure, in contrast the Alcore samples exhibited predominantly cohesive failure in the polyamide adhesive. After vacuum recovery the Alcore samples exhibited 100% cohesive failure area, as seen for the control sample. The Hexcel sample still exhibited a small amount of adhesive failure after vacuum drying, in contrast to the 100% cohesive failure area observed for the control sample. Visual inspection of the failure surface for the Hexcel sample will not be capable of identifying



cohesive failure near the interface, which may explain the apparent adhesive failure observed, despite the 100% recovery in bond strength.

#### 4.6.2 Hexcel and Alcore Node Bond Peel strength versus Temperature

The node bond peel strength as a function of test temperature for the Alcore and Hexcel honeycomb samples is shown in Figure 4.6.2. The Alcore product indicates a superior initial strength and maintains superior performance in comparison to the Hexcel product as a function of test temperature.

Additionally, Alcore and Hexcel honeycomb samples were aged for 4 days at 95°C and 28 days at 70°C. In both cases no observable reduction in honeycomb peel strength was observed. The failure surfaces of these samples, predictably exhibited 100% cohesive failure area.

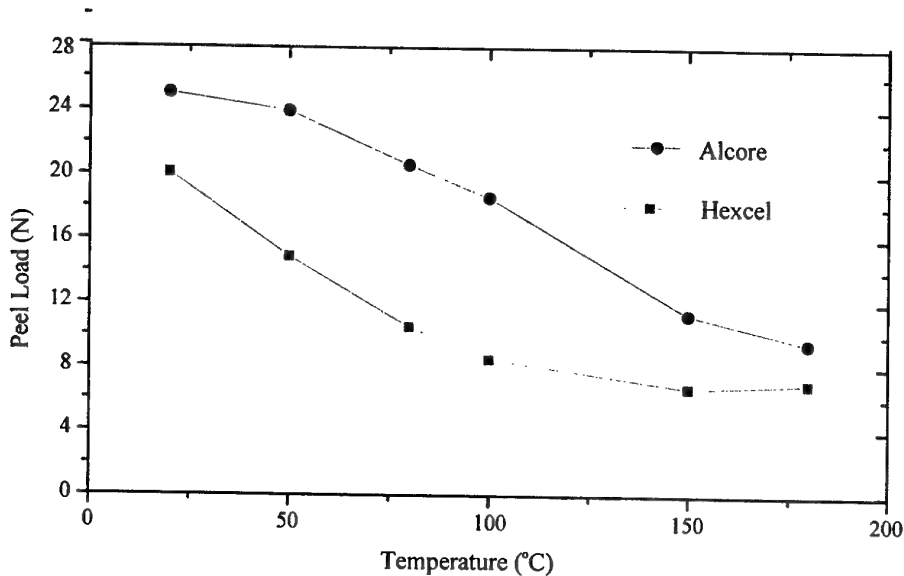


**Figure 4.6.2** Node bond peel load as a function of test Temperature for Alcore and Hexcel honeycomb using the method shown in Figure 2.5.

#### 4.6.3 Hexcel CR3 Honeycomb, prebond node conditioning, Pull-off strength

Three Elcometer samples were prepared in which the Hexcel CR3 honeycomb core was conditioned at 180°C for 500 hours. This conditioning was shown to reduce the node bond peel strength by 70% compared to the as received condition [14]. Table 4.6.3 indicates the pull-off tension measured for the pre-conditioned node bonds relative to control samples. The data in Table 4.6.3 suggests that even for cases where node bond degradation is significant, no obvious drop in pull-off tension for the sandwich panel occurs.

**Table 4.6.3** *Pull-Off tension measured for the Hexcel CR3 honeycomb sandwich samples in which node bonds were pre-conditioned at 180°C for 500 hours.*

Node Bond Conditioning	Pull-Off tension Strength (psi)	Failure Mode
NIL	1100 ± 100	Cohesive
500 hours at 180°C	990 ± 120	Cohesive

#### 4.6.4 Hexcel CR3 Honeycomb, prebond node conditioning, bend strength

Two Beam samples were prepared in which the Hexcel CR3 honeycomb core was conditioned at 180°C for 500 hours, as described for the Elcometer samples in section 4.6.3. The effect of an 80% reduction in the node bond peel strength on the bending properties of beam samples is indicated in Table 4.6.4. As with the pull-off tension data, there does not appear to be a significant effect on bending properties when node bonds of the honeycomb have been degraded. The result for the three point bend sample actually suggests an improvement in ultimate load, although variation expected over a range of samples may be expected to account for this higher value.

**Table 4.6.4** *Bending properties measured for the Hexcel CR3 honeycomb sandwich samples in which node bonds were pre-conditioned at 180°C for 500 hours.*

Condition/ Loading	P(N)	$\tau$ (MPa)	$\sigma$ (MPa)	D (N-mm <sup>2</sup> )	G(MPa)	U(N)
NIL/3 point	2260	1.4	240	2.5x10 <sup>8</sup>	250	2.2x10 <sup>5</sup>
NIL/4 point	3710	2.2	198			
500 hours at 180°C/ 3 point	2716	1.6	288	2.3x10 <sup>8</sup>	262	2.3x10 <sup>5</sup>
500 hours at 180°C/ 4 point	3532	2.1	188			

## 4.7 Water Diffusion Tests

A series of studies were undertaken with double sided honeycomb sandwich panels constructed from Hexcel CR3 honeycomb and bonded to 0.5mm thick skins using FM-300. The aim of the experiment was to determine if diffusion occurred preferentially along the node bond direction of the honeycomb core or through the fillet bond region of the sandwich panel.

### 4.7.1 Hexcel CR3 Honeycomb, Water uptake at 70°C

Initial experiments examined the water uptake for the Hexcel CR3 sandwich panel in 70°C water. Moisture ingress along a specific direction of the honeycomb sandwich was assessed by adhesively bonding aluminium strips along the side walls of the honeycomb sandwich using

FM-73 structural adhesive. In one instance strips were bonded normal to the ribbon direction of the panel, thereby exposing node bonds to the moisture. A second sample had strips bonded parallel to the ribbon direction and the final sample had all sides bonded. The ribbon direction and node bond locations are shown diagrammatically in Figure 4.7.1.

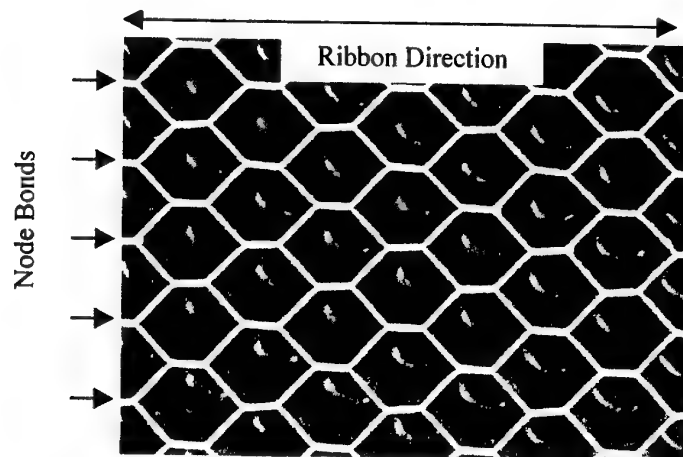


**Figure 4.7.1** Honeycomb core top view indicating the direction of the ribbon and the position of the node bonds.

Weight uptake for the respective samples was measured over two hundred hours and the results are shown in Figure 4.7.2.

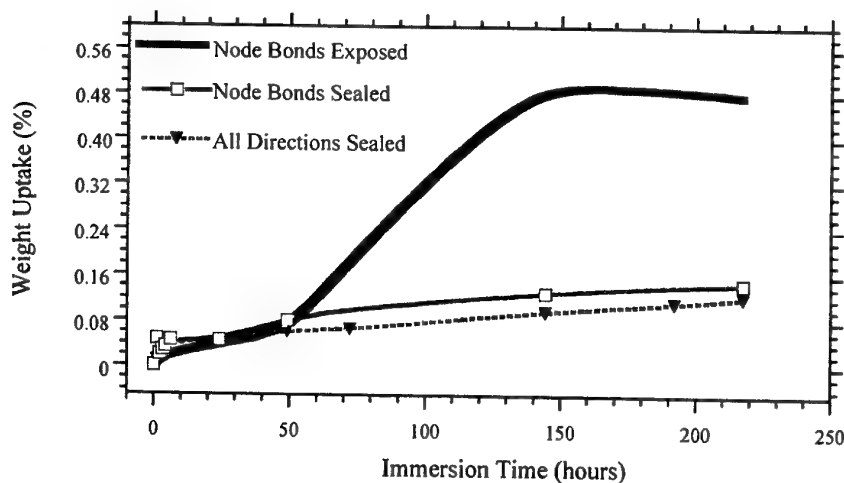


**Figure 4.7.2** Weight uptake as a function of immersion time in 70°C water for Hexcel CR3 honeycomb sandwich panels bonded with FM-300.

The data suggests in the initial stages of water uptake there is a preference for diffusion of water in the direction where node bonds are directly exposed to the water. When the ribbon direction is sealed or when all directions are sealed there appears to be minimal moisture uptake.

The top skin of the samples from the experiment shown in Figure 4.7.2 were manually peeled off to determine if any fillet bond degradation had resulted from the immersion in the 70°C water. Figure 4.7.3 shows the failure surfaces of the samples where the node and ribbon directions were sealed.

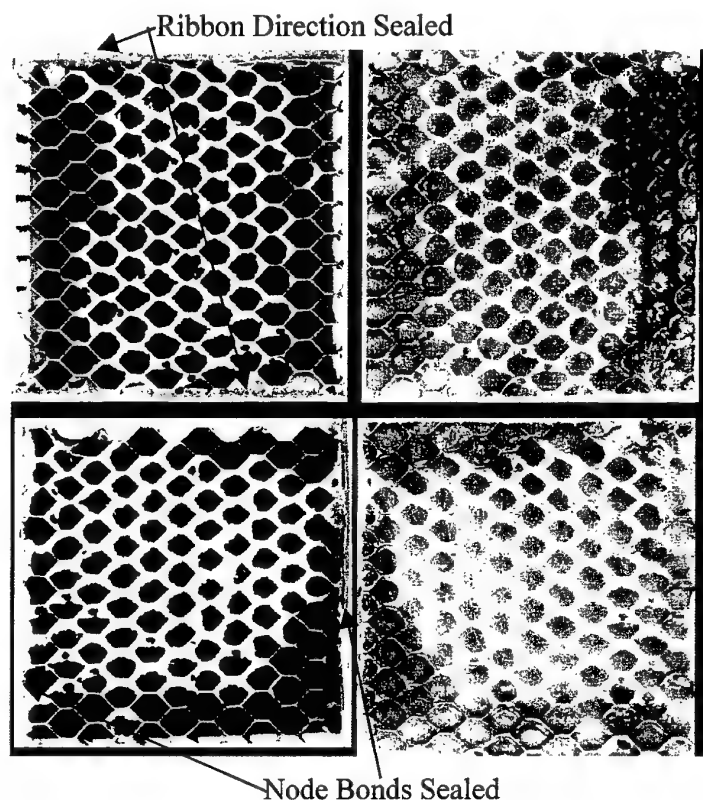


**Figure 4.7.3** Failure surfaces produced after immersion of sandwich panels in 70°C water for a sealed ribbon direction (Top) and sealed node direction (Bottom)

Figure 4.7.3 suggests that there is a preference for diffusion along the node bond direction, although in the case of the sample where the node bonds were sealed there appears to be some moisture ingress from the corners of the sample, suggesting poor sealing in this region and some exposure of the node bonds. Figure 4.7.4 shows the failure surface for a sample where all sides of the sandwich panel were sealed. Minimal fillet bond pull-out was observed for this sample which would suggest that diffusion is retarded by bonding the metal strips with the structural adhesive. This is consistent with diffusion coefficients reported for FM-73 of  $5 \times 10^{-13} \text{ m}^2/\text{s}$  in 70°C humid environments[15].

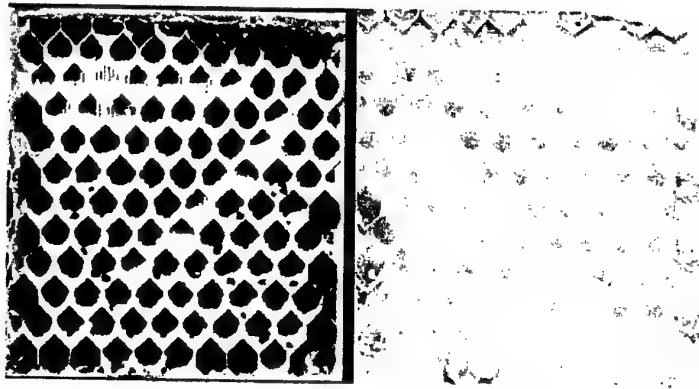


**Figure 4.7.4** Failure surface produced after immersion of the sandwich panel in 70°C water. The panel was sealed in the ribbon and node directions

The process of water diffusion into the honeycomb samples is not consistent. Several experiments indicate that the water uptake can be variable and the extent of fillet bond degradation as measured by manually peeling the top skin off the panel is also irregular. Figure 4.7.5 shows the failure surfaces of a panel which had been immersed in 70°C water for 10 months. The failure surfaces indicated only minor areas of fillet bond pull-out, compared to the sample shown in Figure 4.7.3(Top), which exhibited greater failure after only 4 weeks immersion in 70°C. The sample also showed water had only entered a small number of cells, close to the edge of the sandwich panel. These results may suggest inconsistencies in honeycomb core material or sandwich fabrication.

An additional point of interest was that the cells with water in them all exhibited substantial amounts of cohesive failure of the fillet bond. If water had diffused along the fillet bond in these regions there would possibly be a greater amount of fillet bond pull-out. This result may provide further evidence to support the conclusion that moisture diffusion is occurring preferentially through the honeycomb node bonds.

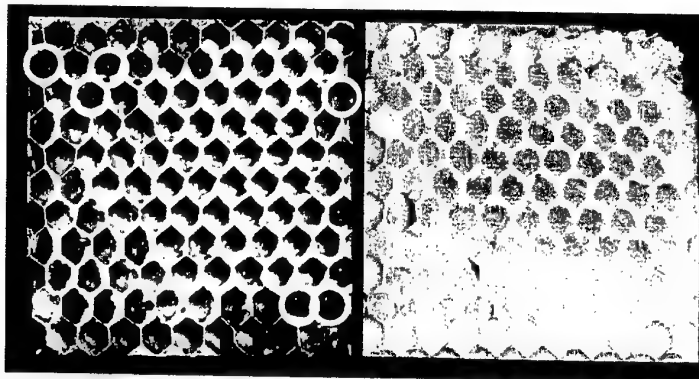


**Figure 4.7.5** Failure surfaces resulting from 10 months immersion of a double aluminium skinned Hexcel CR3 honeycomb sandwich. White circles indicate cells containing water.

#### 4.7.2 Hexcel CR3 Honeycomb, Water uptake at 70°C, Radiography tests

Radiographic inspection of a Hexcel CR3 honeycomb sandwich bonded with FM-300 was undertaken in order to investigate possible moisture ingress paths. The sandwich sample was immersed in a 50%w/w aqueous solution of cerium nitrate in order to provide contrast in the radiographic images for the diffusing solution. The sample was immersed for 10 days and radiographic images acquired over this period.

Upon removal from the cerium solution the sandwich skin was removed and the failure surface photographed. This image is shown in Figure 4.7.6. The failure surface indicates a preference for diffusion along the node bond direction and in most areas where fillet bond pull-out has occurred the node bonds also have failed. There is also substantial evidence of cell wall corrosion in the regions where node and fillet bond failure have occurred. In regions where cohesive failure of the fillet bond has occurred the cell walls appear not to have corroded and some of the node bonds still appear to be intact.

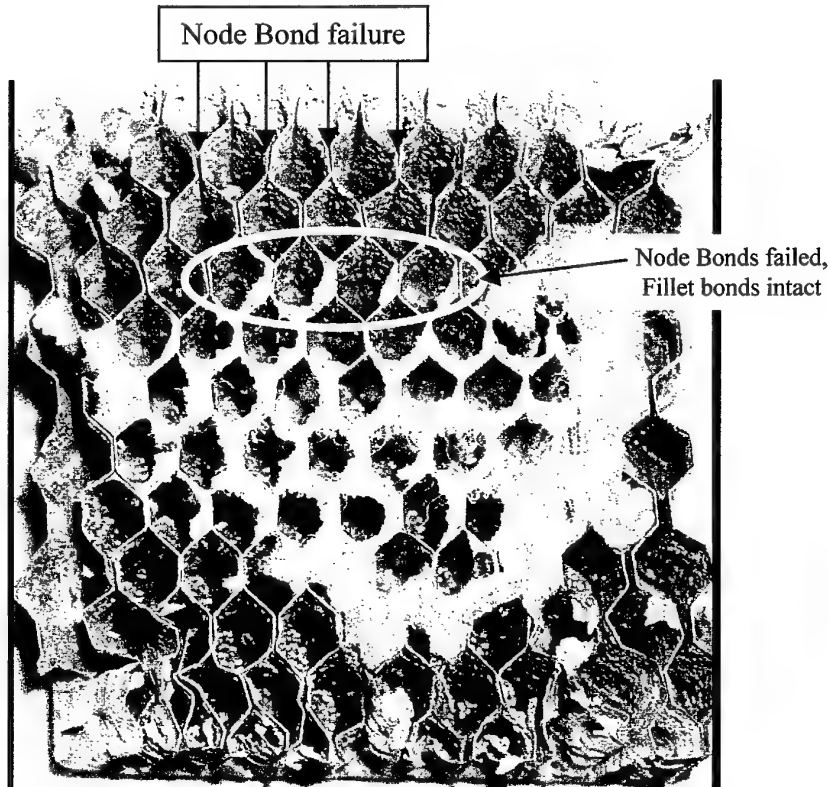


**Figure 4.7.6** Failure surface resulting from immersion of Hexcel CR3 core bonded to 0.5mm thick aluminium skins with FM-300 in 70°C concentrated cerium nitrate solution for 10 days.

The radiographic images acquired as a function of immersion time are presented in *Appendix 1*, together with a discussion of the data. In brief terms, the radiographic data indicated that the radio opaque fluid, cerium nitrate solution, could be observed to migrate along the node bonds

as evidence of the swelling between the two layers of bonded aluminium foil. The fluid appears to move a distance of 3 node bonds during the 10 day exposure and migrates around the cell walls. Whether diffusion occurs through the fillet bond before diffusing through the node bond is not definitive. If diffusion occurred through the fillet bond it may be expected to produce a more symmetric failure surface. The failure surface in Figure 4.7.6, and radiographs presented in the Appendix, suggest greater ingress along the node bond direction than across the node bond direction. The moisture ingress across the node bonds appears to have only progressed by 1 cell or less. Additionally, as noted in Figure 4.7.6, the third row of cells shows that the node bonds have separated, indicating degradation as a result of cerium nitrate ingress. Notably, the fillet bonds do not appear to have been degraded to the same extent, as shown by the larger regions of cohesive failure in the FM-300 adhesive of the fillet bond. This provides further evidence to suggest that the moisture ingress has proceeded through the node bonds in preference to the fillet bond region.

## 4.8 Adhesive Water Diffusion Tests

### 4.8.1 Mass Uptake Studies

Mass uptake of FM-300 disks as a function of immersion time in 50°C, 70°C and 95°C water are shown in Figures 4.8.1 to 4.8.3. The mass uptake for FM-300 exposed to a 70°C and condensing humidity environment is shown in Figure 4.8.4. The plots show mass uptake at time  $t$  ( $M_t$ ) normalised to the saturation mass uptake at infinite time ( $M_0$ ).

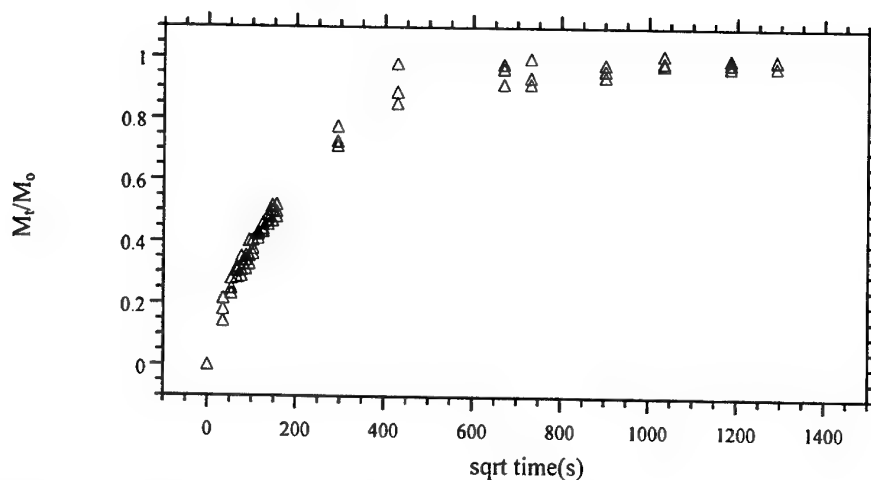


**Figure 4.8.1** Mass uptake of FM-300 immersed in 50°C distilled water as a function of time.

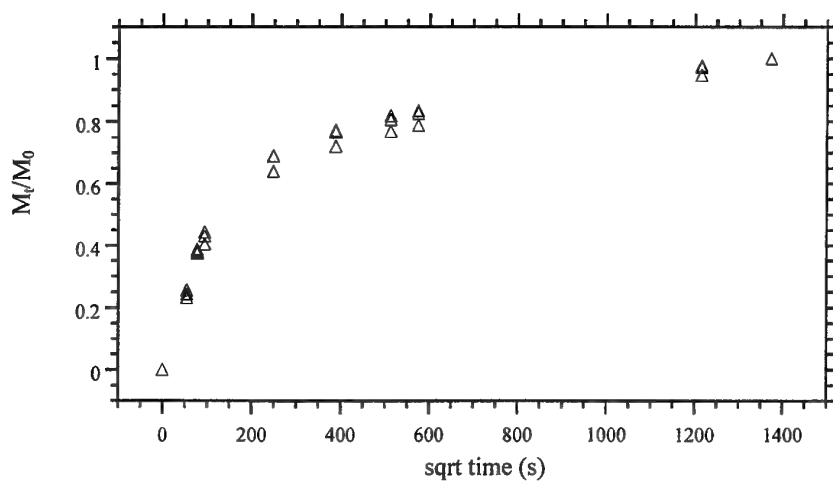


**Figure 4.8.2** Mass uptake of FM-300 immersed in 70°C distilled water as a function of time.

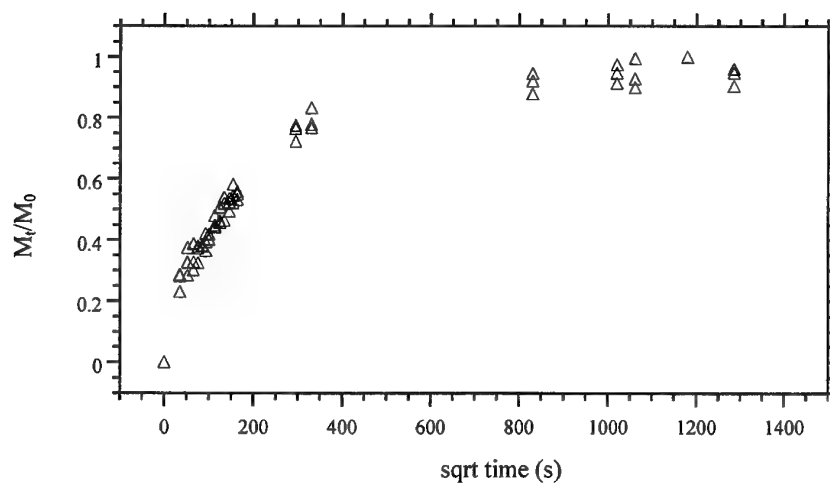


**Figure 4.8.3** Mass uptake of FM-300 immersed in 95°C distilled water as a function of time.



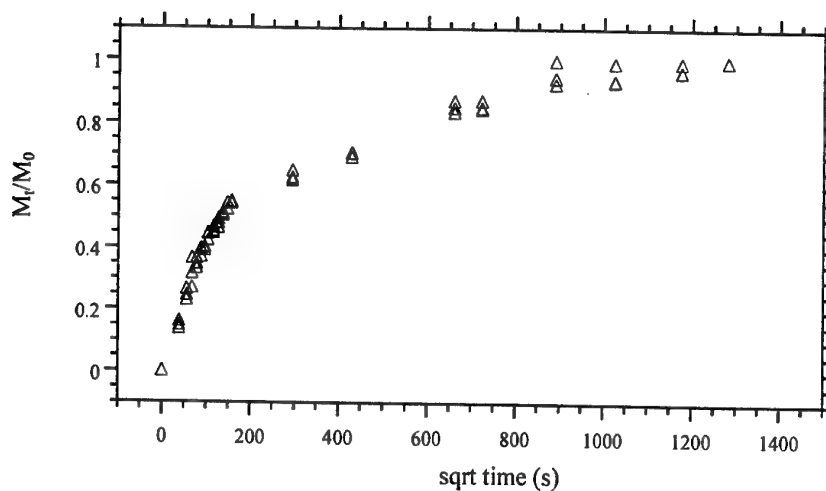


**Figure 4.8.4** Mass uptake of FM-300 exposed to 70°C condensing humidity environment as a function of time.

Mass uptake of FM-300-2K disks as a function of immersion time in 70°C and 95°C water are shown in Figures 4.8.5 and 4.8.6. The mass uptake for FM-300-2K exposed to a 70°C and condensing humidity environment is shown in Figure 4.8.7.

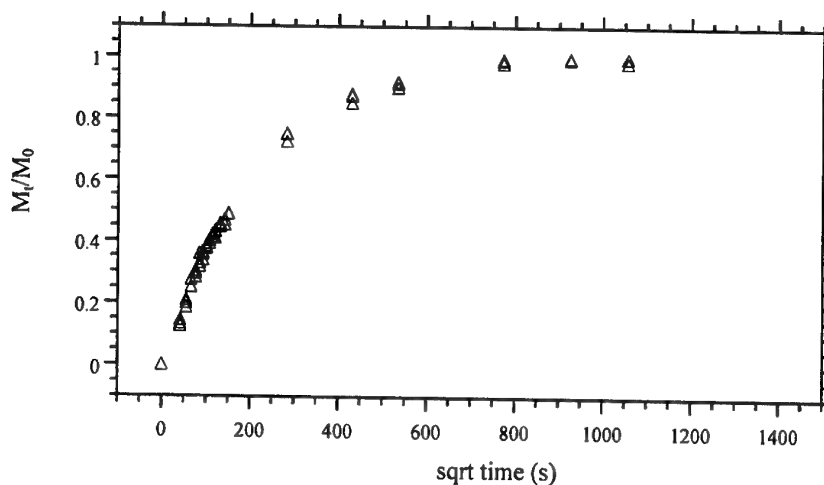


**Figure 4.8.5** Mass uptake of FM-300-2K immersed in 70°C distilled water as a function of time.

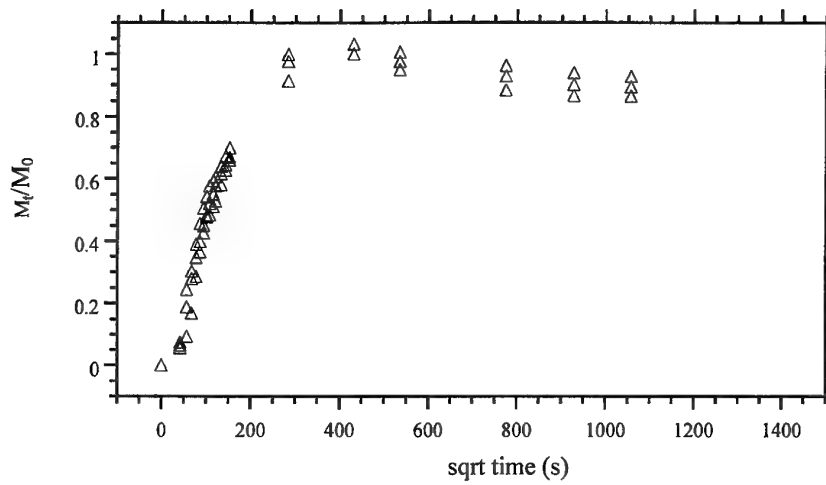


**Figure 4.8.6** Mass uptake of FM-300-2K immersed in 95°C distilled water as a function of time.

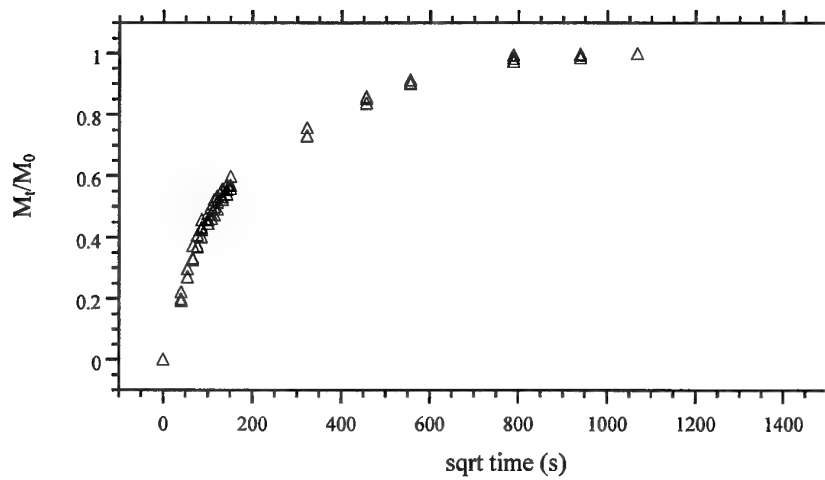


**Figure 4.8.7** Mass uptake of FM-300-2K exposed to 70°C condensing humidity environment as a function of time.

Table 4.8.1 indicates the diffusion coefficients,  $D_t$ , calculated at the different temperatures and exposure conditions for the FM-300 and FM-300-2K adhesive together with the saturation mass uptake,  $M_0$ .

The diffusion coefficient,  $D_a$ , was calculated using equation 4.8, where  $h$  is the thickness of the adhesive disk and  $t$  is the exposure time. The diffusion coefficient was calculated from the linear portion of the plots shown in Figures 4.8.1 to 4.8.7 for  $M_t/M_0$  values less than 0.4 [16].

$$\frac{M_t}{M_0} = \frac{4}{h} \sqrt{\frac{D_a \cdot t}{\pi}} \quad (4.8)$$

**Table 4.8.1** Diffusion coefficients and saturation mass uptake for FM-300 and FM-300-2K.

Exposure	50°C/Immersion		70°C/Immersion		70°C/100%RH		95°C/Immersion	
Adhesive	$D_a(m^2/s)$	$M_0(\%)$	$D_a(m^2/s)$	$M_0(\%)$	$D_a(m^2/s)$	$M_0(\%)$	$D_a(m^2/s)$	$M_0(\%)$
FM-300	$4.2 \times 10^{-13}$	2.7	$7.0 \times 10^{-13}$	4.3	$7.0 \times 10^{-13}$	4.3	$2.2 \times 10^{-12}$	8.4
FM-300-2K	---	---	$7.5 \times 10^{-13}$	4.7	$7.2 \times 10^{-13}$	4.5	$2.6 \times 10^{-12}$	7.6

The data shown in Table 4.8.1 indicates that the diffusion coefficients for the two adhesives examined are very similar and that the water uptake in a condensing humidity environment is similar to full immersion for 70°C. Figure 4.8.8 indicates an Arrhenius plot for the measured diffusion coefficients for FM-300. The calculated activation energy is 37 kJ/mole, similar to previously measured values for water diffusion in epoxy adhesives [17].

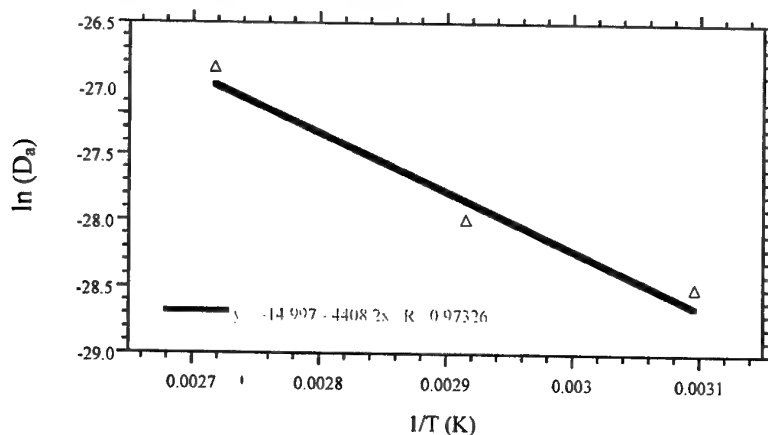


**Figure 4.8.8** Arrhenius plot for moisture diffusion in FM-300 adhesive.

#### 4.8.2 Moisture Saturated Adhesive Drying Rate at 80°C

Mass loss of FM-300 and FM-300-2K adhesive disks that had reached saturation moisture uptake over a several month period was measured in an 80°C isothermal oven. Typical plots of  $M_t/M_0$  as a function of time are indicated in Figures 4.8.9 and 4.8.10 for FM-300 adhesive and in Figures 4.8.11 and 4.8.12 for FM-300-2K adhesive. The diffusion coefficients measured for drying of the two types of adhesive are indicated in Table 4.8.2, together with the saturation

mass uptake and the relative change in the diffusion coefficient measured for the mass uptake studies, indicated in Table 4.8.1.

The data in Table 4.8.2 indicates that drying the adhesives in a 80°C environment results in rapid loss of moisture. The drying rate for the FM-300 adhesive appears to slightly greater than the FM-300-2K adhesive. The relative increase in drying rate, as expected, is independent of the mass uptake of the adhesive. The data suggests that drying the sandwich samples at 80°C would result in a significant reduction in the adhesive water content within a matter of hours.

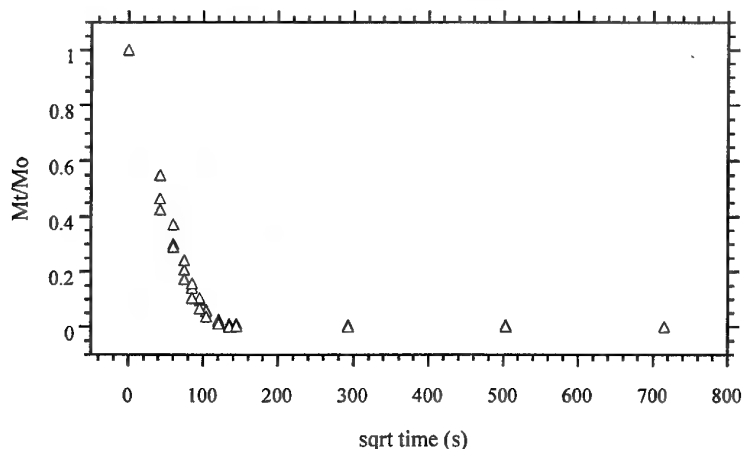


**Figure 4.8.9** Drying rate in a 80°C isothermal oven for FM-300 adhesive saturated by immersion in 95°C water

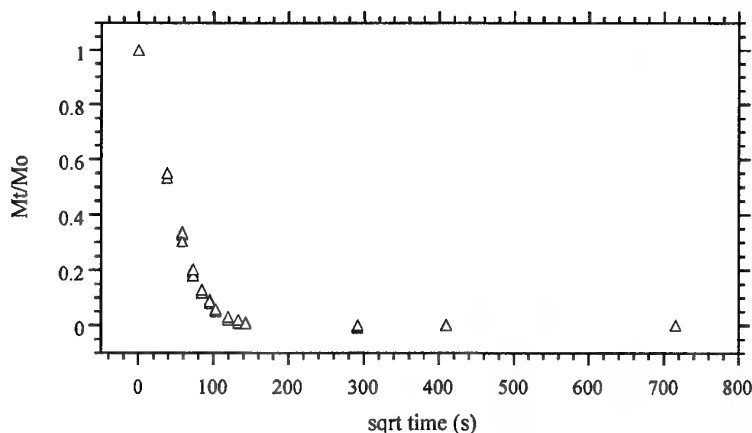


**Figure 4.8.10** Drying rate in a 80°C isothermal oven for FM-300 adhesive saturated by exposure to a 70°C/100%RH environment.

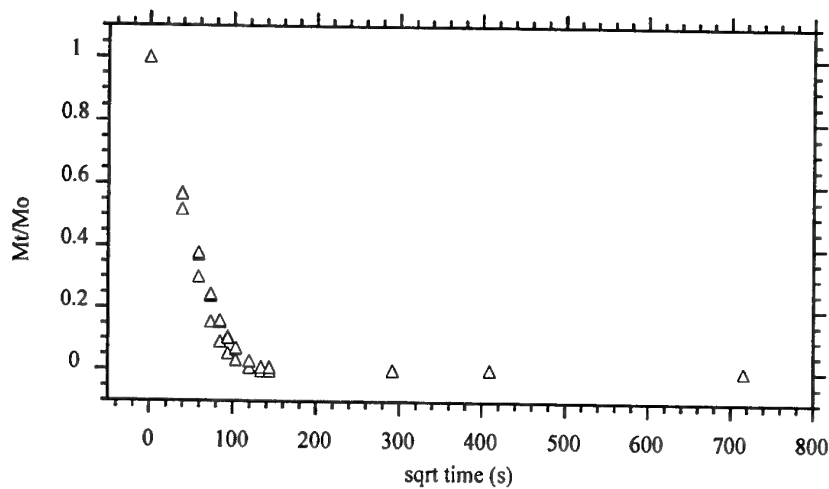


**Figure 4.8.11** Drying rate in a  $80^{\circ}\text{C}$  isothermal oven for FM-300-2K adhesive saturated by immersion in  $95^{\circ}\text{C}$  water

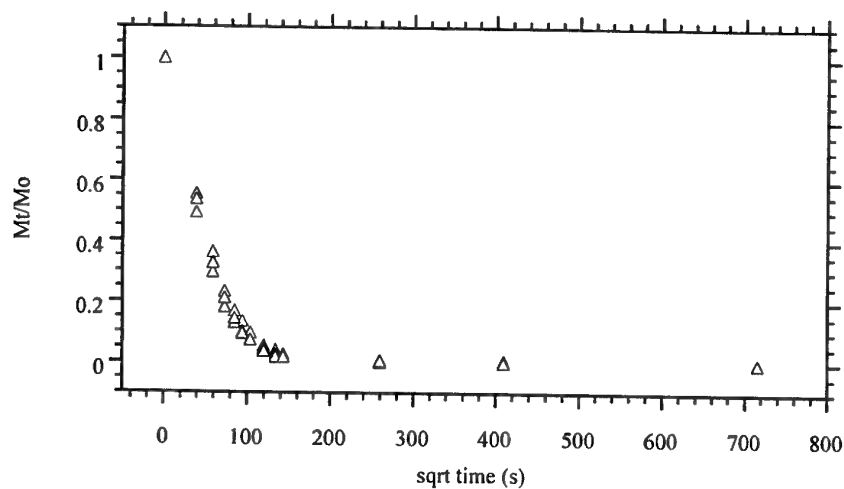


**Figure 4.8.12** Drying rate at in a  $80^{\circ}\text{C}$  isothermal oven for FM-300-2K adhesive saturated by immersion in  $70^{\circ}\text{C}$  water

**Table 4.8.2** The diffusion coefficients measured for drying of the adhesives, the saturation mass uptake and the relative change in the diffusion coefficient.

Adhesive	Mass Uptake/Temp	$D_a(\text{drying})$	$D_a(\text{moisture uptake})$	$D_a(\text{drying})/D_a(\text{moisture uptake})$
FM-300	4.3 / $70^{\circ}\text{C}$ immersion	$7 \times 10^{-13}$	$4.5 \times 10^{-12}$	6.4
FM-300	4.3 / $70^{\circ}\text{C}$ C.H.	$7 \times 10^{-13}$	$5.2 \times 10^{-12}$	7.4
FM-300	8.4 / $95^{\circ}\text{C}$ immersion	$2.2 \times 10^{-12}$	$5.0 \times 10^{-12}$	2.3
FM-300-2K	4.7 / $70^{\circ}\text{C}$ immersion	$7.5 \times 10^{-13}$	$3.7 \times 10^{-12}$	4.9
FM-300-2K	4.5 / $70^{\circ}\text{C}$ C.H.	$7.2 \times 10^{-13}$	$3.7 \times 10^{-12}$	5.1
FM-300-2K	7.6 / $95^{\circ}\text{C}$ immersion	$2.6 \times 10^{-12}$	$3.5 \times 10^{-12}$	1.3

## 5. Discussion

### 5.1 Honeycomb Characterisation

#### 5.1.1 Honeycomb Node Bonds

The relative durability performance of the node bonds in the Hexcel and Alcore samples suggest that differences in node bond adhesive may be an important factor. Alcore node bond peel strength does not degrade as significantly in water as the Hexcel node bond, refer Figure 4.6.1, and the percentage of adhesive failure is also markedly less in the Alcore case. The strontium chromate fibres present in the polyamide adhesive of the Alcore node bonds, refer Figure 3.5, may offer more corrosion resistance than the Hexcel nitrile rubber modified phenolic node bonds, refer Figure 3.2.

The incomplete coverage of both the Hexcel and Alcore node bond adhesive, refer Figure 3.1 and Figure 3.4, may also be expected to provide paths for moisture ingress into the adhesive bond and facilitate bond degradation. Given the Alcore node bond adhesive coverage appears to be less than the Hexcel case, and yet does not degrade in a moist environment as rapidly as the Hexcel node bonds, this may suggest that the coverage of the adhesive is not a dominant factor. Node bond durability may depend more on the properties of the node adhesive and the hydrolytic stability of the node adhesive bond with the honeycomb metal surface.

For both the Alcore and Hexcel honeycomb, 100% recovery of the peel strength of the node bonds could be achieved after vacuum drying, suggesting that the moisture uptake by the node adhesives was a reversible process. This result is significant for repair of old honeycomb panels and suggests panel drying may be beneficial for recovery of some panel mechanical properties.

#### 5.1.2 Honeycomb Surface Coatings

Chemical analysis of the coatings on the Hexcel and Alcore honeycomb suggests some subtle differences. The Hexcel CR3 honeycomb appears to have a chromium oxide layer which is coated with a very thin silicon containing organic layer. The Alcore Dura-Core coating also appears to have a chromium oxide layer which may be marginally thinner than the Hexcel CR3 chromium layer, but does not appear to be coated with an organic layer. The durability performance of these Alcore and Hexcel honeycomb samples was notably different for a range of the durability tests carried out and may suggest that the organic coating on the Hexcel CR3 surface is critical in the production of more durable adhesive bonds.

Analysis of the Alcore PAA honeycomb suggests that a thick polyamide top-coat exists on the metallic surface which is of the order of 1µm thick. This analysis is consistent with data reported by the Swiss [11] for Hexcel PAA core and indicates the anodised surfaces of the honeycomb prepared by both manufacturers are primed directly after anodisation. Hexcel PAA core should be analysed in future so direct comparison of the Alcore and Hexcel products can be performed. The topcoat of the Alcore PAA honeycomb is substantially thicker and of different chemical composition to the Hexcel CR3 product. The significantly improved durability performance of the PAA product relative to the Dura-Core and CR3 honeycomb may depend significantly on the chemical character of the polyamide type top-coat layer.

## 5.2 Flatwise Tension Testing

The analysis of the Flatwise tension (FWT) testing carried out in section 4.1 presents difficulties associated with the procedure employed to test the conditioned honeycomb panels. There is a substantial amount of evidence to suggest that the procedure of bonding the testing blocks to the conditioned samples at 80°C for 16 hours resulted in some recovery of the FWT strength. This was particularly evident when comparing the FWT data in Figure 4.1.3 with the Elcometer data in Figure 4.2.1 for FM-300 adhesive bonded to Hexcel CR3 honeycomb. The Elcometer testing in Figure 4.2.1 clearly indicates that after only 1 day of immersion the pull-off tension decreases to a plateau value of about 400psi. The data in Figure 4.1.3 for the FWT testing shows erratic behaviour which suggests drying effects are recovering FWT strength. Failure analysis of representative FWT and Elcometer samples in sections 4.4.1 and 4.4.3, respectively, indicated that the FWT sample exhibited a greater proportion of fracture in the FM-300 layer than the interfacial failure observed for the Elcometer sample. This result is consistent with moisture removal from the FWT sample recovering adhesive bond strength.

Further evidence to support this conclusion is provided by the adhesive diffusion studies carried out in section 4.8.2. Adhesives that have reached saturation mass uptake are nearly completely dry within three hours at 80°C. Hence, single sided honeycomb panels would be expected to recover mechanical strength as a function of drying time in a reasonably short time frame. Double sided samples, however, may be expected to take longer to dry given there is not a direct path for moisture vapour to escape from the bondline. This would partly explain the differences in the Flat-wise tension measurements conducted for the single and double skin samples in Figures 4.1.2 and 4.1.3.

Whilst there are clearly some difficulties in directly comparing the FWT results in section 4.1, the general trends observed for a number of the experiments helped validate the Elcometer test method. The Elcometer test indicated a linear relationship between adhesion failure and pull-off strength, refer Figure 4.2.7, as was observed in Figure 4.1.1 for the FWT test. Similarly, the dry FWT strength and plateau FWT strength of conditioned Hexcel CR3, refer Figure 4.1.2, was comparable to the Elcometer values, refer Figure 4.2.1.

Comparison of the durability tests conducted using Elcometer measurements provide a more reliable guide to the relative performance of the different honeycomb and adhesive combinations. Drying effects resulting in partial recovery of the original FWT strength should be minimised for the Elcometer testing, given the sample preparation procedure employed.

## 5.3 Modelling Moisture Degradation in Honeycomb Structure

The influence of humid exposure on the measured strength of honeycomb panels involves understanding the complex nature of moisture diffusion in adhesively bonded structure. The different modes of failure that may result from moisture diffusion along the various paths available needs to be considered.

### 5.3.1 The Influence of Moisture on the Locus of Fracture

Fracture analysis conducted in section 4.4 indicated that in most cases the ingress of moisture into the fillet bond region of the honeycomb panel resulted in fillet bond pull-out, refer Figure 4.4.6. This mode of failure involved moisture displacing adhesive bonds at the FM-300 to

honeycomb interface. In both the peel and Elcometer testing there appeared to be a linear correlation between the percentage of adhesion failure resulting from fillet bond pull-out and honeycomb panel strength. Clearly, in this instance moisture diffusion either through the adhesive to the interfacial region and/or along the honeycomb-adhesive interface was responsible for the bond degradation observed. Whilst a plateau value in adhesion strength corresponded with adhesion failure area approaching 90 to 100%, in some cases extended exposure resulted in further reduction in bond strength, refer Figure 4.2.2. Fracture analysis suggested that this continued reduction in bond strength resulted from moisture at the honeycomb and adhesive interface reacting with the honeycomb surface and producing a weakened hydrated layer, refer Figure 4.4.8. This suggests that honeycomb sandwich panel degradation may involve two phases. In the initial stage moisture diffusion displaces adhesive bonds and in the second stage this moisture can react with the honeycomb surface and produce a weakened hydrated layer.

Whilst fillet bond pull-out was the most common mode of failure observed, moisture ingress into the honeycomb panel also produced adhesion failure at the skin and adhesive interface. This mode of failure was observed for the Hexcel CR3 honeycomb bonded to FM-300-2K, refer Figure 4.3.2. The initial peel strength of the honeycomb bond was not significantly affected from exposure to moisture, however, between 3 and 6 months the skin to adhesive failure increased to 100%. This mode of failure suggests that in cases where the adhesive to honeycomb fillet bonds are hydrolytically more stable than the skin to adhesive bonds that failure will eventually propagate at this interface. Some indication of this failure mode was also observed for the FM-300 and PAA honeycomb peel samples. At extended exposure the corners of the skin indicated skin to adhesive failure. The PAA honeycomb to FM-300 bonds were clearly the most resistant to moisture degradation of any of the conditioned specimens.

The durability of the untreated Alcore honeycomb bonded to FM-300 and FM-300-2K indicated the most unusual behaviour of all the honeycomb samples tested. Generally, the initial bond strength degraded at a rapid rate in the first few weeks of environmental exposure and then recovered to a strength value similar to or greater than the dry strength value, refer Figures 4.2.2 and 4.3.1. In this case failure changed from fillet bond pull-out to fillet bond fracture, or cohesive failure of the fillet adhesive layer. This result suggested that moisture ingress at the honeycomb to adhesive interface was altering the hydrolytic stability of the fillet bonds in a favourable manner. In some instances the degradation of the peel strength after 6 months of exposure to humid conditions resulted from skin to adhesive failure, refer Figure 4.3.1. This failure was observed for the honeycomb samples that had exhibited excellent fillet bond hydrolytic stability and indicates the improvement in bond durability caused by moisture ingress in the fillet bond for the untreated honeycomb samples.

SEM analysis in section 4.4.3 of failed untreated honeycomb peel panels revealed some explanation for the apparent improvement in the peel strength as a function of conditioning time. The moisture which diffused to the honeycomb and adhesive interface appeared to react with the aluminium over time and produce localised areas of hydrated oxide. The density of these hydrated oxide islands increased as a function of humid exposure time and suggested that the improved peel strength was related to their presence. Possibly, the oxide nodules act as microscopic wedges which increase the force required to break the adhesive to honeycomb bonds, forcing either cohesive failure of the fillet adhesive or, at extended exposure times, failure at the skin to adhesive interface.



The failure modes observed for the conditioned honeycomb samples provides an indication of the locus of fracture expected based on the relative hydrolytic stability of the skin-adhesive and honeycomb-adhesive bonds.

### 5.3.2 Bond Degradation as a Function of Moisture Diffusion Rates

Previous work has formulated theories based on the relationship between the retention of adhesion strength and the moisture content of the bonded sample [17] [18] [19]. The basis of these theories is that moisture uptake in an epoxy adhesive joint can be modelled as Fickian type diffusion. One theory considered that a critical concentration of water in the adhesive was required for bond degradation to proceed [17]. By calculating the adhesive moisture concentration as a function of distance into the joint, on the basis of the diffusion rate in the bulk adhesive, it was shown that a critical concentration of water had diffused a distance into the joint that corresponded to the observed progression of adhesion failure. An alternative theory modelled the mass uptake of moisture in an adhesive joint as a function of time and related this value through a proportionality constant to the measured adhesion strength [18]. The proportionality constant was a sensitivity factor which described the efficiency of the absorbed moisture in producing adhesion loss. This theory enabled a diffusion coefficient for moisture uptake in the bulk adhesive and adhesive joint to be compared and thereby provided an indication of whether diffusion in the adhesive or along the interface was responsible for bond degradation. These two theories provide complementary information that can be used to understand moisture diffusion in adhesive joints.

#### 5.3.2.1 *Modelling the Decay of Tension Strength in Humid Environments*

The degradation in pull-off tension strength (POTS) of the conditioned honeycomb samples was modelled on the basis of moisture mass uptake rate of the single sided honeycomb sample, assuming Fickian type diffusion using the theory discussed in section 5.3.2 [18]. The diffusion was considered to be one dimensional and the diffusion distance of 0.6mm was estimated from cross-sectional analysis of the fillet bonds formed in the honeycomb panels using an optical micrograph. A typical cross-section is shown in Figure 5.3.1. This distance approximately corresponds to either diffusion through the adhesive to the honeycomb metal surface or along the interfacial region between the adhesive and honeycomb which would result in 100% adhesion failure area.

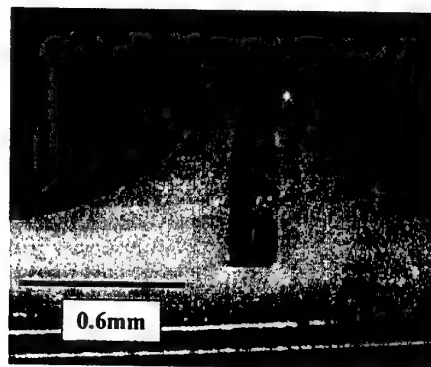


**Figure 5.3.1** *Cross-section of the FM-300 adhesive fillet bond.*

Equation 5.3.1 indicates the relationship between moisture diffusion in the adhesive joint and bond strength used to model the data in section 4.2 [18].

$$S/S_0 = 1 - P(M_t/M_0) \quad 5.3.1$$

$$P = pM_0/S_0 \quad 5.3.2$$

where  $S_0$  is the initial dry strength of the honeycomb sample,  $S$  is the strength of the joint at time  $t$  of exposure,  $M_t$  is the mass uptake of moisture at time  $t$ ,  $M_0$  the saturation mass uptake,  $P$ , defined in equation 5.3.2, is the ratio at which water contributes to bond breakage and  $p$  is the adhesion breakage parameter that provides the sensitivity of the honeycomb bond sample to moisture uptake in the adhesive.

$M_t/M_0$  was calculated using the first 30 terms in the convergent series of equation 5.3.3.

$$\frac{M_t}{M_0} = 1 - \frac{8}{\pi^2} \sum_{n=0}^{100} \frac{1}{(2n+1)^2} \cdot e \left[ - \frac{(2n+1)^2 \cdot \pi^2 \cdot D \cdot t}{4l^2} \right] \quad 5.3.3$$

where  $D$  is the diffusion coefficient and  $l$  is the diffusion length.

Data was fitted by adjusting the values of  $D$  and  $P$  to produce the closest approximation. Table 5.3.1 indicates the values of  $D_j$ , diffusion coefficient for the honeycomb joint,  $P$  and  $p$  calculated for the conditioned honeycomb samples tested in tension. The relative difference in  $D_j$  and  $D_a$ , diffusion coefficient for the bulk adhesive, is also provided. Figures 5.3.2 to 5.3.8 indicate the fit to the data for the conditioned honeycomb samples tested in tension. The blue line indicates the fit generated using the values in Table 5.3.1.

**Table 5.3.1** Values of  $D_j$ ,  $P$  and  $p$  calculated for the conditioned honeycomb samples tested in tension (imm.=fully immersed CH=condensing humidity).

Honeycomb	Adhesive	Exposure	$D_j(m^2/s \times 10^{-13})$	P	p (psi/wt%)	$D_j/D_a$ (%)
Hexcel CR3	FM-300	95°C/imm	24	0.6	83	109
Hexcel CR3	FM-300-2K	95°C/imm	24	0.5	69	109
Hexcel CR3	FM-300	70°C/imm	0.8	0.6	150	18
Hexcel CR3	FM-300-2K	70°C/imm	0.8	0.4	100	18
Hexcel CR3	FM-300	70°C/CH	0.8	0.35	88	18
Hexcel CR3	FM-300-2K	70°C/CH	0.8	0.2	50	18
Duracore	FM-300	70°C/imm	2	0.7	175	43
Duracore	FM-300-2K	70°C/imm	2	0.7	175	43
Duracore	FM-300	70°C/CH	2	0.7	175	43
Duracore	FM-300-2K	70°C/CH	2	0.7	175	43
Untreated*	FM-300	70°C/imm	2	0.7	175	43
Untreated*	FM-300-2K	70°C/imm	2	0.7	175	43

\* fit only for initial exposure times, extended exposure actually increases bonded panel strength.

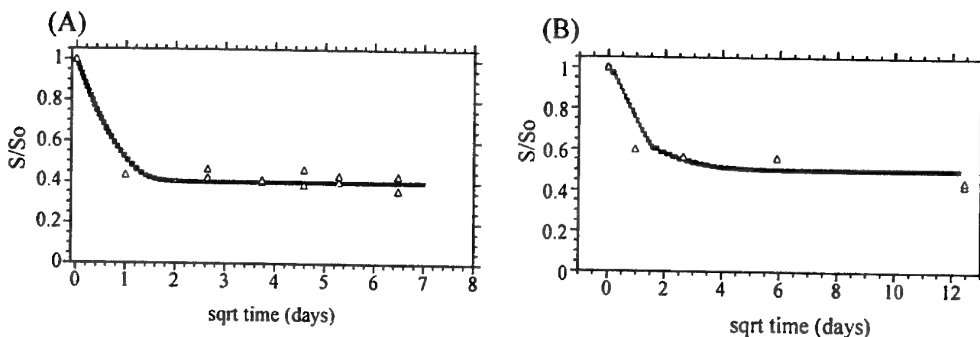


**Figure 5.3.2** Data fit using equation 5.5 for Hexcel CR3 bonded to (A) FM-300 and (B) FM-300-2K, immersed in 95°C water.

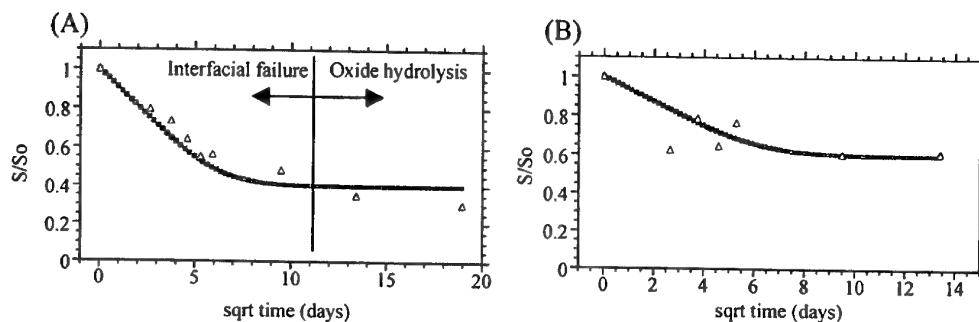


**Figure 5.3.4** Data fit using equation 5.5 for Hexcel CR3 bonded to (A) FM-300 and (B) FM-300-2K, immersed in 70°C water.

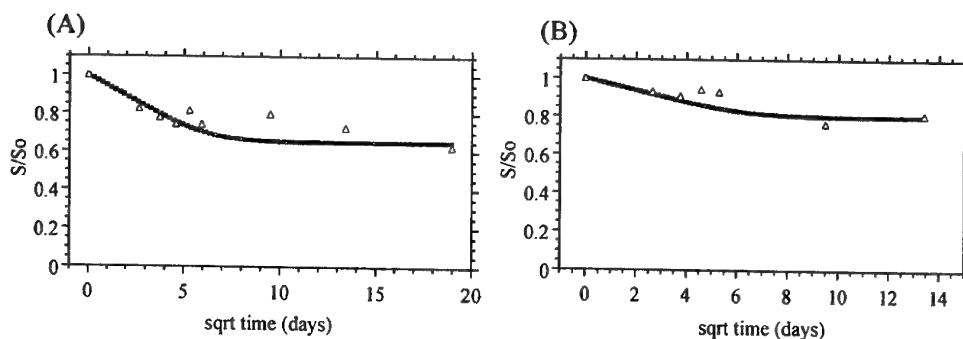


**Figure 5.3.5** Data fit using equation 5.5 for Hexcel CR3 bonded to (A) FM-300 and (B) FM-300-2K, exposed to 70°C condensing humidity.

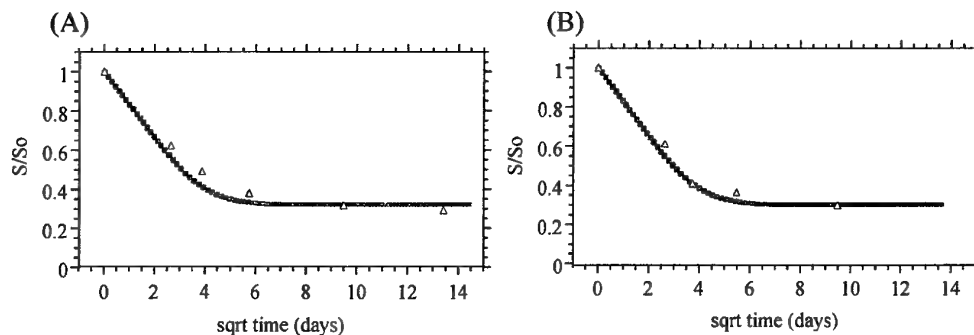


**Figure 5.3.6** Data fit using equation 5.5 for Duracore bonded to (A) FM-300 and (B) FM-300-2K, immersed in 70°C water.

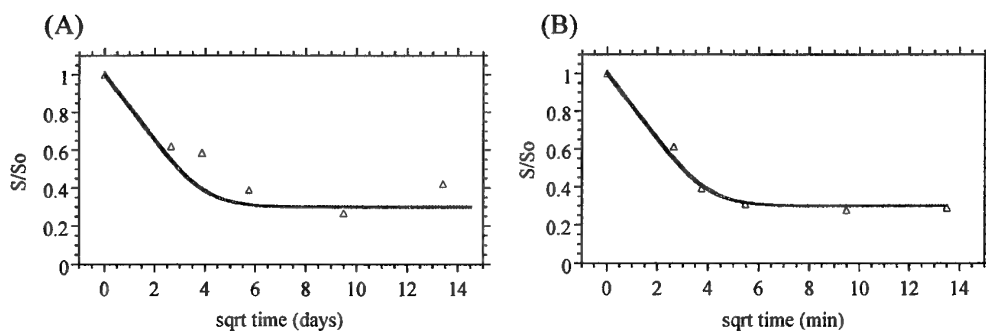


**Figure 5.3.7** Data fit using equation 5.5 for Duracore bonded to (A) FM-300 and (B) FM-300-2K, exposed to 70°C condensing humidity.

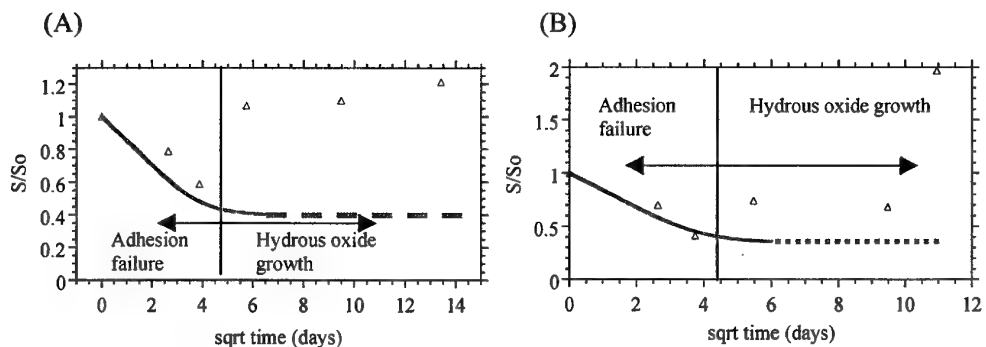


**Figure 5.3.8** Data fit using equation 5.5 for Untreated Alcore bonded to (A) FM-300 and (B) FM-300-2K, immersed in 70°C water.

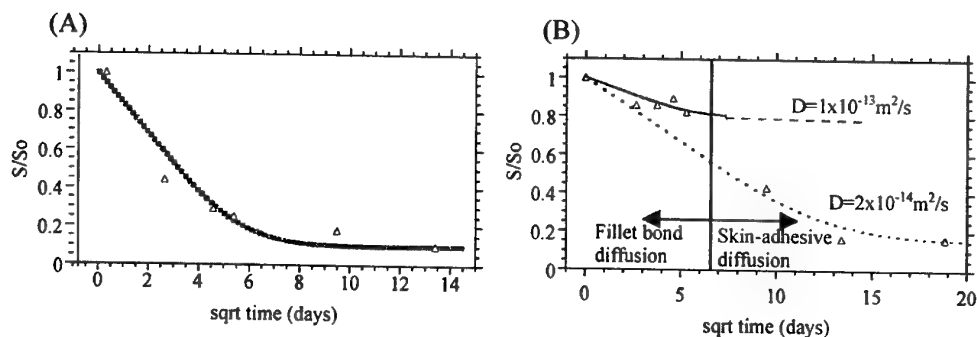
### 5.3.2.2 Modelling the Decay of Peel Strength in Humid Environments

Table 5.3.2 indicates the values of  $D$ ,  $P$  and  $p$  calculated for the conditioned honeycomb samples tested in peel. Figures 5.3.9 to 5.3.11 indicate the fit to the data for the conditioned honeycomb samples tested in peel. The blue line indicates the fit generated using the values in Table 5.3.2

**Table 5.3.2** Values of  $D$ ,  $P$  and  $p$  calculated for the honeycomb samples tested in peel, conditioned in a  $70^{\circ}\text{C}$ , condensing humidity.

Honeycomb	Adhesive	$D$ ( $\text{m}^2/\text{s} \times 10^{-13}$ )	$P$	$p$ ( $\text{kg} \cdot \text{mm}/\text{mm}/\text{wt}\%$ )	$D_f/D_s$ (%)
Hexcel CR3	FM-300	1	0.9	2.5	23
Hexcel CR3	FM-300-2K	0.2*	0.85	2.3	23
		1&	0.2	0.5	
Duracore	FM-300	7	0.9	2.5	160
Duracore	FM-300-2K	7	0.85	2.3	160
Untreated	FM-300	7	0.9	2.5	160

\*moisture diffusion resulting in skin to adhesive failure  
&moisture diffusion leading to fillet bond pull-out.



**Figure 5.3.9** Data fit using equation 5.5 for Hexcel CR3 bonded to (A) FM-300 and (B) FM-300-2K, exposed to  $70^{\circ}\text{C}$  condensing humidity.

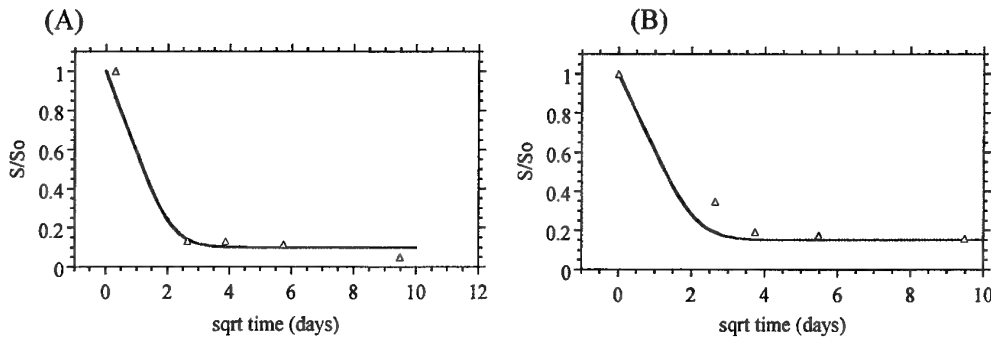


**Figure 5.3.10** Data fit using equation 5.5 for Duracore bonded to (A) FM-300 and (B) FM-300-2K, exposed to 70°C condensing humidity.

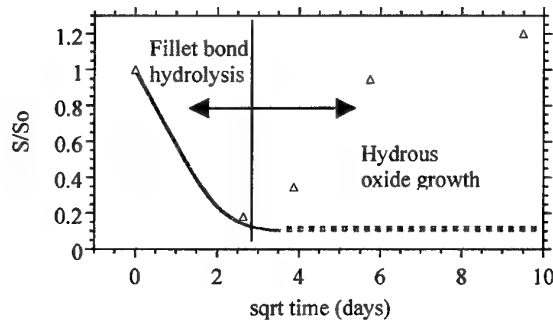


**Figure 5.3.11** Data fit using equation 5.5 for untreated honeycomb bonded to FM-300 and exposed to a 70°C condensing humidity.

## 5.4 Bond Degradation in Honeycomb Structure

### 5.4.1 Tension Strength

The diffusion coefficients values,  $D_j$ , reported in Table 5.3.1, for conditioned honeycomb samples tested in tension, are substantially lower than the diffusion coefficient values calculated in Table 4.8.1, for moisture uptake in the bulk adhesive,  $D_a$ . This is indicated by the values in the last column for  $D_j/D_a$  that are nearly all well below 100. The lower values for  $D_j$  in the honeycomb samples suggests that moisture uptake by the adhesive does not result in degradation of bond strength. If this were the case, the rate of decay of tension strength would have been appreciably greater than observed.

If the theory discussed in section 5.3.2 is correct, then a critical concentration of water uptake by the adhesive is required to disbond the adhesive at the interface. Possibly, the critical concentration is only achieved when additional moisture can gain access to the interfacial region. The most likely source of additional moisture will come from diffusion along the interface between the adhesive and honeycomb. Hence, the low values of  $D_j$  may represent moisture diffusion rates along the interfacial region. This may suggest that interfacial moisture

diffusion is a critical step leading to decay of tension strength in the honeycomb samples for temperatures below 95°C. The slow rate of interfacial diffusion implied by the calculation may indicate that the interfacial diffusion length is substantially greater than the geometrical distance measured from Figure 5.3.1. Typically, diffusion along the interface is expected to be more rapid than through the adhesive so an increased diffusion distance may be one explanation for the values calculated. In the case of the Hexcel CR3 and FM-300 sample immersed in 95°C water,  $D_j/D_a$  is slightly higher than 100. This result would suggest that the critical concentration of water at the interface may be achieved through moisture uptake of the adhesive. The faster diffusion rate for the bonded sample may also suggest that the critical concentration of water required for interfacial disbonding to occur is approximately 7 weight percent. This value was determined from the distance the moisture is required to diffuse into the adhesive, as a function of time, that would correlate with the measured adhesion failure. The critical concentration value would also explain why saturation mass uptake of the adhesive at 70°C is not sufficient to degrade the tension strength of the Hexcel CR3 and FM-300 honeycomb sample.

The values for P in Table 5.3.1 are also significant. In the case of conditioning in a 70°C humid environment the diffusion coefficients are similar for the Hexcel CR3 samples, however, values of P are lower for the FM-300-2K adhesive, suggesting equivalent concentrations of moisture are more effective at displacing the FM-300 adhesive bonds. The values of P determined for the 95°C immersion of the Hexcel CR3 samples also indicate the bonds formed with FM-300-2K are more resistant than the FM-300 case.

The values of  $D_j$  and P determined for the Dura-core and Untreated Alcore honeycomb samples indicate that the interfacial moisture diffusion and the hydrolytic resistance of the adhesive bonds are similar. The Alcore samples indicate notably poorer durability performance than the Hexcel CR3 samples. The correlation in the increased values of  $D_j$  and P for the Alcore samples suggests that in cases where the hydrolytic stability of the adhesive to honeycomb bonds is inferior, the interfacial diffusion rate of moisture increases.

Table 5.3.1 also indicates that the value of P is lower for the Hexcel CR3 specimens exposed to a condensing humidity environment, although the diffusion coefficients are similar. This suggests that the concentration of moisture resulting from interfacial diffusion is lower in a condensing humidity than for water immersion.

The values reported in Table 5.3.1 provide some insight into the initial stages of moisture diffusion paths in a single sided honeycomb panel exposed to humid environments. The data however cannot provide additional information about processes occurring at extended exposure periods, for example, at exposures greater than 1 year. Figures 5.3.2(A) and 5.3.8(A) indicate change in tension strength caused by moisture reacting with the honeycomb surface. In these instances, prediction of tension strength as a function of exposure will require information about the concentrations of moisture at the interface and details of the chemical reactions with the honeycomb. In the case of Figure 5.3.2(A), the hydrolysis of the chromium coating on the oxide increases the amount of cohesive failure of the coating layer, leading to a further reduction in tension strength. In the case of Figure 5.3.8(A), the hydrolysis of the metal surface produces oxide nodules which appear to increase the tension strength through a mechanical interaction.

#### 5.4.2 Decay of Peel Strength

The decay in the peel strength of the conditioned honeycomb samples reveals important differences in comparison with the tension strength decay, discussed in section 5.4.1. The values in Table 5.3.2 indicate only the Hexcel CR3 samples have lower values of  $D_j$  than  $D_a$ . Values of  $D_j$  are 1.3 times faster than  $D_j$  values measured for the tension samples in Table 5.3.1. The values of  $P$  also indicate substantial increases. Given the peel and tension samples were exposed under identical conditions, it can be assumed the real diffusion rates in both types of bonded specimen would be the same. The increase in the values of  $D_j$  and  $P$  can, therefore, be explained on the basis that a lower concentration of moisture at the adhesive-honeycomb interface is required to cause disbonding when the sandwich panels are loaded in peel, compared with loading in tension.

The values of  $D_j$  and  $P$  determined for the Duracore and untreated Alcore honeycomb are also greater than the tension samples. The values of  $D_j$  are 3.5 times that measured for the tension samples. Notably, for these samples the values of  $D_j/D_a$  are greater than 100 and indicate that the moisture uptake by the adhesive is sufficient to cause decay of peel strength. The Duracore and untreated Alcore samples degrade with an adhesive moisture concentration of approximately 3 weight percent, calculated by determining the water concentration for the diffusion distance resulting in the observed interfacial failure.

An unusual result determined for the peel samples is indicated in Figure 5.3.9(B). The slower diffusion rate determined for the Hexcel CR3 -FM-300-2K sample is based on skin-adhesive failure. Due to the complexity in determining the geometry of diffusion in this case, a diffusion length of 6mm was used simply for the basis of comparison with the other studies. Clearly, this is an oversimplification, but it does provide some indication of the relative rates of diffusion resulting in the different types of failure. In this case, the excellent hydrolytic stability of the honeycomb to adhesive bonds results in moisture diffusion disbonding the skin to adhesive, which appears to occur at a markedly slower rate.

#### 5.4.3 General Comments on the Decay in Mechanical Properties caused by Moisture

The diffusion modelling reported in section 5.3 does not include any of the Alcore PAA samples. In the peel and tension testing carried out, there was no obvious degradation in mechanical properties. This may indicate that the critical concentration of moisture required to degrade the mechanical properties of these samples is higher than the concentration of moisture resulting from uptake of the adhesive or interfacial diffusion. The hydrolytic stability of the honeycomb to adhesive bonds is clearly superior to the other honeycomb types tested. If the correlation between  $D_j$  and  $P$  observed for the tension samples exposed at 70°C in Table 5.3.1 is extrapolated to the PAA honeycomb samples, then the excellent durability of these samples may result from superior hydrolytic stability of the adhesive to honeycomb bonds retarding interfacial diffusion.

Modelling the tension and peel strength decay in humid environments for single sided honeycomb panels provides useful information about diffusion processes and the relative performance of the different honeycomb material. Alcore PAA honeycomb provides the best durability, followed by Hexcel CR3. Both Duracore and untreated Alcore honeycomb provided the poorest durability performance. Whilst untreated Alcore honeycomb provided improved



response at extended exposure due to growth of hydrated oxide nodules at the interface, extended exposure times indicated failure at the skin-adhesive interface had occurred.

There were no peel or Elcometer samples conditioned by immersion in 50°C water. The values for  $D_a$  in Table 4.8.1 for 50°C immersion in water would suggest that decay of tension and peel strength at these temperatures would be significantly slower than for 70°C and 95°C. This would be indicated by the Arrhenius plot in Figure 4.8.8, that indicates diffusion decreases exponentially as a function of temperature, and the saturation mass uptake of only 2.7%, being notably lower than the 70°C or 95°C cases. Therefore, the critical concentration of moisture required for interfacial disbonding to occur would rely on interfacial moisture diffusion that should be exponentially slower than the higher temperature cases.

## 5.5 Beam Mechanical Properties

The beam stiffness properties of honeycomb sandwich samples indicate decay in strength properties can be expected as a result of humid exposure. Four point bending experiments provided a more even distribution of load over the panel specimen and indicated an approximate linear decrease as a function of adhesion area. When single sided beam samples were constructed in which the second side of the panel was bonded with a paste adhesive, a similar response in beam properties was observed as a function of adhesion area, refer Figure 4.5.6. This indicates that the beam properties are determined by load transfer to the face of the beam with the reduced adhesion area. In terms of accelerated exposure experiments, exposure of single sided beam samples to the conditioning environment is clearly an option. Degradation of the fillet bond properties will dictate the beam strength when tested with a second skin, bonded after humid exposure, using a room temperature adhesive.

Exposure of a double skinned Hexcel CR3/FM-300 adhesive beam to a 95°C humid environment for a period of 9 months indicated the reduction in strength of the beam properties that could be expected with 100% fillet bond pull-out. Elcometer measurements indicated the tension strength of the beam specimen had reduced by approximately 90% relative to the dry strength value. Additionally, experiments carried out in section 4.6.1 indicated that the node bond peel strength of the honeycomb would also be expected to drop by at least 53% as a result of the conditioning. The ultimate load for the beam decreased by 66% for 4 point loading. This result suggests that the decrease in beam mechanical properties may not be as great as for the tension or peel loading cases.

## 5.6 Node Bond Strength Influence on Honeycomb Panel Properties

Tests were carried out in which the node bonds were also degraded by thermal conditioning, refer section 4.6.4. This data indicated an 80% reduction in node bond peel strength resulted in a minimal decrease in the mechanical properties of the Hexcel CR3 honeycomb samples bonded to FM-300 and tested in tension or 3 and 4 point bending. This data suggests that the major reduction in mechanical properties of the sandwich panels may be caused by fillet bond degradation. Clearly, these experiments do not give an indication of the reduction of honeycomb sandwich panel mechanical properties when the node strength approaches zero. A non-linear relationship between panel strength and node strength may exist.

Results in section 4.6.1 also suggest that node bond peel strength can be recovered with moisture removal through drying. This would represent situations where moisture ingress into

the node bond has contributed to adhesive plasticisation and adhesive failure. At longer periods where oxide hydration and corrosion of the honeycomb substrate has occurred, it is unlikely drying would have as a dramatic effect in recovering dry strength properties of the honeycomb.

### 5.7 Moisture Diffusion in Honeycomb Sandwich Panels.

Experiments conducted in section 4.7.1 provided some indication of a preference for moisture diffusion in sandwich panels through the node bonds of the honeycomb. The rate of the diffusion, however, appeared to be quite slow once access to the first row of cells was achieved. The diffusion also appeared to be very inconsistent. In some panels moisture would diffuse into the first row of cells within a matter of weeks, whereas, other samples only showed diffusion into individual cells after several months of exposure. These results would suggest that in cases where there is *no applied load*, moisture rates would be extremely slow and unlikely to lead to significant degradation of honeycomb panels over extended periods of service.

Additional evidence to support the preference for node bond moisture diffusion was provided by experiments carried out in section 4.7.2. Radiographic analysis of cerium nitrate ingress into a sandwich panel suggested a preference for the radio opaque fluid to migrate around the cell walls and through the node bonds. Moisture ingress along the skin to adhesive interface also appeared to proceed, but at a slower rate than observed for the node bond diffusion. Further chemical analysis of the node and fillet bond areas of the radiography sample is required to confirm this work.

The radiographic images provided in the Appendix indicate the ability to identify moisture ingress and node bond degradation in sandwich panels. Digital scanning is a process that should be employed to further aid the analysis of radiographic images.

## 6. Conclusions

A number of conclusions can be drawn from the studies into the effect of moisture on the mechanical properties of honeycomb sandwich panels.

Characterisation of the honeycomb indicated that Alcore node bonds were polyamide containing strontium chromate fibres, whereas, the Hexcel nodes bonds used nitrile rubber modified phenolic. Although the Alcore node adhesive covered less area than the Hexcel product, the peel strength did not degrade as rapidly when exposed to hot water. The peel strength of the conditioned Hexcel and Alcore node bonds could almost be 100% recovered with drying.

The surface chemistry of the Alcore and Hexcel honeycomb showed obvious differences. The Hexcel honeycomb surface was a chromium oxide layer with an ultrathin silicon containing organic layer. The Alcore Duracore honeycomb surface had a slightly thinner chromium oxide layer compared to the Hexcel CR3 product, but did not have an organic film on the surface. Alcore PAA honeycomb was characterised by a thick, several micron, polyamide primer layer. The differences in surface chemistry appeared to be related to the apparent differences in durability performance of the different honeycomb materials.

Flatwise tension (FWT) testing indicated a dry strength of approximately 1200 psi that decreased to 400psi for extended exposure in 95°C water. Manufacture of the single sided FWT samples resulted in significant scatter of measured strength values from conditioned samples. Measurements of moisture removal rates from saturated adhesive disks and tension tests conducted with the Elcometer method indicated the variation was due to drying of the fillet bond adhesive and consequent recovery of tension strength. Despite difficulties encountered with the preparation of FWT samples, trends in data helped validate results recorded using the Elcometer test. FWT data indicated that untreated honeycomb recovered an initial loss in strength at extended exposure times in humid environments. FWT data also suggested that the relative performance of the Alcore PAA may be alloy dependent. Alcore PAA treated Al-5056 performance was notably poorer than for the Al-5052 alloy.

Elcometer measurements indicated that tension strength could be accurately recorded using a portable adhesion testing system. The test offered advantages over the FWT test in that conditioned samples could be tested without complications caused by moisture removal during the preparation stage.

Tension strength of single sided Al-5052 alloy honeycomb samples indicated durability performance in the order: Alcore PAA >> Hexcel CR3 > Alcore Dura-core, Alcore Untreated. Degradation of tension strength of double sided panels exposed to humid environments was significantly slower than the single sided samples. The relative performance of the honeycomb material also depended on the adhesive used. FM-300-2K produced more durable fillet bonds with Hexcel CR3 than FM-300. Notably, bonds formed between untreated Alcore and FM-300-2K showed greater variability in dry strength than for bonds formed with FM-300. The simple degrease pretreatment step may not be reliable when bonding untreated honeycomb to the lower temperature curing adhesive. The untreated honeycomb sample showed a similar trend to that observed with the FWT measurements. After an initial decrease in strength, the untreated honeycomb sample strength recovered to values similar to or higher than the dry strength value at extended exposure times.

The decrease in tension strength as a function of exposure time to a high humidity environment indicated a linear relationship in fillet bond pull-out or adhesional failure. The tension strength decreased to a plateau value that was 80% lower than the dry strength. The rate of decrease depended on the exposure environment. Aqueous immersion of the honeycomb sample resulted in a more rapid decrease of strength than exposure to a condensing humidity.

Peel torque measured with the climbing drum method indicated similar trends to the tension data. The peel torque, however, appeared to decrease at a more rapid rate than the tension strength under similar humidity exposure. The decrease in peel strength showed a linear trend in adhesional failure area and showed a 90% reduction in the dry strength value, greater than the decrease observed for the Elcometer testing.

SEM and surface analysis of the failed honeycomb samples revealed details about the degradation mechanisms in humid environments. In the case of the tension testing, fracture appeared to propagate along the honeycomb-adhesive interface. At extended exposures, the fracture also seemed to begin to propagate into a hydrated chromium oxide layer for the Hexcel CR3 sample. The FWT samples indicated evidence for drying in specimen manufacture, with a small amount of cohesive failure in the adhesive region near the top of the honeycomb cell. Peel fracture surfaces indicated 100% adhesive failure of the honeycomb-adhesive interface. The

unusual behaviour of the untreated honeycomb sample could be explained by the appearance of oxide nodules on the surface of the honeycomb in the fillet bond region. The density of these areas of localised oxide hydration increased as a function of exposure in the humid environment and, presumably, offered mechanical advantage to the fillet bond. The honeycomb to adhesive bonds that exhibited excellent hydrolytic resistance, such as the PAA honeycomb samples, showed failure at the skin to adhesive interface at exposure periods greater than 3 months. This suggests that further improvement in durability performance of the PAA sandwich panels would require improvement in the durability of the surface pretreatment used for the aluminium skin.

The decrease in ultimate load for beam specimens loaded in 4 point bending mode indicate a linear relationship with adhesion area of the fillet bond. Single sided samples, in which a second skin was bonded with paste adhesive, exhibited similar load response to the two sided samples and suggested that accelerated conditioning of beam samples could be undertaken as with the peel and tension testing. A fully degraded beam sample exposed to 95°C water indicated the reduction in ultimate load was less than fully degraded samples loaded in peel or tension.

Experiments in which the node bonds were artificially degraded prior to sandwich panel preparation indicated minimal effect on strength in beam and tension testing. The peel strength of the node bonds was degraded by 80% using thermal treatment at 180°C, the effect on bending properties of beams made from honeycomb with nodes having greater degradation is not clear.

There is evidence to suggest diffusion of moisture into double sided honeycomb sandwich panels proceeded at a faster rate in the node bond direction. Moisture uptake in sandwich panels, however, appeared to be variable. The time taken for moisture to fill the first row of cells may vary from weeks to several months. Diffusion past the first row of cells, however, appeared to be substantially slower. Radiographic images of radio opaque fluid suggested moisture migrated along cell walls and through node bonds at a faster rate than diffusion through the fillet bond.

Drying of honeycomb panels would appear to be beneficial in recovering mechanical properties. Node bonds exposed to 95°C water for brief periods recovered 100% of their dry strength and moisture saturated adhesive disks dried within hours at 80°C. Double sided panels would not provide a direct path for moisture removal from the fillet and node bond regions and, therefore, would not be expected to dry at as fast a rate.

Modelling the diffusion of moisture into the fillet bond region of single sided honeycomb panels revealed a number of features about the bond degradation process. There was evidence to suggest that less water was required at the adhesive-honeycomb interface to produce adhesive failure when the bond was loaded in peel compared with tension. Moisture uptake by the adhesive was sufficient to describe the decay of peel strength for most samples. In contrast, the decay in tension strength could not be explained solely on the basis of moisture uptake by the adhesive, for the majority of specimens. One explanation provided was that interfacial diffusion of moisture between the adhesive and honeycomb was also required for the critical concentration of water required for disbonding of the adhesive to proceed. In the case where interfacial diffusion of moisture was proposed to be leading to bond degradation, a correlation between the adhesion breakage parameter,  $P$ , and the diffusion coefficient in the joint,  $D_j$ , was identified. This may suggest increases in the hydrolytic stability of interfacial bonds led to reduced rates of interfacial diffusion. Further evidence to support the role of interfacial diffusion in bond degradation was provided by the difference in degradation rates of the honeycomb

samples immersed in water or exposed to a condensing humidity. The degradation rate in a condensing humidity was slower than aqueous immersion, despite the fact that the moisture diffusion rates and the saturation mass uptake of water in the bulk adhesive are identical for both environments. The concept of a critical concentration of moisture in the interfacial region could be used to explain the bond durability data observed.

## 7. Future Work

The work conducted to date has raised a number of issues that should be investigated in more detail. The future work will improve the current understanding of the factors influencing the durability of honeycomb panels currently in service on F-111 aircraft and provide valuable information that will assist in maintenance and repair of bonded structure.

The current experiments have conditioned the honeycomb panels in humid environments without any load being present. In service the bonded panels will be expected to be exposed to a range of temperatures and humidities, whilst simultaneously experiencing loads. It is known that stress can lower the energy for processes such as diffusion. Given the above experiments indicate the importance of moisture diffusion processes in bond degradation it is necessary to examine the combined influence of load and humidity on panel degradation processes. Initial experiments carried out with static loads have failed to accelerate the bond degradation rates of sandwich panels. This may indicate fatigue loading is required to accelerate the degradation process. Clearly, additional factors are influencing panel degradation given service experience indicates panels degrading over large areas in time frames significantly shorter than those predicted by the tests conducted in this report [1].

The ability to predict the rate of panel degradation in humid environments requires more information about concentrations of moisture at the bond interface. Whilst diffusion models used in this report are capable of qualitatively comparing the relative performance of different honeycomb and adhesive sandwich panels, critical concentration values will aid in developing more quantitative models.

Whilst initial investigations suggest a preference for moisture diffusion in the node bond direction of sandwich panels, more refined experiments are required to unequivocally establish moisture diffusion paths and their rates in sandwich panels. This information will be valuable for successful maintenance of bonded panels. If damaged regions of panels are identified, the extent of moisture damage could be estimated and procedures for drying panels to recover mechanical properties could be established.

Further examination of the different honeycomb materials available for repairs, or currently used in service panels, is required to establish their relative durability performance. Work in this report indicates that Alcore PAA treated honeycomb may offer superior performance to alternative surface pretreatments. PAA treated honeycomb from Hexcel should also be examined given the superior performance of the Hexcel CR3 product relative to the equivalent Alcore product. There is also evidence to suggest that different alloys will influence durability performance of the honeycomb bonded structure. This is important information in maintenance of bonded panels, where a variety of alloys may be expected to have been used in panel construction. The information would identify panels that may be more susceptible to environmental damage.

This report details the durability performance of bonded panels constructed from materials that would be used or encountered in repairs. Additional research is required to assess the durability that would be expected from bonded panels constructed from original and reworked materials. These investigations will be undertaken in AIR Task 98/186 and reported in a future technical report.

## 8. Acknowledgements

The author would like to acknowledge the efforts of a considerable number of people at AMRL who assisted with the research planning and experimental work undertaken to provide the data required for production of this comprehensive report. These people include: Mr John Backhouse, Mr John Retchford, Mr Peter Pearce, Mr Tony Camileri, Dr David Arnott, Mr Michael Ryan, Mr Richard Muscat and Mr Louie Lambrianidis.

## 9. References

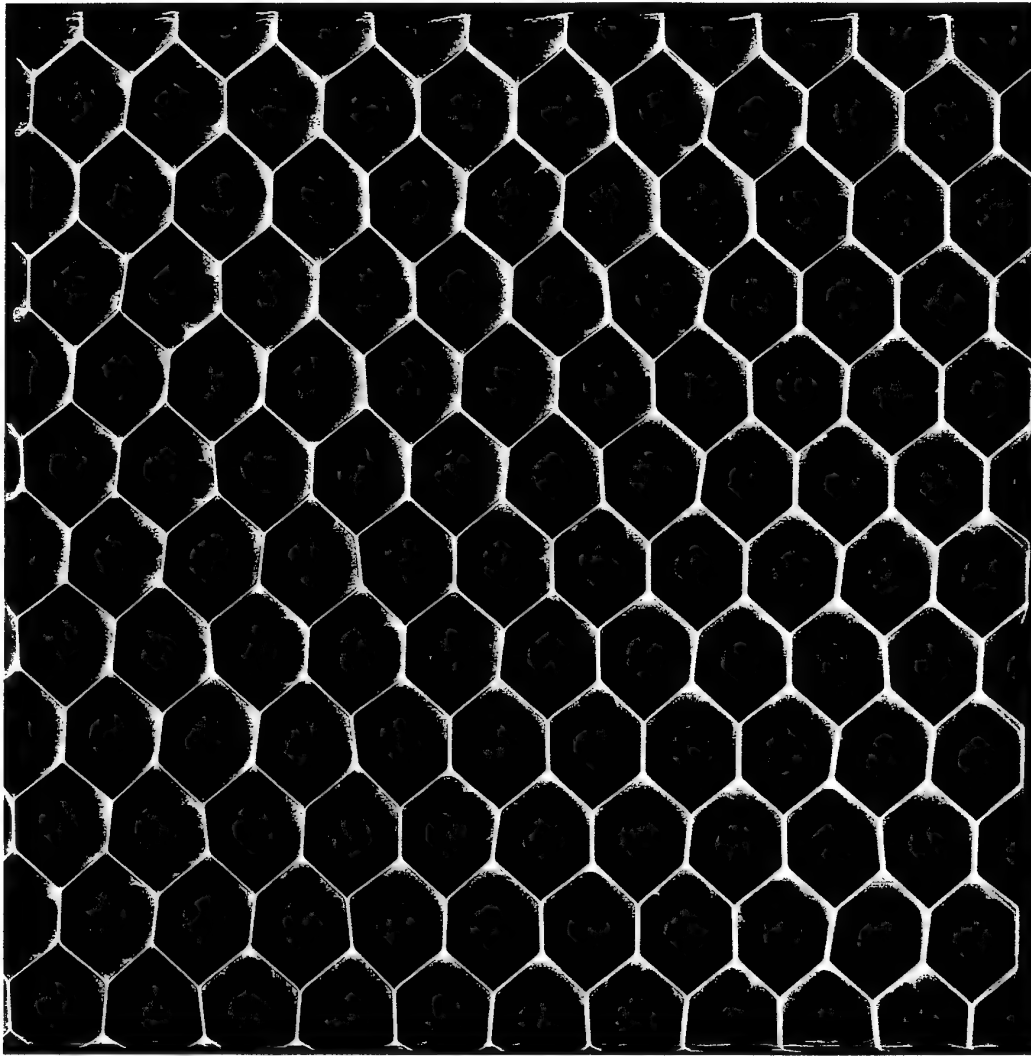
- [1] A. N. Rider, "*F-111 Bonded Panel Repair Status*", DSTO-TR-0803, DSTO-AMRL, Melbourne, April, 1999.
- [2] Royal Australian Airforce Engineering Standard C5033, "*Composite Materials and Adhesive Bonded Repairs*", RAAF Headquarters Logistics Command, Melbourne, September, 1995.
- [3] Royal Australian Airforce Draft Document AAP 7021.016-2, "*Composite Materials and Adhesive Bonded Repairs. Repair Fabrication and Application Procedures*", RAAF Headquarters Logistics Command, Melbourne, September, 1995.
- [4] ASTM C297-94, "*Standard Test Method for Flat-wise Tensile Strength of Sandwich Constructions*", 1996 Annual Book of ASTM Standards, Section 15, Volume 15.03, pp. 9-10, ASTM, Pennsylvania, 1996.
- [5] ASTM D4541-95, "*Standard Test Method for Pull-Off Strength of Coatings Using Portable Adhesion Testers*", 1995 Annual Book of ASTM Standards, Section 6, Volume 6.01, ASTM, Pennsylvania, 1995.
- [6] ASTM D1781-98, "*Standard Test Method for Climbing Drum Peel Test for Adhesives*", 1998 Annual Book of ASTM Standards, Section 15, Volume 15.06, pp. 106-109, ASTM, Pennsylvania, 1998.
- [7] ASTM C393-94, "*Standard Test Method for Flexural Properties of Sandwich Constructions*", 1996 Annual Book of ASTM Standards, Section 15, Volume 15.03, pp. 21-24, ASTM, Pennsylvania, 1996.
- [8] R. L. Pecsok, L. D. Shields, T. Cairns, I. G. McWilliam, "*Modern Methods of Chemical Analysis*", 2<sup>nd</sup> ed., Chapter 11, pp. 165-201, John Wiley, New York, 1976.
- [9] M. P. Seah, D. Briggs in "*Practical Surface Analysis*", 2<sup>nd</sup> ed., D. Briggs and M. P. Seah (Ed.), Chapter 1, pp. 1-16, John Wiley, Chichester, 1990.

- [10] M. J. Davis, D. A. Bond, "*The Importance of Failure Mode Identification in Adhesive Bonded Aircraft Structures and Repairs*", presented at the International Conference on Composite Materials 12, Paris, July 5-9, 1999.
- [11] M. Zog, "*Degradation Effects at FA-18 Sandwich Structures*", Report KOR-TE99-0045, Swiss Aircraft and Systems Enterprise Corporation, January, 1999.
- [12] T. C. Radtke, A. Charon, R. Vodicka, "Hot/Wet Environmental Degradation of Honeycomb Sandwich Structure Representative of F/A-18: Flatwise Tension Strength", DSTO-TR-0908, September, 1999.
- [13] A. N. Rider, C. L. Olsson-Jacques, D. R. Arnott, "*Influence of Adherend Surface Preparation on Bond Durability*", Surface Interface Analysis, 27, 1055-1063, 1999.
- [14] R. Vodicka, CREDP 15<sup>th</sup> International Meeting, *Minutes of Meeting*, Hull, Quebec, Canada, December, 1999. .
- [15] P. D. Chalkley, "*A Critical Compendium of Material Property Data for Bonded Composite Repairs*", DSTO-DDP-0274, pp. 5, DSTO-AMRL, Melbourne, 1997.
- [16] C. L. Soles, F. T. Chang, D. W. Gidley, A. F. Yee, " *Contributions of the Nanovoid Structure to the Kinetics of Moisture Transport in Epoxy Resins*", Journal of Polymer Science: Part B: Polymer Physics, 38, 776-791, 2000.
- [17] R. A. Gledhill, A. J. Kinloch, S. J. Shaw, "*A Model for Predicting Joint Durability*", Journal of Adhesion, 11, 3-15, 1980.
- [18] K. Nakamura, T. Maruno, S. Sasaki, , "*Theory for the decay of wet Shear Strength of Adhesion and its application to Metal/Epoxy/Metal Joints*", International Journal of Adhesion and Adhesives, 7(2), 97-102, 1987.
- [19] K. Nakamura, T. Ueda, S. Hosono, T. Maruno, "*Theoretical Analysis of the decay of Shear Strength of Adhesion in Metal/Epoxy/Metal Joints in an Aqueous Environment*", International Journal of Adhesion and Adhesives, 7(4), 209-212, 1987.

## Appendix A: Radiographic Analysis of Moisture Diffusion in Metal Honeycomb Sandwich Panels

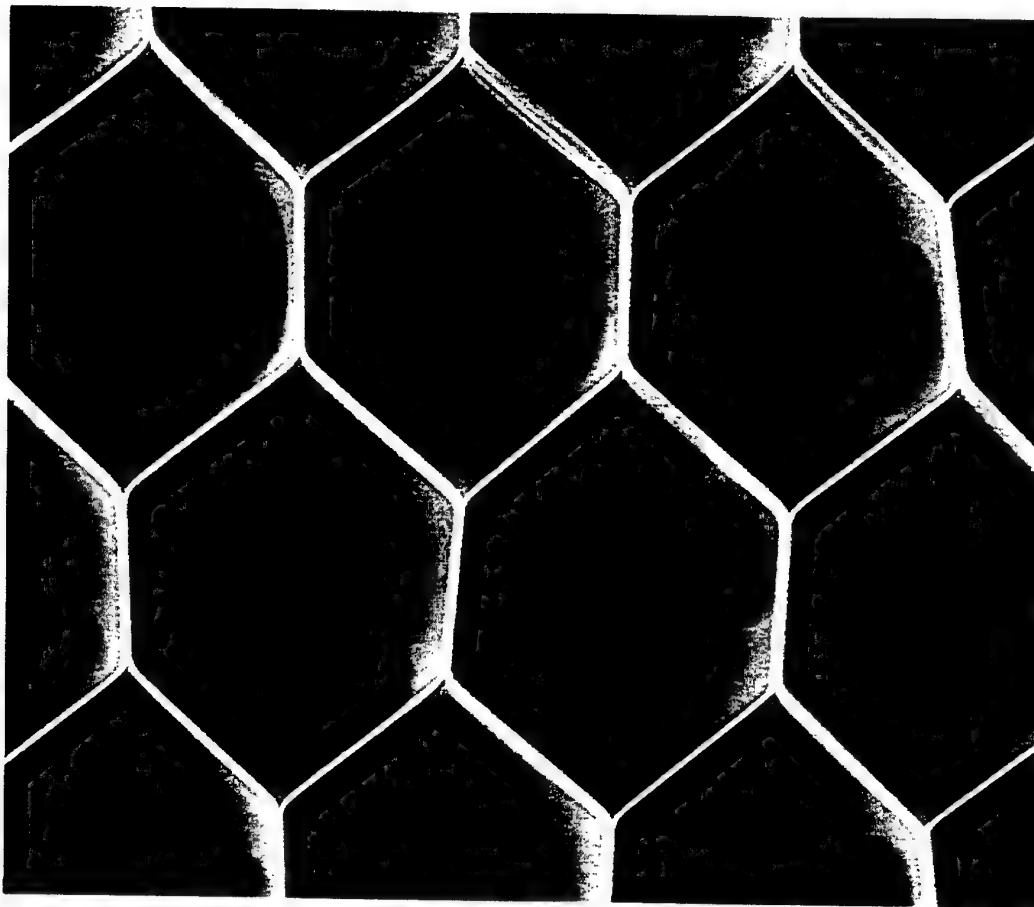
### A.1 Control Specimen

Figure A1.0 indicates the radiographic image acquired using Kodak M film with 50kV X-rays and 12mA/s exposure. The image was acquired at normal incidence relative to the plane of the sandwich skins.

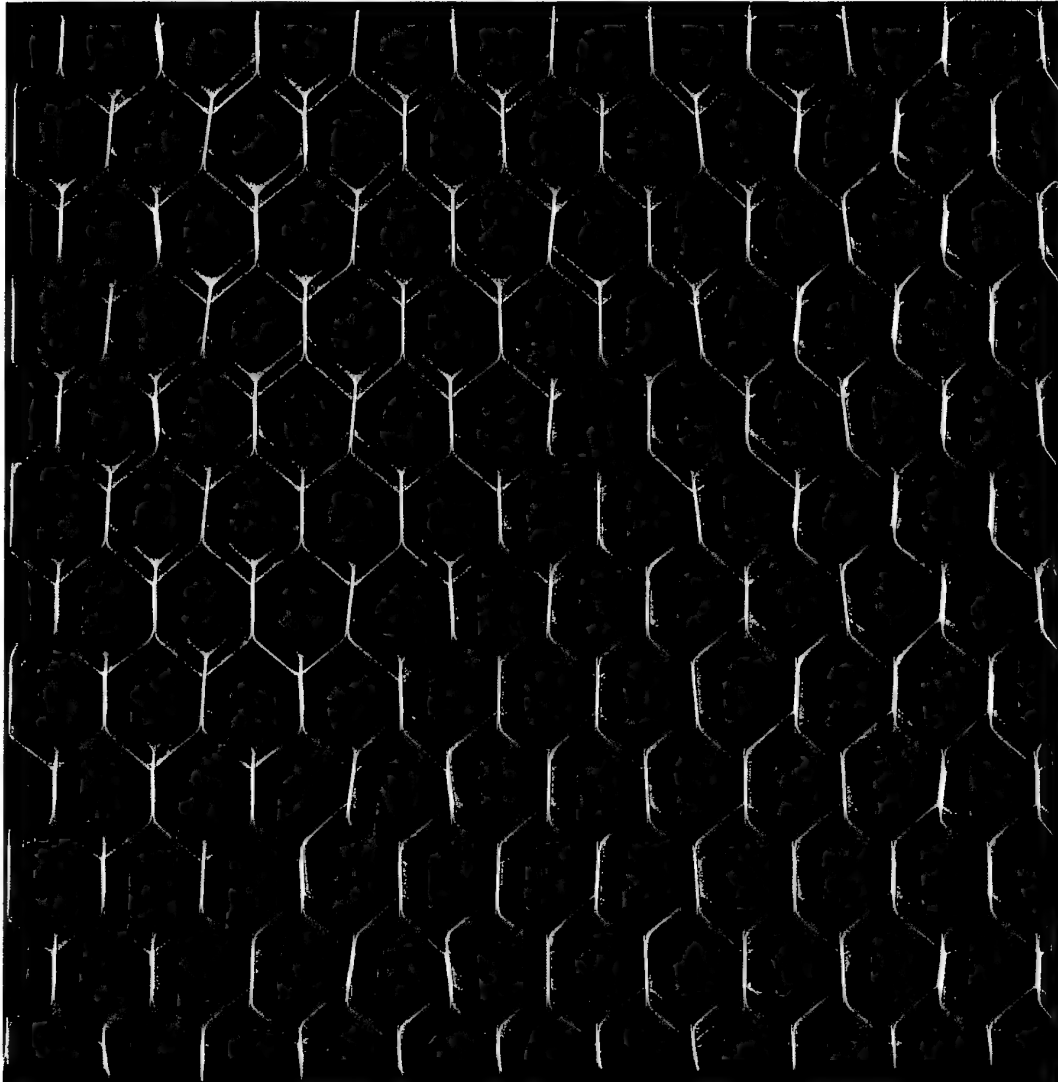


**Figure A1.0** *Hexcel CR3 honeycomb sandwich panel bonded with FM-300 and 0.5mm skins. Image acquired with Kodak M film at 50kV, 12mA/s. Image acquired at normal incidence.*

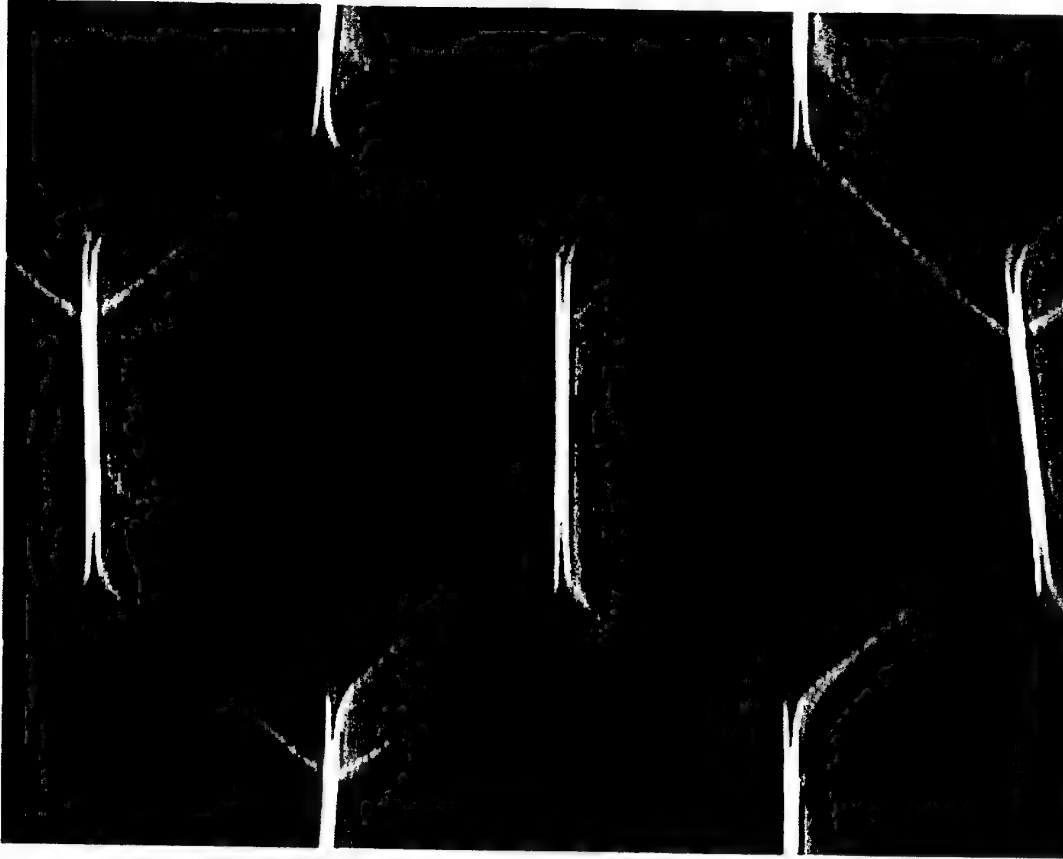




**Figure A1.1** *Hexcel CR3 honeycomb sandwich panel bonded with FM-300 and 0.5mm skins. Image acquired with Kodak M film at 50kV, 12mA/s. Image acquired at normal incidence.*



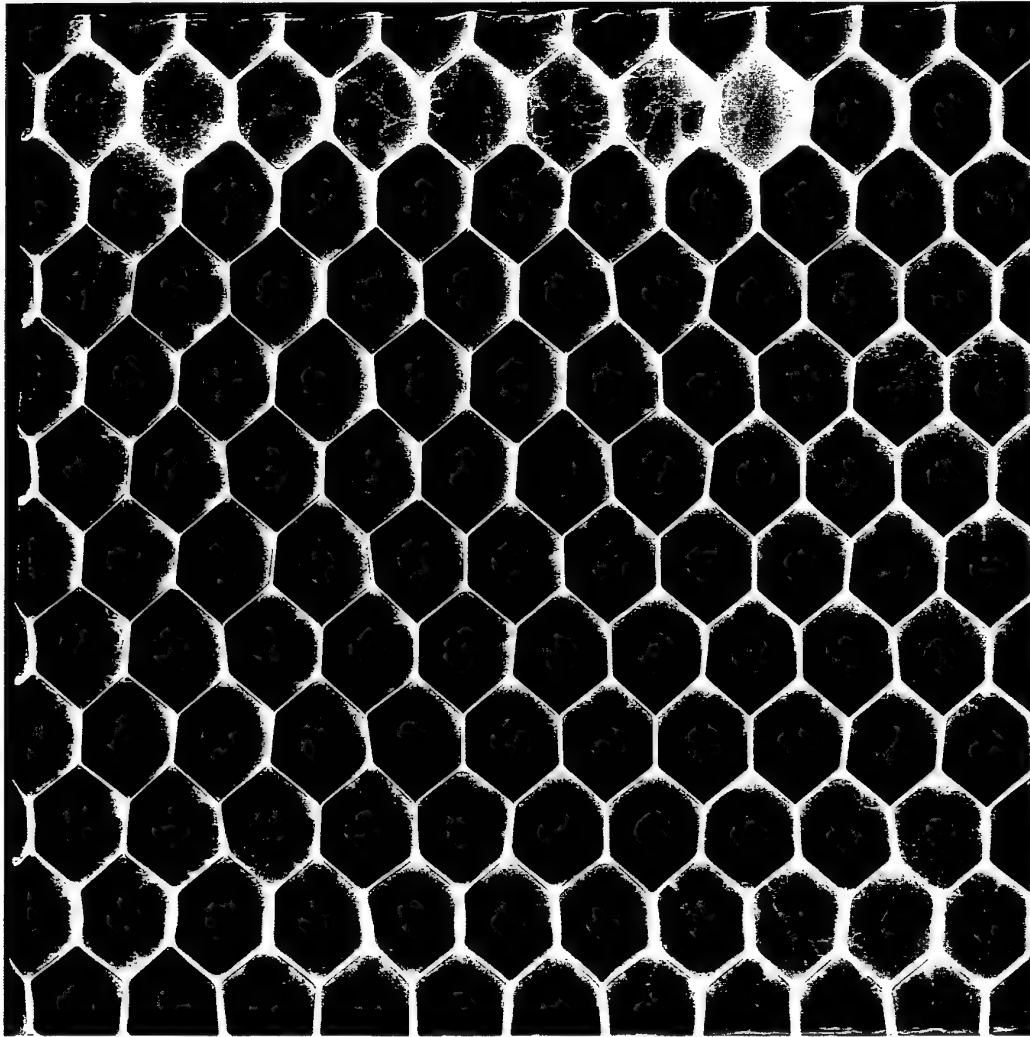
**Figure A1.2** *Hexcel CR3 honeycomb sandwich panel bonded with FM-300 and 0.5mm skins. Image acquired with Kodak M film at 50kV, 12mA/s. Image acquired at 5 degrees off normal incidence.*



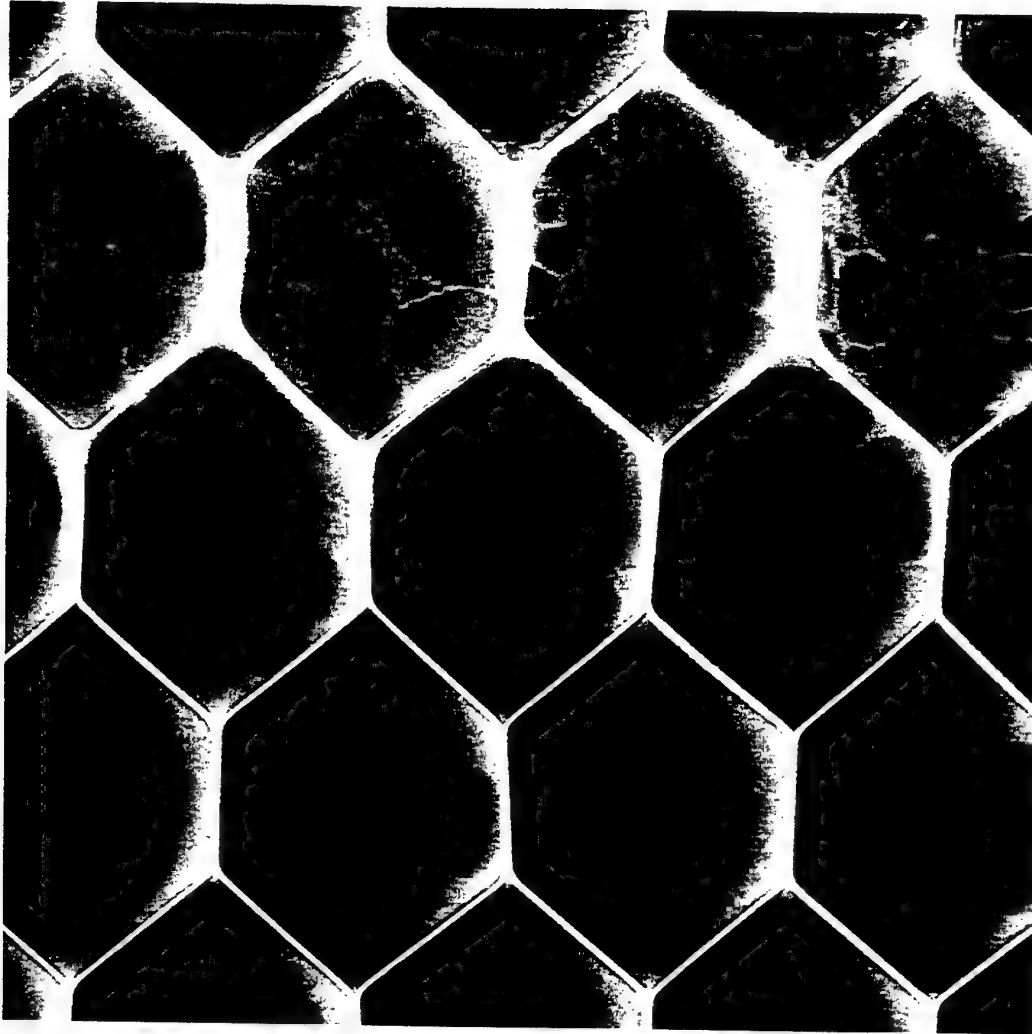
**Figure A1.3** *Hexcel CR3 honeycomb sandwich panel bonded with FM-300 and 0.5mm skins. Image acquired with Kodak M film at 50kV, 12mA/s. Image acquired at 5 degrees off normal incidence.*

## A.2 Two Days Immersion in 70°C Cerium Solution

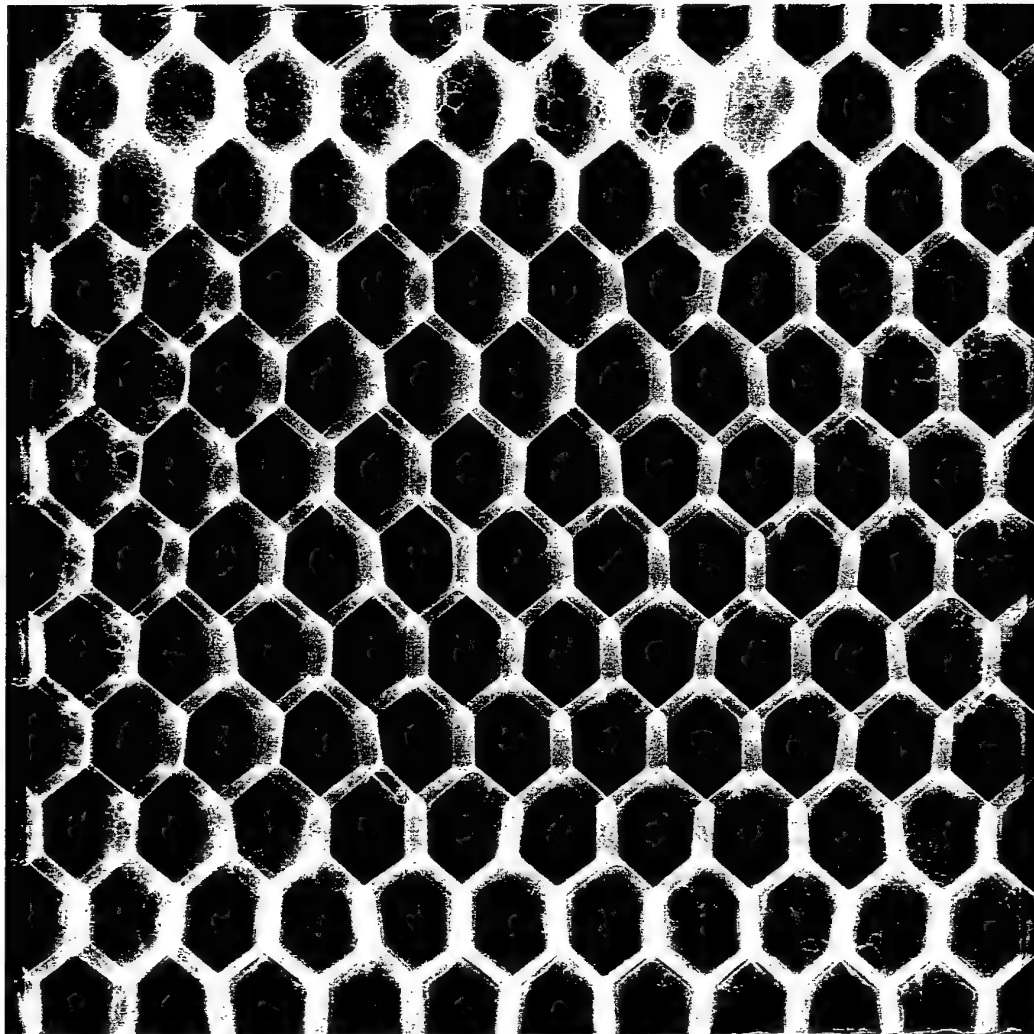
Figure A2.0 indicates the radiographic image acquired using Kodak M film with 50kV X-rays and 12mA/s exposure. The image was acquired at normal incidence relative to the plane of the sandwich skins after immersion in 70°C Cerium Nitrate solution for 2 days.



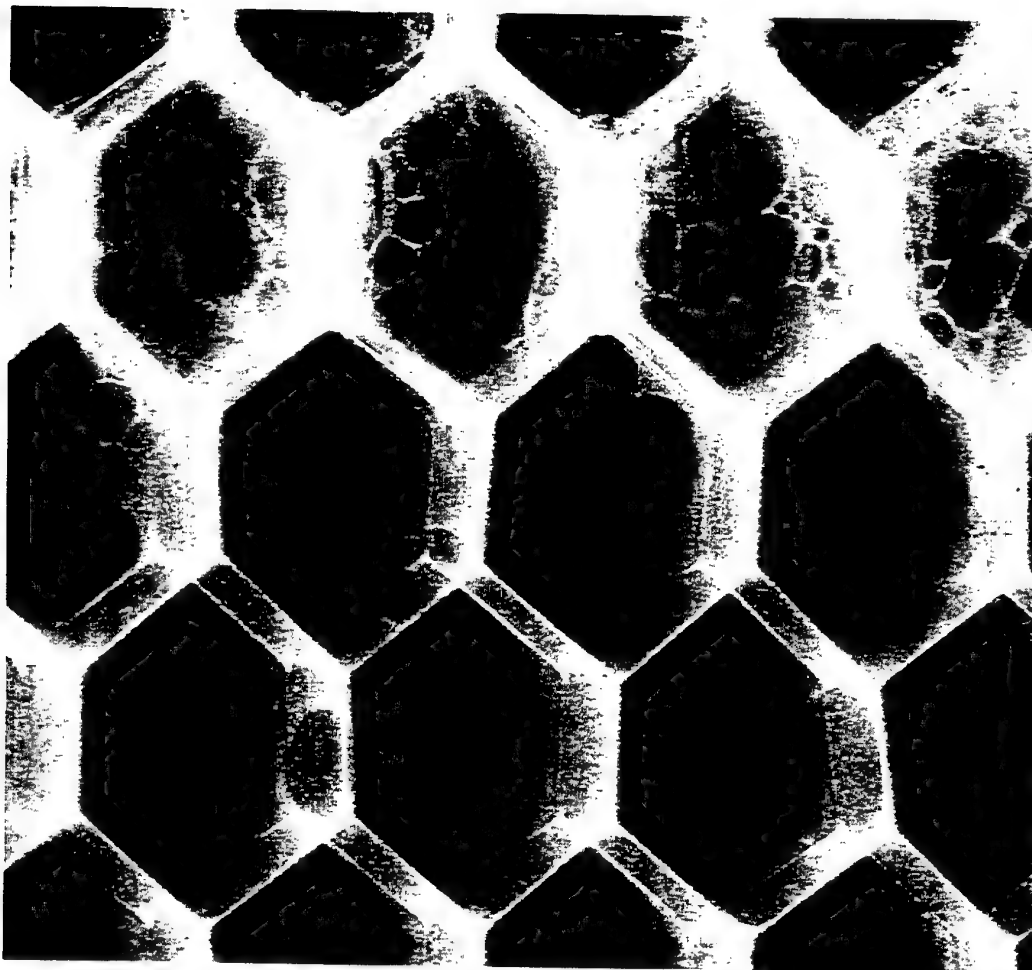
**Figure A2.0** *Hexcel CR3 honeycomb sandwich panel bonded with FM-300 and 0.5mm skins. Image acquired with Kodak M film at 50kV, 12mA/s at normal incidence after 2 days immersion in Cerium Nitrate solution.*



**Figure A2.1** *Hexcel CR3 honeycomb sandwich panel bonded with FM-300 and 0.5mm skins. Image acquired with Kodak M film at 50kV, 12mA/s at normal incidence after 2 days immersion in Cerium Nitrate solution.*



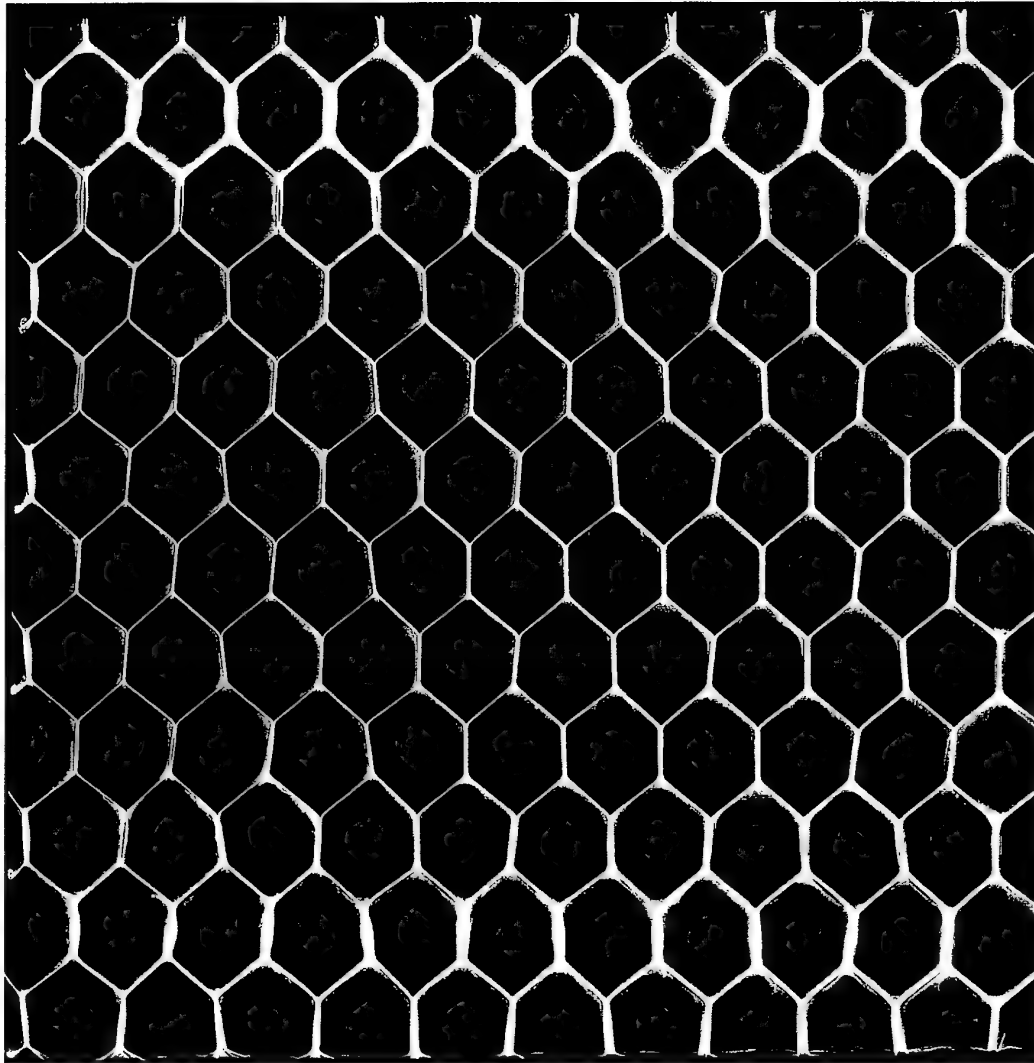
**Figure A2.2** *Hexcel CR3 honeycomb sandwich panel bonded with FM-300 and 0.5mm skins. Image acquired with Kodak M film at 50kV, 12mA/s at 5 degrees off normal incidence after 2 days immersion in Cerium Nitrate solution.*



**Figure A2.3** *Hexcel CR3 honeycomb sandwich panel bonded with FM-300 and 0.5mm skins. Image acquired with Kodak M film at 50kV, 12mA/s at 5 degrees off normal incidence after 2 days immersion in Cerium Nitrate solution.*

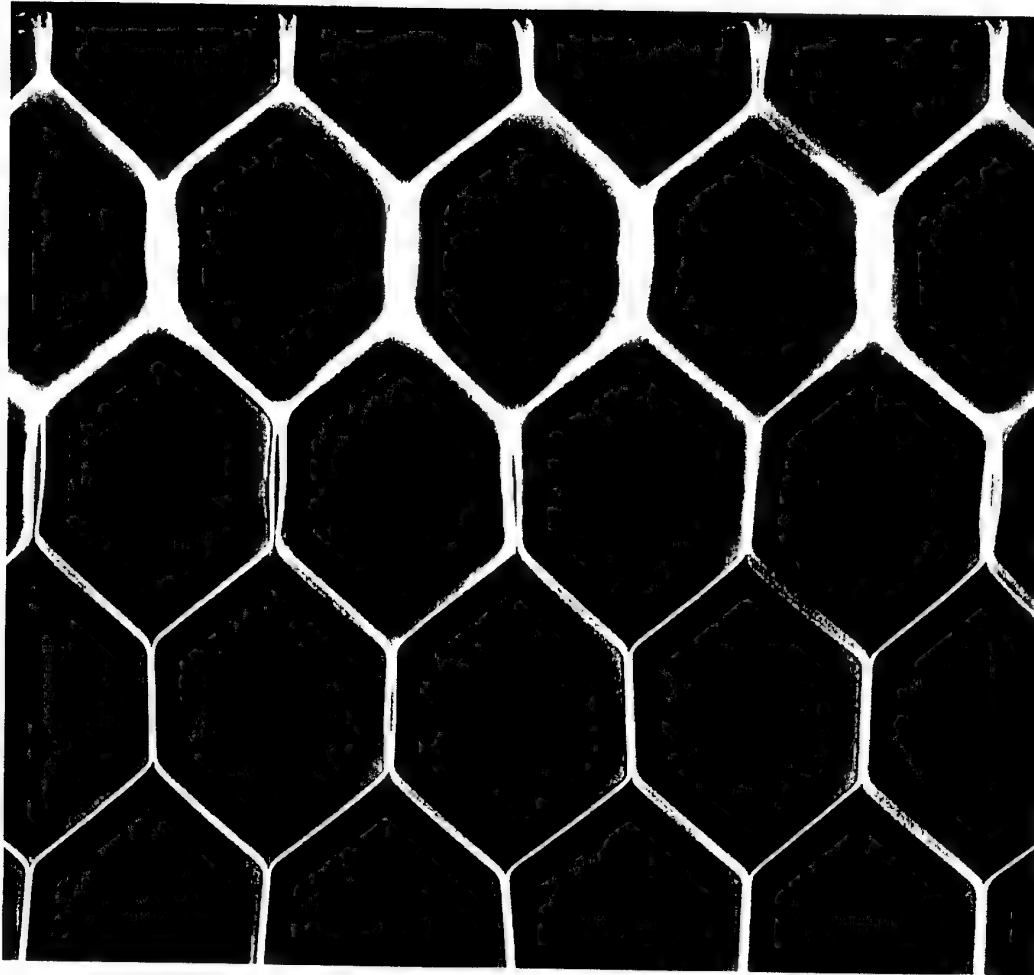
### A.3 Three Days Immersion in 70°C Cerium Solution

Figure A3.0 indicates the radiographic image acquired using Kodak M film with 50kV X-rays and 12mA/s exposure. The image was acquired at normal incidence relative to the plane of the sandwich skins after 3 days immersion in Cerium Nitrate solution at 70°C.

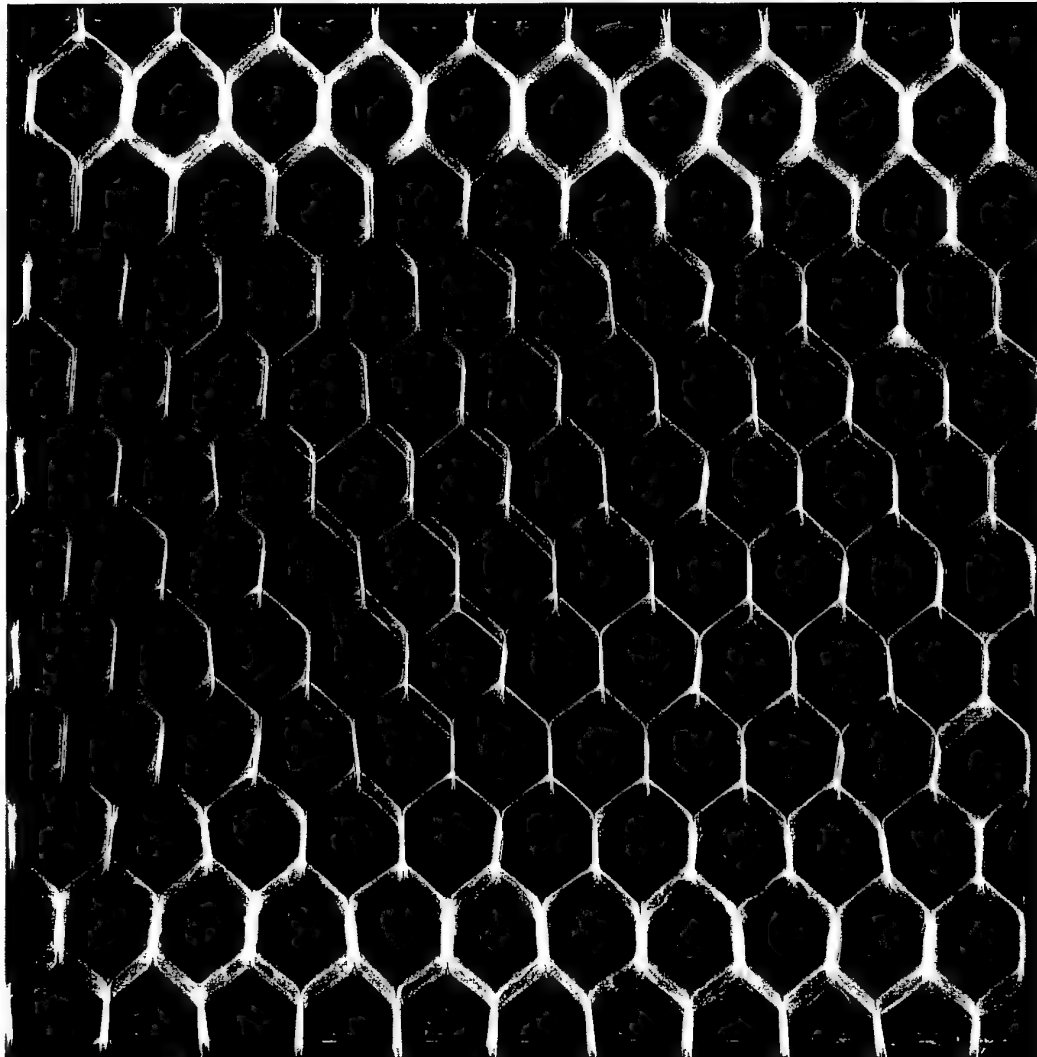


**Figure A3.0** *Hexcel CR3 honeycomb sandwich panel bonded with FM-300 and 0.5mm skins. Image acquired with Kodak M film at 50kV, 12mA/s and normal incidence. after 3 days immersion in Cerium Nitrate solution at 70°C.*

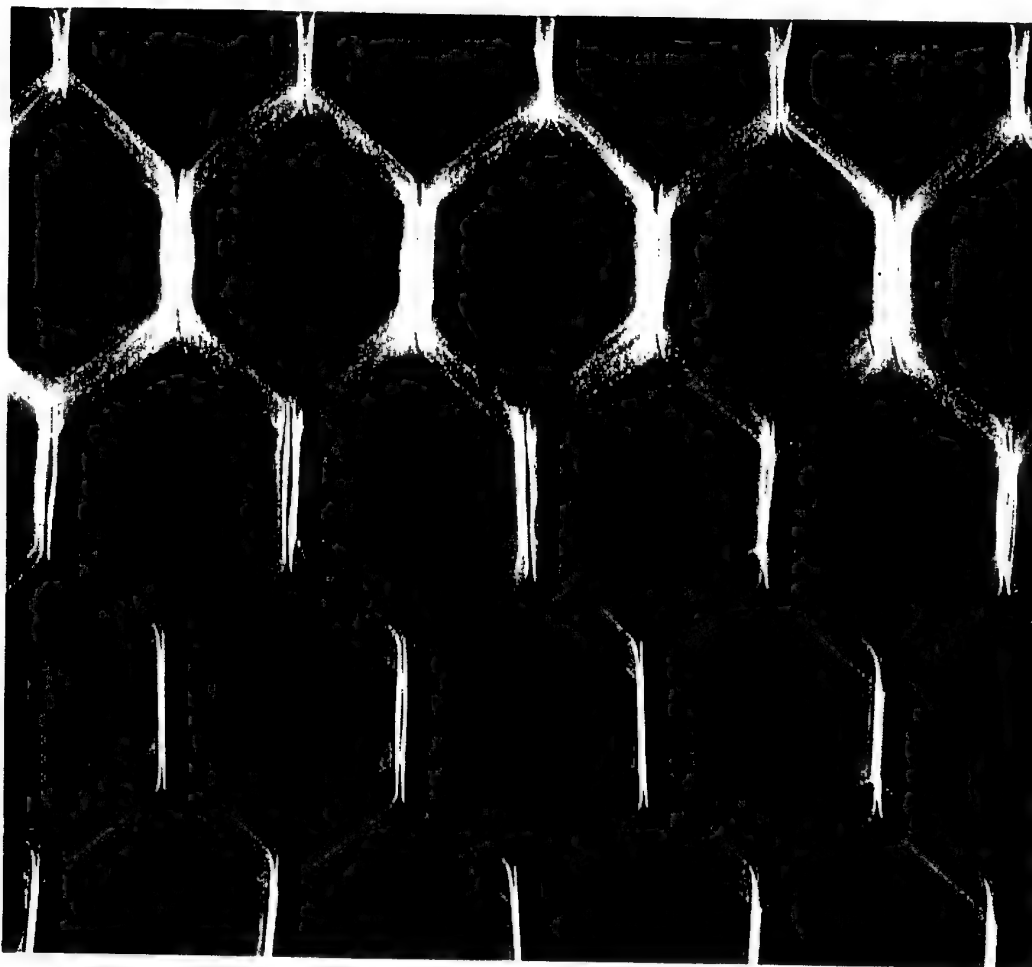




**Figure A3.1** *Hexcel CR3 honeycomb sandwich panel bonded with FM-300 and 0.5mm skins. Image acquired with Kodak M film at 50kV, 12mA/s and normal incidence. after 3 days immersion in Cerium Nitrate solution at 70°C.*



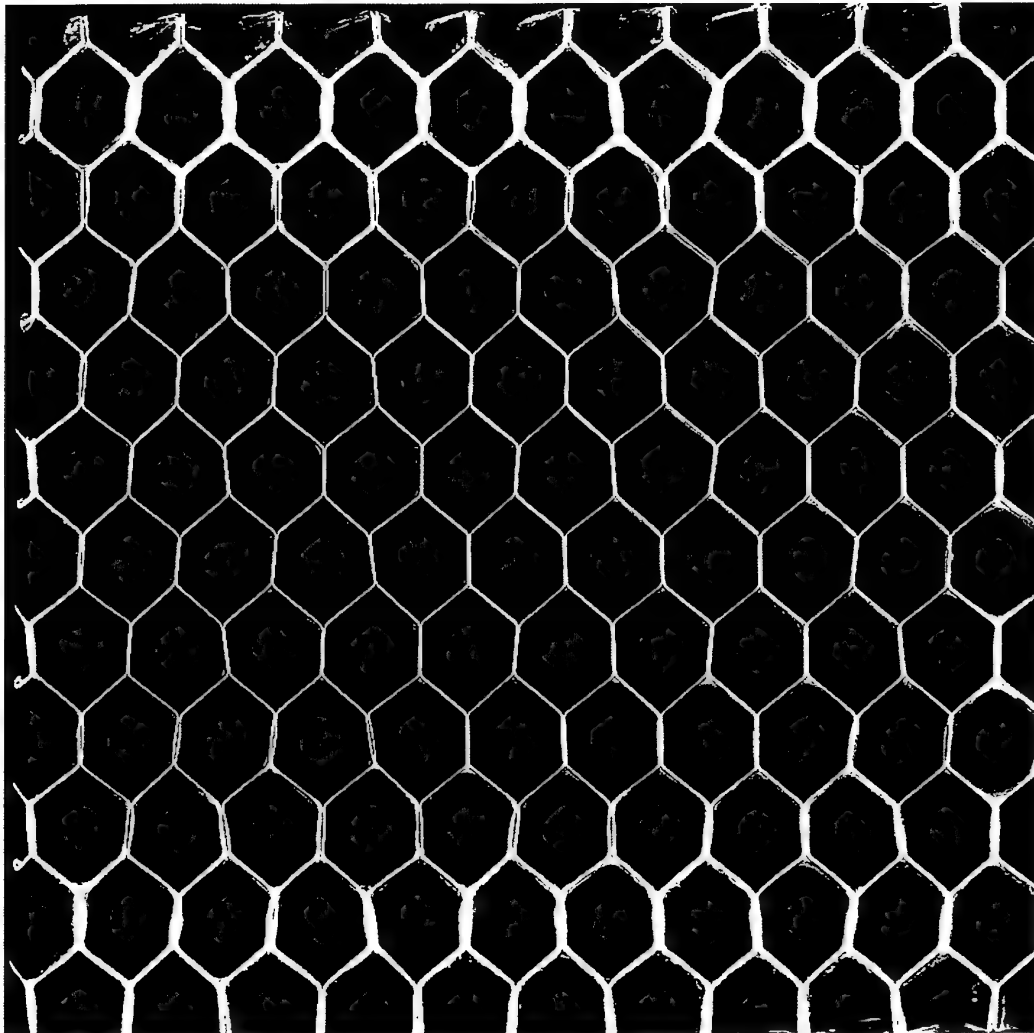
**Figure A3.2** *Hexcel CR3 honeycomb sandwich panel bonded with FM-300 and 0.5mm skins. Image acquired with Kodak M film at 50kV, 12mA/s and 5 degrees off normal incidence after 3 days immersion in Cerium Nitrate solution at 70°C.*



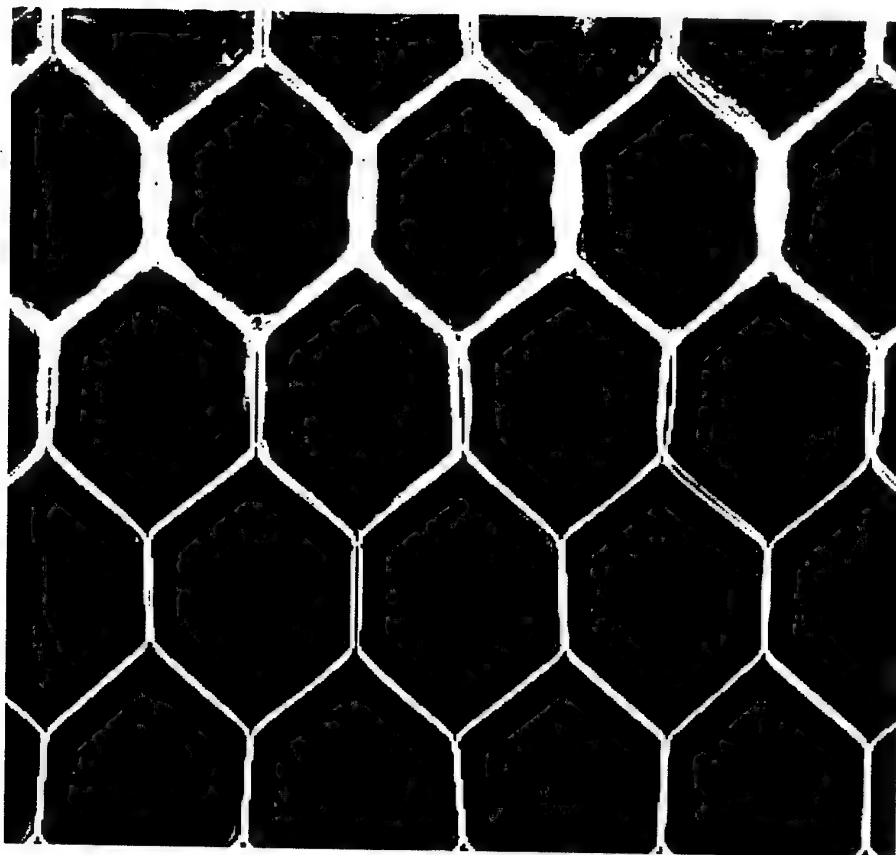
**Figure A3.3** *Hexcel CR3 honeycomb sandwich panel bonded with FM-300 and 0.5mm skins. Image acquired with Kodak M film at 50kV, 12mA/s and 5 degrees off normal incidence after 3 days immersion in Cerium Nitrate solution at 70°C.*

#### A.4 Five Days Immersion in 70°C Cerium Solution

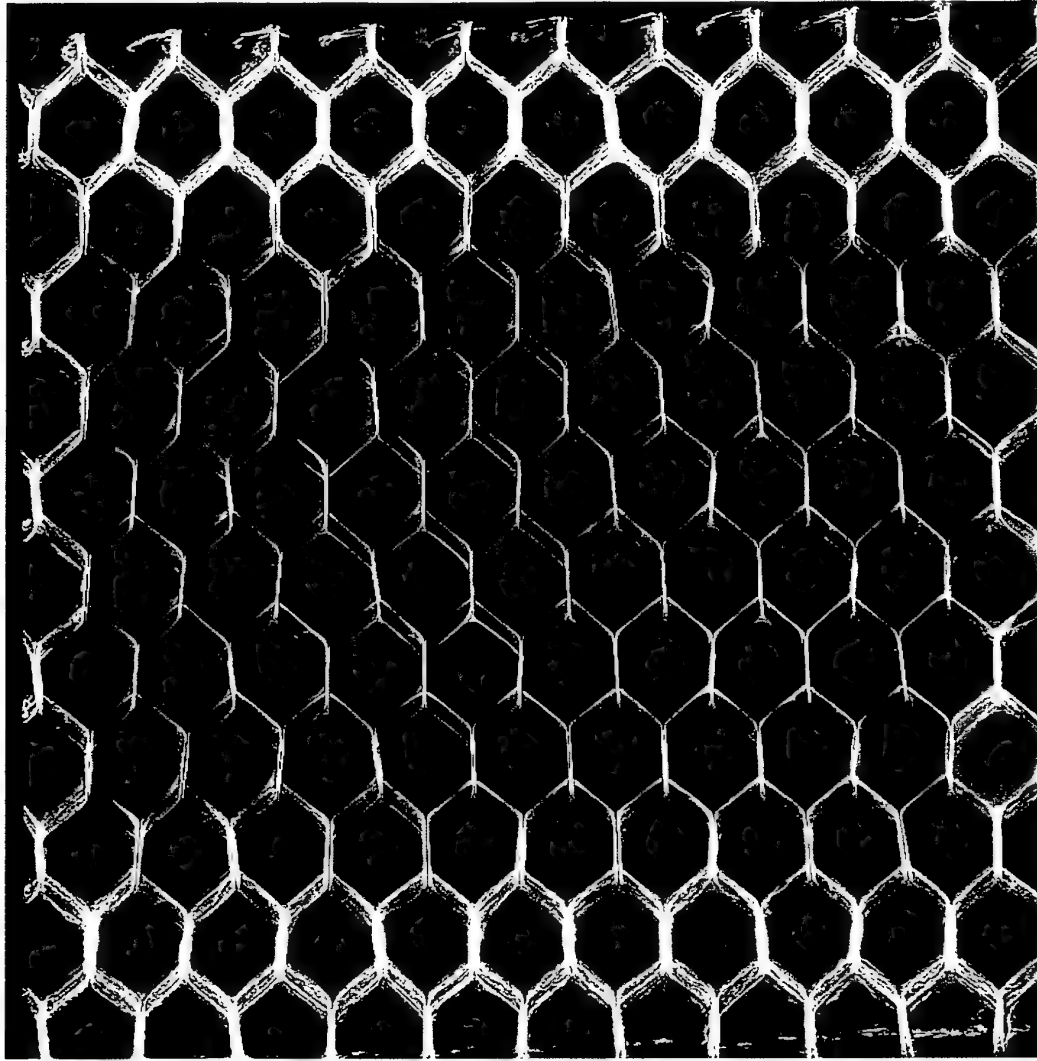
Figure A3.0 indicates the radiographic image acquired using Kodak M film with 50kV X-rays and 12mA/s exposure. The image was acquired at normal incidence relative to the plane of the sandwich skins after 5 days immersion in Cerium Nitrate solution at 70°C.



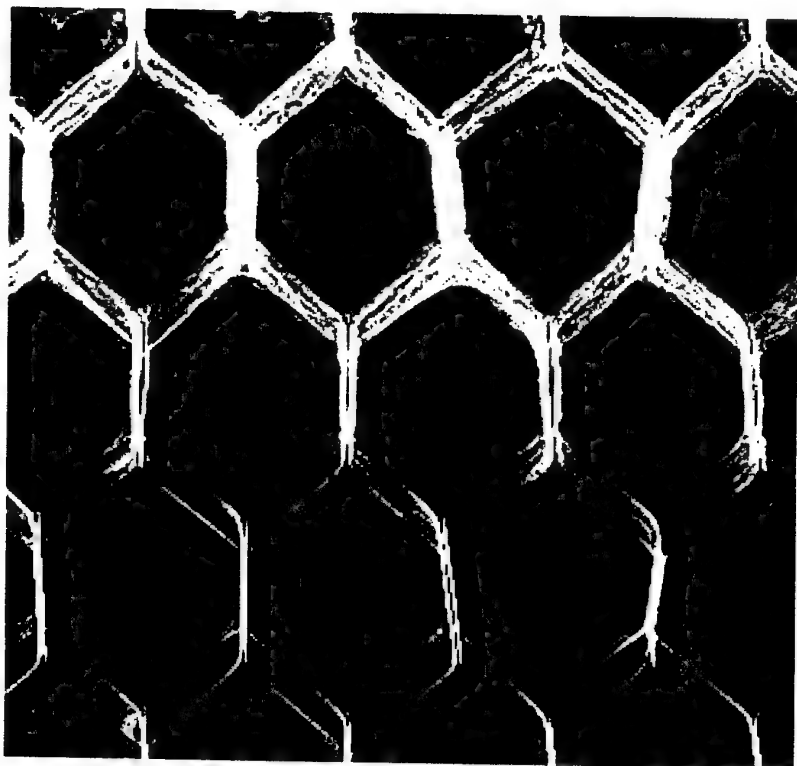
**Figure A4.0** *Hexcel CR3 honeycomb sandwich panel bonded with FM-300 and 0.5mm skins. Image acquired with Kodak M film at 50kV, 12mA/s and normal incidence after 5 days immersion in Cerium Nitrate solution at 70°C.*



**Figure A4.1** *Hexcel CR3 honeycomb sandwich panel bonded with FM-300 and 0.5mm skins. Image acquired with Kodak M film at 50kV, 12mA/s and normal incidence after 5 days immersion in Cerium Nitrate solution at 70°C.*



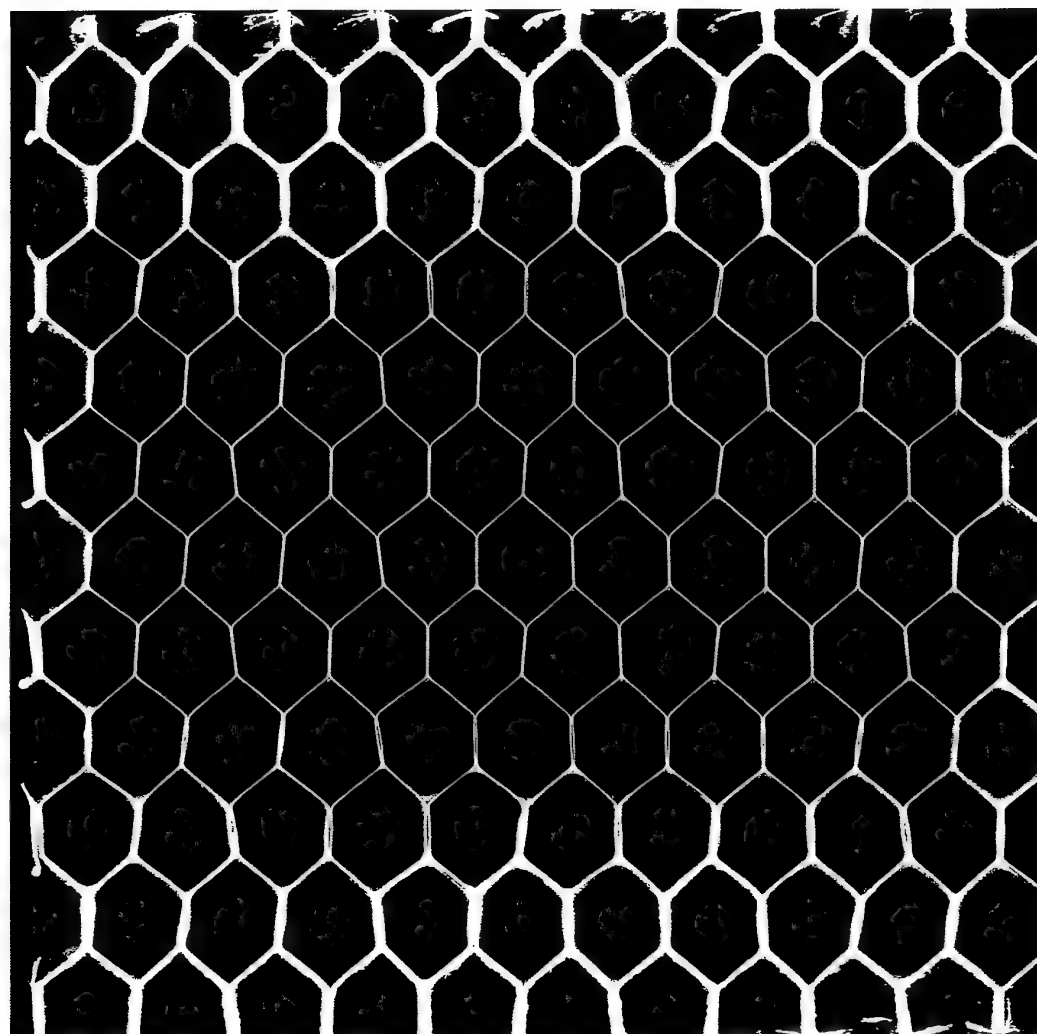
**Figure A4.2** *Hexcel CR3 honeycomb sandwich panel bonded with FM-300 and 0.5mm skins. Image acquired with Kodak M film at 50kV, 12mA/s and 5 degrees off normal incidence after 5 days immersion in Cerium Nitrate solution at 70°C.*



**Figure A4.3** *Hexcel CR3 honeycomb sandwich panel bonded with FM-300 and 0.5mm skins. Image acquired with Kodak M film at 50kV, 12mA/s and 5 degrees off normal incidence after 5 days immersion in Cerium Nitrate solution at 70°C.*

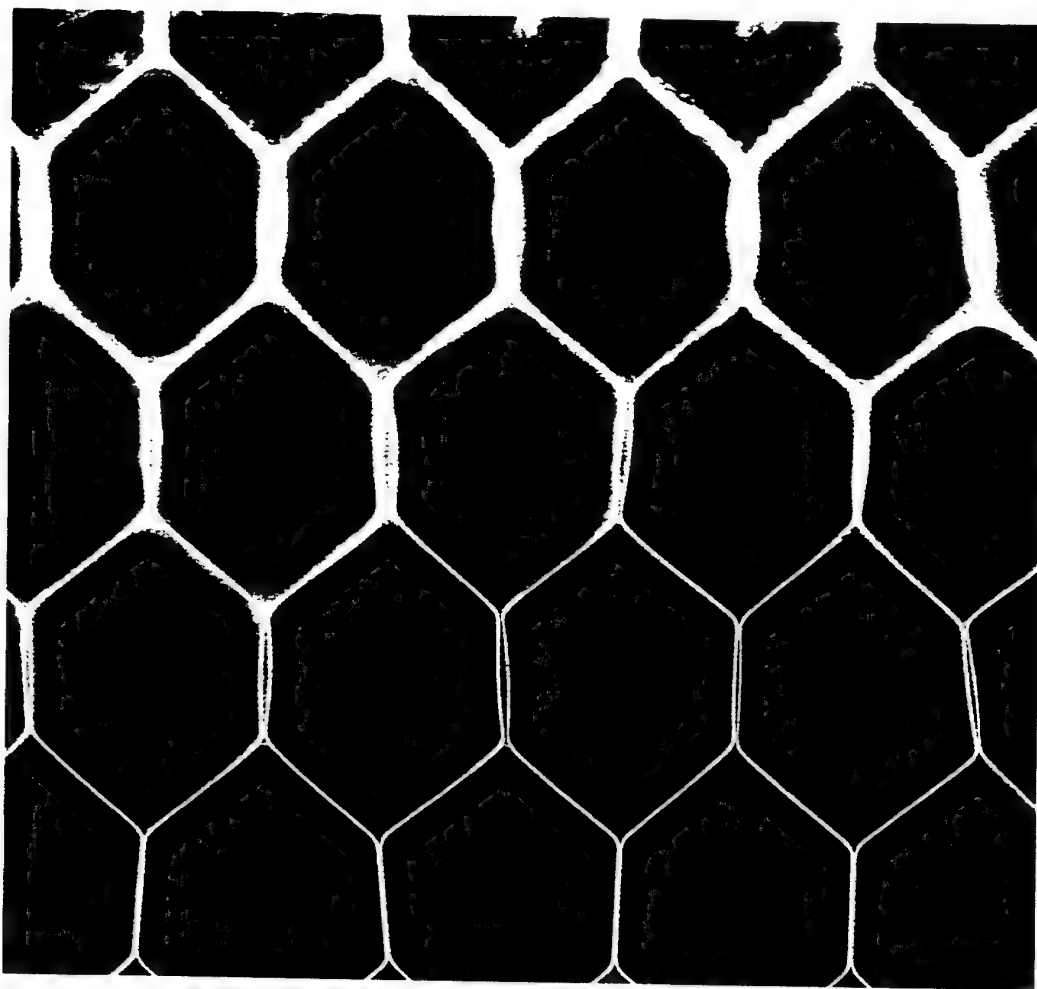
## A.5 Ten Days Immersion in 70°C Cerium Solution

Figure A3.0 indicates the radiographic image acquired using Kodak M film with 50kV X-rays and 12mA/s exposure. The image was acquired at normal incidence and 3 degrees relative to the plane of the sandwich skins after 10 days immersion in Cerium Nitrate solution at 70°C.



**Figure A5.0** *Hexcel CR3 honeycomb sandwich panel bonded with FM-300 and 0.5mm skins. Image acquired with Kodak M film at 50kV, 12mA/s and normal incidence after 10 days immersion in Cerium Nitrate solution at 70°C.*





**Figure A5.1** *Hexcel CR3 honeycomb sandwich panel bonded with FM-300 and 0.5mm skins. Image acquired with Kodak M film at 50kV, 12mA/s and normal incidence after 10 days immersion in Cerium Nitrate solution at 70°C.*

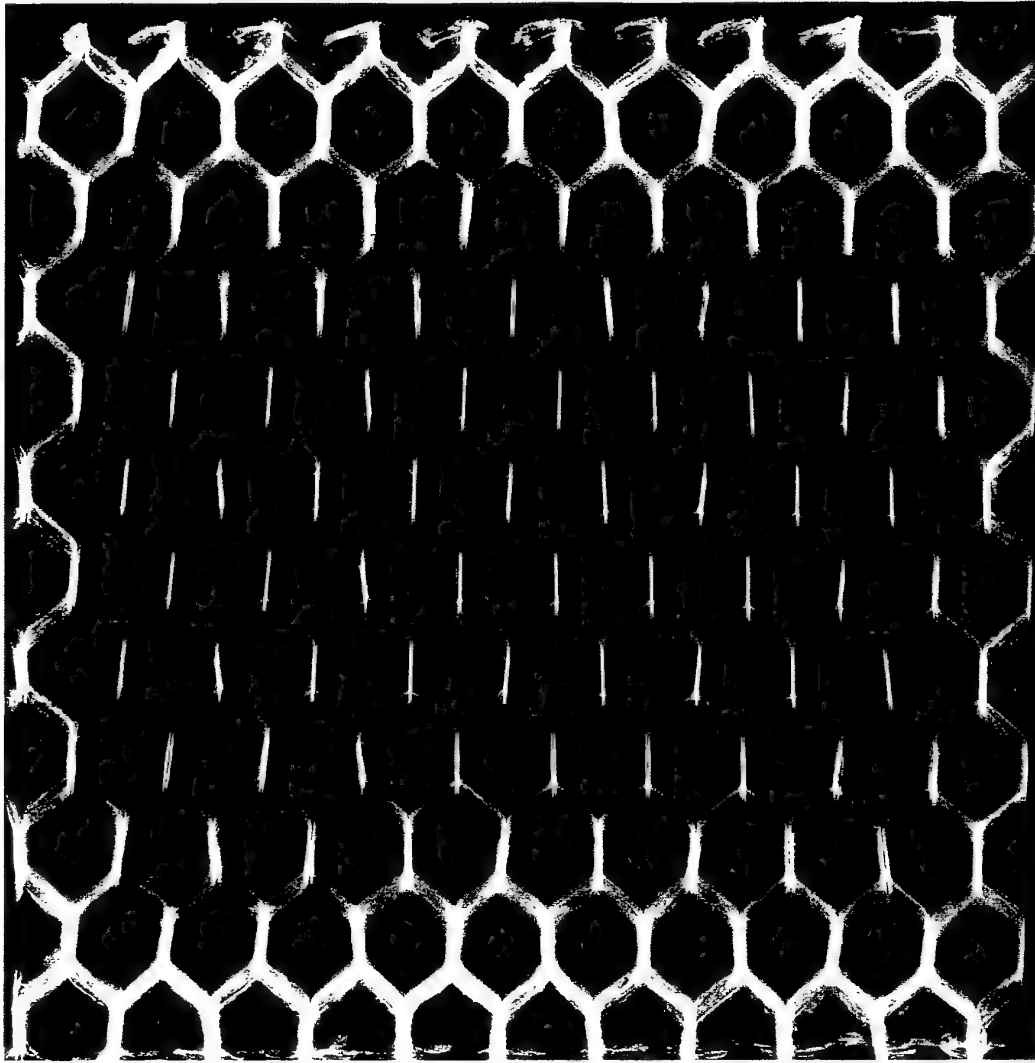


**Figure A5.2** *Hexcel CR3 honeycomb sandwich panel bonded with FM-300 and 0.5mm skins. Image acquired with Kodak M film at 50kV, 12mA/s and 5 degrees off normal incidence after 10 days immersion in Cerium Nitrate solution at 70°C.*

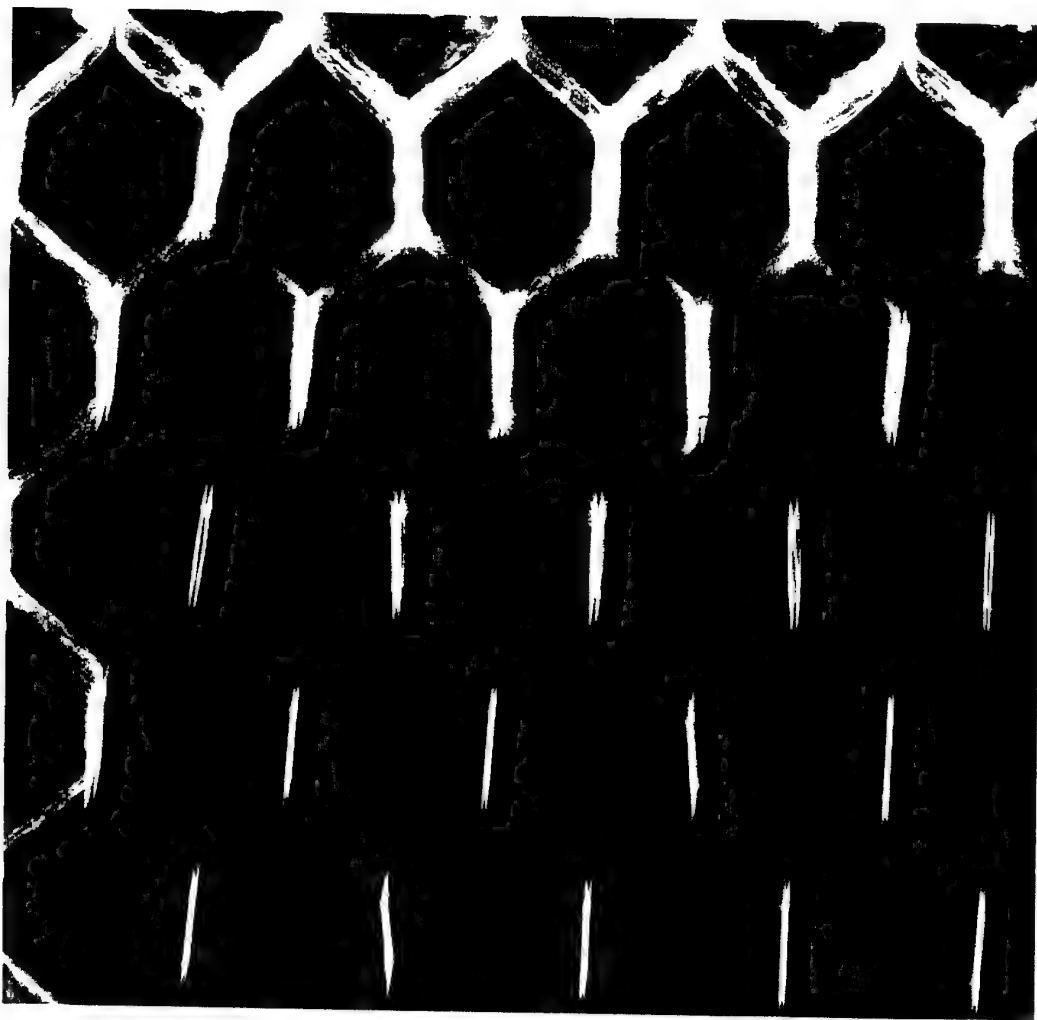


**Figure A5.3** *Hexcel CR3 honeycomb sandwich panel bonded with FM-300 and 0.5mm skins. Image acquired with Kodak M film at 50kV, 12mA/s and 5 degrees off normal incidence after 10 days immersion in Cerium Nitrate solution at 70°C.*

## **Appendix A: Radiographic Analysis of Moisture Diffusion in Metal Honeycomb Sandwich Panels**

### **A.6 Discussion**

The radiographs presented in sections A.1 to A.5 indicate the changes which occur to the honeycomb core material as a function of exposure in a 50% aqueous solution of cerium nitrate. The control sample, refer A.1, shows that the core material appears to be regularly shaped and that the node bonds are all similar in nature. Figure A1.3 indicates the structure of the node bonds, with two sheets of aluminium bonded and a thin dark line indicative of the presence of the node adhesive in between. All images in the Appendix are presented with the node bond or ribbon direction running from the top to bottom of the page. The ends of the individual node bonds show small separation in the higher magnification shots, refer figure A1.3. Some evidence of voiding in the fillet bond adhesive is also evident the figures A1.0 to A1.3 as indicated by the spherical shaped regions present in the majority of cells.

After two days immersion in cerium nitrate solution at 70°C, figures A2.0 to A2.3 indicate some notable changes in the radiographs. The node bonds of the first row of complete cells all appear to have separated in the centre as seen in figure A2.1. In contrast, there does not appear to be any change in the node bonds for the direction normal to the ribbon. The cerium nitrate diffusion path can be identified by the brighter regions at the edge of the honeycomb core at the top and bottom of the page, refer figure A2.0 and A2.2. Closer examination of cells, figure A2.1 and A2.3, suggests there is an outline of cerium around the cell wall of the first complete cell and a small increase in the brightness of the first half of the second cell, suggesting some cerium has migrated into the second layer of node bonds.

After three days immersion in the cerium solution the radiographs indicate the moisture has diffused almost completely into second row of node bonds, as indicated by the swelling in the centre of the node bonds in this row, refer figure A3.1. Migration into the third cell row is only evident in a couple of node bonds for either end of the sandwich sample, refer figure A3.1. Figures A3.2 and A3.3 suggest the cerium solution hasn't completely diffused around the second row of cells.

After five days immersion in the cerium solution there does not appear to be any significant changes from the radiographs acquired for the three days immersion in the salt solution. Only node bonds up to the second row of cells still appear to be swollen, refer figures A4.1 and A4.3, with diffusion along around the cell walls only obvious for the first one and half rows.

After ten days immersion in the salt solution all node bonds along the third row are swollen, showing evidence of diffusion of the salt solution, refer figure A5.0 and A5.1. The diffusion of the cerium solution around the cell walls appears to have occurred for the first two rows of cells and has begun developing along the node bond of the third row of cells, refer figures A5.2 and A5.3. After 10 days immersion in the salt solution there still appears to be evidence that diffusion along the node bond direction is proceeding at a notably faster rate than the direction normal to the

node bonds. Cerium solution does not appear to have migrated beyond the outer edge of the first column of cells.

## **A.7 Conclusion**

Cerium nitrate solution can be identified in radiographs of honeycomb sandwich panels as regions of higher contrast.

The results presented in the appendix suggest there is a preference for the 70°C concentrated cerium nitrate solution to diffuse into the honeycomb sandwich panel along the ribbon direction. The progress of diffusion can be identified by progressive swelling of the row of node bonds from the perimeter of the sandwich panel to about the third row in a 10 day period. The rate of diffusion appears to slow after the first two days. The solution also appears to diffuse along the cell walls in the node direction.

In contrast to the apparent diffusion along the ribbon direction, there did not appear to be significant ingress of the cerium nitrate solution in the direction normal to the ribbon direction. Cerium nitrate only appeared to be present on the outer wall of the first column of honeycomb cells.

Some cells in the honeycomb sandwich panel were observed to fill during the test in a more random nature than the apparently ordered diffusion path seen in the radiographs. Node bond swelling and cell wall wetting of the core did not appear to require large volumes of salt solution for the diffusion to proceed.

Due to the apparently corrosive nature of the concentrated solution of cerium nitrate the diffusion path observed may be unique for this solution. Separate studies examining water diffusion should also be undertaken to observe if similar diffusion processes occur.

## DISTRIBUTION LIST

The Durability of Metal-Honeycomb Sandwich Structure Exposed to  
High Humidity Conditions

Andrew Rider

### AUSTRALIA

#### DEFENCE ORGANISATION

##### Task Sponsor

ASI4A

##### S&T Program

Chief Defence Scientist	}	shared copy
FAS Science Policy		
AS Science Corporate Management		
Director General Science Policy Development		
Counsellor Defence Science, London (Doc Data Sheet)		
Counsellor Defence Science, Washington (Doc Data Sheet)		
Scientific Adviser to MRDC Thailand (Doc Data Sheet )		
Scientific Adviser Joint		
Navy Scientific Adviser (Doc Data Sheet and distribution list only)		
Scientific Adviser - Army (Doc Data Sheet and distribution list only)		
Air Force Scientific Adviser		
Director Trials		

##### Aeronautical and Maritime Research Laboratory

Director (Doc Data Sheet only)  
Chief of Airframes and Engines Division  
RLACS  
Roger Vodicka  
Andrew Rider

##### DSTO Library and Archives

Library Fishermans Bend (Doc Data Sheet )  
Library Maribyrnong (Doc Data Sheet )  
Library Edinburgh  
Australian Archives  
Library, MOD, Pyrmont (Doc Data sheet only)  
US Defense Technical Information Center, 2 copies  
UK Defence Research Information Centre, 2 copies  
Canada Defence Scientific Information Service, 1 copy  
NZ Defence Information Centre, 1 copy  
National Library of Australia, 1 copy

##### Capability Systems Staff

Director General Maritime Development (Doc Data Sheet only)  
Director General Aerospace Development (Doc Data Sheet only)

##### Knowledge Staff

Director General Command, Control, Communications and Computers (DGC4) (Doc  
Data Sheet only)

**Army**

ABCA National Standardisation Officer ( 4 copies)  
Land Warfare Development Sector  
Tobruk Barracks  
PUCKAPUNYAL VIC 3662  
SO (Science), Deployable Joint Force Headquarters (DJFHQ) (L), MILPO Gallipoli  
Barracks, Enoggera QLD 4052 (Doc Data Sheet only)  
NPOC QWG Engineer NBCD Combat Development Wing, Tobruk Barracks,  
Puckapunyal, 3662 (Doc Data Sheet relating to NBCD matters only)

**Air Force**

ASI-SRS

**Intelligence Program**

DGSTA Defence Intelligence Organisation  
Manager, Information Centre, Defence Intelligence Organisation

**Corporate Support Program**

Library Manager, DLS-Canberra  
MS Sam Doran  
Defence Library Service - Sydney West  
Building N157, Defence Establishment  
The Northern Road  
Orchard Hills NSW 2748

**UNIVERSITIES AND COLLEGES**

Australian Defence Force Academy (Doc Data Sheet only)  
Library (Doc Data Sheet only)  
Head of Aerospace and Mechanical Engineering (Doc Data Sheet only)  
Senior Librarian, Hargrave Library, Monash University (Doc Data Sheet only)

**OTHER ORGANISATIONS**

NASA (Canberra)  
AusInfo  
Aerostructures (Doc Data Sheet only)

**OUTSIDE AUSTRALIA****ABSTRACTING AND INFORMATION ORGANISATIONS**

Library, Chemical Abstracts Reference Service  
Engineering Societies Library, US  
Materials Information, Cambridge Scientific Abstracts, US  
Documents Librarian, The Center for Research Libraries, US

**INFORMATION EXCHANGE AGREEMENT PARTNERS**

Acquisitions Unit, Science Reference and Information Service, UK  
Library - Exchange Desk, National Institute of Standards and Technology, US  
National Aerospace Laboratory, Japan  
National Aerospace Laboratory, Netherlands  
SPARES (5 copies)

**Total number of copies: 42**

<b>DEFENCE SCIENCE AND TECHNOLOGY ORGANISATION DOCUMENT CONTROL DATA</b>					
				1. PRIVACY MARKING/CAVEAT (OF DOCUMENT) (U)	
2. TITLE  The Durability of Metal-Honeycomb Sandwich Structure Exposed to High Humidity Conditions			3. SECURITY CLASSIFICATION (FOR UNCLASSIFIED REPORTS THAT ARE LIMITED RELEASE USE (L) NEXT TO DOCUMENT CLASSIFICATION)  Document (U) Title (U) Abstract (U)		
4. AUTHOR(S)  Andrew Rider			5. CORPORATE AUTHOR  Aeronautical and Maritime Research Laboratory 506 Lorimer St Fishermans Bend Vic 3207 Australia		
6a. DSTO NUMBER DSTO-TR-1276		6b. AR NUMBER AR-012-154		6c. TYPE OF REPORT Technical Report	
7. DOCUMENT DATE March 2002					
8. FILE NUMBER M1/9/778		9. TASK NUMBER AIR 01/123		10. TASK SPONSOR DGTA	
				11. NO. OF PAGES 108	
				12. NO. OF REFERENCES 19	
13. URL on the World Wide Web  <a href="http://www.dsto.defence.gov.au/corporate/reports/DSTO-TR-1276.pdf">http://www.dsto.defence.gov.au/corporate/reports/DSTO-TR-1276.pdf</a>				14. RELEASE AUTHORITY  Chief, Airframes and Engines Division	
15. SECONDARY RELEASE STATEMENT OF THIS DOCUMENT  <i>Approved for public release</i>					
OVERSEAS ENQUIRIES OUTSIDE STATED LIMITATIONS SHOULD BE REFERRED THROUGH DOCUMENT EXCHANGE, PO BOX 1500, EDINBURGH, SA 5108					
16. DELIBERATE ANNOUNCEMENT  No Limitations					
17. CASUAL ANNOUNCEMENT Yes					
18. DEFTTEST DESCRIPTORS  adhesive bonding, bonded repair, honeycomb panels					
19. ABSTRACT Metal-honeycomb structure plays an important role in the structural integrity of RAAF F-111 aircraft. When F-111 is retired from service honeycomb panels will have experienced extended exposure to hostile environments. The processes leading to degradation of metal-honeycomb sandwich structure and its effect on the structural integrity of F-111 structure is critical information required for successful, long term aircraft management.  The work presented in this report summarises initial investigations into the mechanical strength response of metal-honeycomb sandwich structure exposed to high humidity environments. Honeycomb sandwich panels constructed from core and structural adhesives materials currently used for repairs at RAAF-Amberley have been conditioned in high humidity environments and examined using flatwise tension, peel and bending tests. The durability performance of honeycomb panels depended on the construction materials and the mode of loading employed. In some cases, characterisation of the honeycomb revealed differences that could be related to the durability performance.					